Mechanism underlying the anticontractile effect of perivascular adipose tissue

A thesis submitted to The University of Manchester for the degree of

Doctor of Philosophy

in the Faculty of Medical and Human Sciences

2013

Yiwen Dong

School of Medicine

Table of contents

Final word count: 45,644

List of figures

Chapter 1

Chapter 2

Chapter 3

Chapter 4

Chapter 5

Chapter 6

Chapter 7

Abbreviations

5-HT	5-Hydroxytryptamine
ACC	CoA carboxylase
ACE	Angiotensin-converting enzyme
ADHF	Adipocyte-derived hyperpolarisation factor
AdipoR	Adiponectin receptor
ADRF	Adipocyte-derived relaxing factor
AICAR	5-aminoimidazole-4-carboxamide ribonucleoside
AMPK	AMP-activated protein kinase
Ang	Angiotensin
ANOVA	Analysis of variance
ANP	Atrial natriuretic peptide
ATP	Adenosine-5'-triphosphate
BK_{Ca}	Large conductanceCa^{2+}-activated K^{+}
BNP	Brain natriuretic peptide
CaMKKβ	Ca^{2+}/calmodulin dependent protein kinase kinase
cAMP	Cyclic adenosine monophosphate
CBS	Cystathionine β-synthase
cGMP	Cyclic guanosine monophosphate
CoA	Acetyl-coenzyme A
COX	Cyclooxygenases
CSE	Cystathionine γ-lyase
DMSO	Dimethyl sulfoxide
EC_{50}	Half maximal effective concentration
eNOS	Endothelial nitric oxide synthase
G6P	Glucose-6-phosphate
G6P-D	Glucose-6-phosphate dehydrogenase
GTP	Guanosine triphosphate
H_2O_2	Hydrogen peroxide

H_2S	Hydrogen sulphide
HMG	3-hydroxy-3-methylglutaryl
HSL	Hormone-sensitive lipase
$I_{BK(Ca)}$	BK_{Ca} channel current
$I_{K(V)}$	K_V channel current
IK_{Ca}	Intermediate conductance Ca^{2+}-activated K^+
iNOS	Inducible nitric oxide synthase
IP_3	Inositol 1,4,5-trisphosphate
K_{ATP}	ATP-sensitive K^+
K_{Ca}	Ca^{2+}-activated K^+
K_V	voltage-gated K^+
LKB1	Liver kinase B1
L-NMMA	NG-monomethyl-L-arginine
MLC	Myosin light chain
MLCK	Myosin light chain kinase
MST	3-mercapro-sulphurtransferase
NADPH	Nicotinamide adenine dinucleotide phosphate
NED	N-1-napthylethylenediamine
nNOS	Neuronal nitric oxide synthase
NO	Nitric oxide
NO_2^-	Nitrite
NO_3^-	Nitrate
NOS	Nitric oxide synthase
pEC_{50}	Negative logarithm of EC_{50}
PBS	Phosphate buffered saline
PDE	Cyclic nucleotide phosphodiesterases
PIP_2	Phosphatidylinositol bisphosphate
PKA	cAMP-dependent protein kinase
PKG	cGMP-dependent protein kinase
PLC	Phospholipase C

PSS	Physiological saline solution
PVAT	Perivascular adipose tissue
RCK	Regulator of conductance for K^+
ROS	Reactive oxygen species
RT-PCR	Reverse transcription polymerase chain reaction
SEM	Standard error of the mean
SK_{Ca}	Small conductance Ca^{2+}-activated K^+
SOD	Superoxide dismutase
STOC	Spontaneous transient outward current
SUR	Sulphonylurea receptors
TAK1	Transforming growth factor-β-activated protein kinase 1
TNF-α	Tumor necrosis factor-α
ZMP	Monophosphate AICAR

Abstract

This thesis, entitled 'Mechanism underlying the anticontractile effect of perivascular adipose tissue', has been submitted by author Yiwen Dong for a degree of Doctor of Philosophy (PhD) in the Faculty of Medical and Human Sciences at the University of Manchester, September 2013.

Most systemic blood vessels are surrounded by layers of adipocytes forming perivascular adipose tissue (PVAT). Healthy PVAT can act as an endocrine organ to release different factors which can reduce vessel contractility. The exact anticontractile mechanism is still unclear, although recent evidence suggests that PVAT-derived factors may activate the large conductance Ca^{2+}-dependent K^+ (BK_{Ca}) channels on the vascular myocytes possibly via AMP-activated protein kinase (AMPK). Additionally, cGMP-dependent protein kinase (PKG) within the adipocytes seemed to be important for the anticontractile function of PVAT. This project aims to investigate the mechanism of the anticontractile effect of PVAT by determining the functions of PKG within adipocytes, as well as to assess the importance of vascular AMPK and BK_{Ca} channels to the PVAT anticontractile mechanism.

Experiments were carried out mainly with male rat mesenteric arteries and aortas. Whole vessels with or without PVAT were mounted on wire myographs to detect changes in vessel tension induced by pharmacological agents. Single myocytes were freshly-isolated from mesenteric artery or aorta and were voltage-clamped in the whole-cell configuration. BK_{Ca} channel current was triggered by voltage steps.

Vascular tension experiments showed that sildenafil (an indirect PKG activator) did not enhance the anticontractile effect of PVAT. However, the vasorelaxant effect of sildenafil was reduced when endothelium was removed, but only in PVAT-denuded vessels. Nitric oxide (NO) synthase inhibition reversed the vasorelaxant effect of sildenafil regardless of the presence of endothelium or PVAT.

In electrophysiology recordings, application of an AMPK activator A-769,662 increased BK_{Ca} channel current, an effect that was inhibited by iberiotoxin (a selective BK_{Ca} channel blocker), but not by dorsomorphin (an AMPK inhibitor). PT1 (an alternative AMPK activator) mimicked the effect of A-769,662 and increased the BK_{Ca} channel current. Again, this was not sensitive to dorsomorphin.

In solution transfer experiments, the PVAT bath solution increased BK_{Ca} channel activity, an effect that was similarly observed with adiponectin. The effect of the PVAT bath solution was not inhibited by catalase. Furthermore, in tension studies, PVAT isolated from adiponectin deficient mouse had lost its anticontractile effect under basal conditions.

The results indicate that, under basal conditions, PVAT exerts anticontractile effect by release NO to activate PKG in vascular myocytes. In addition, PVAT can also release an unknown factor which can activate the BK_{Ca} channels on the myocytes to cause membrane hyperpolarisation. The identity of this factor is unknown, but is unlikely to be hydrogen peroxide. AMPK activators as well as adiponectin, a putative AMPK activator, increased BK_{Ca} channel current, suggesting that AMPK activation can cause myocyte relaxation via opening BK_{Ca} channels. Thus, PVAT may release adiponectin which can cause vascular myocyte hyperpolarisation by opening of BK_{Ca} channels.

Declaration

I declare that no portion of the work referred to in the thesis has been submitted in support of an application for another degree or qualification of this or any other university or other institute of learning.

Yiwen Dong Date

Copyright statement

Acknowledgements

It is with immense gratitude that I acknowledge my supervisors Prof. A Heagerty and Dr. G Edwards for their help and advice during the past three years. I am truly grateful for the generous support provided by Dr. G Edwards. This project would not have come this far without her insightful discussions and constructive recommendations. I would like to acknowledge Prof. Heagerty for providing me the opportunity to explore this truly fascinating area and for placing confidence in me when I have doubted myself. I would also like to thank Prof. A Weston for his words of encouragement.

I thank the current and former members of the Heagerty and Edwards labs, especially Dr. I Egner for entertaining me both in the lab and during our breaks from science.

I am also grateful for the generous help given by Dr. Y Li. She guided me onto the right track at a time when I was deeply lost. Dr. Li is also a wonderful friend who I will keep in touch with. To all my friends (the 'lunchtime gang') who made my life so much fun, I will miss you all and will treasure the times we spent joking and laughing.

Finally, I would like to express my very great appreciation to my mum and dad for providing unconditional care and support. My mum especially, for the immense amount of love. I would not be where I am without her. I am grateful to my boyfriend for the support and for looking after me in the final few weeks of my PhD. My cat Tigger, whose purring cured every bit of stress that came from a long day of unsuccessful experiments.

Funding for this research was provided by the British Heart Foundation. I am grateful for the dedicated volunteers and fundraisers who made this research happen.

Publications

Dong Y, Edwards G & Heagerty A (2013). Effect of perivascular adipose tissue and AMPK activation on vascular myocytes BKCa currents [abstract]. 37th Congress of IUPS, available at http://www.physoc.org/proceedings/abstract/Proc%2037th%20IUPSPCB418

Weston AH, Egner I, Dong Y, Porter EL, Heagerty AM & Edwards G (2013). Stimulated release of a hyperpolarizing factor (ADHF) from mesenteric artery perivascular adipose tissue; involvement of myocyte BKCa channels and adiponectin. *Br J Pharmacol*, 169, pp.1500-1509.

Chapter 1

General introduction

1.1 The cardiovascular system and blood vessel composition

The role of the blood vessels is to deliver blood from heart to the rest of the body to allow gaseous and substance exchange before returning the blood back to heart. There are two circulation systems within the body: pulmonary and systemic. The pulmonary artery delivers blood to the lungs for oxygenation; this oxygen-rich blood is then carried by the systemic circulation to distribute oxygen to the rest of the body. Depending on their functions, the blood vessels can be divided into three types. The arteries carry blood away from the heart and branch progressively from muscular arteries to smaller arterioles and eventually to capillaries. The capillaries are sites for substance exchange and form extensive networks to supply nutrients for various tissues within the body. Capillaries then coalesce to form bigger venules which progressively increase in size to form the large veins which return the blood back to the heart. Apart from capillaries, all blood vessels consist of three layers: tunica intima, a layer of endothelial cells; media, the middle smooth muscle layer and adventitia. The adventitia can then be further divided into two components: adventitia compacta, a layer of mainly fibroblasts and perivascular adipose tissue (PVAT) which surrounds most blood vessels (See Figure 1.01). Capillaries are the smallest vessels in the body. Their vessel walls comprise a single layer of endothelial cells, so the rate of substance exchange between blood and tissue is maximized.

1.1.1 Vascular smooth muscle cells

The media layer of vessels consists of layers of circumferentially-arranged smooth muscle cells. Generally, arteries tend to have thicker media layer (thus, more smooth muscle cells) than veins. The smaller arteries and arterioles are the resistance arteries which are in a partially constricted state under physiological conditions, also known as the basal arterial tone. This vascular tone is determined by the resulting actions of various influences including the myogenic mechanism, endothelium-derived factors, sympathetic adrenergic stimulation and local hormones. The myogenic mechanism is intrinsic to the vascular myocytes in response to transmural pressure or stretch (as reviewed by Schubert & Mulvany 1999). Constriction occurs when transmural pressure or stretch increases and *vice versa.* The other mechanisms that participate in regulating the arterial tone will be introduced in later sections. Depending on the perfusion demand of the tissue, these arteries can constrict further or dilate to control blood flow. Vascular myocyte contraction causes vasoconstriction and conversely, relaxation causes vasodilation.

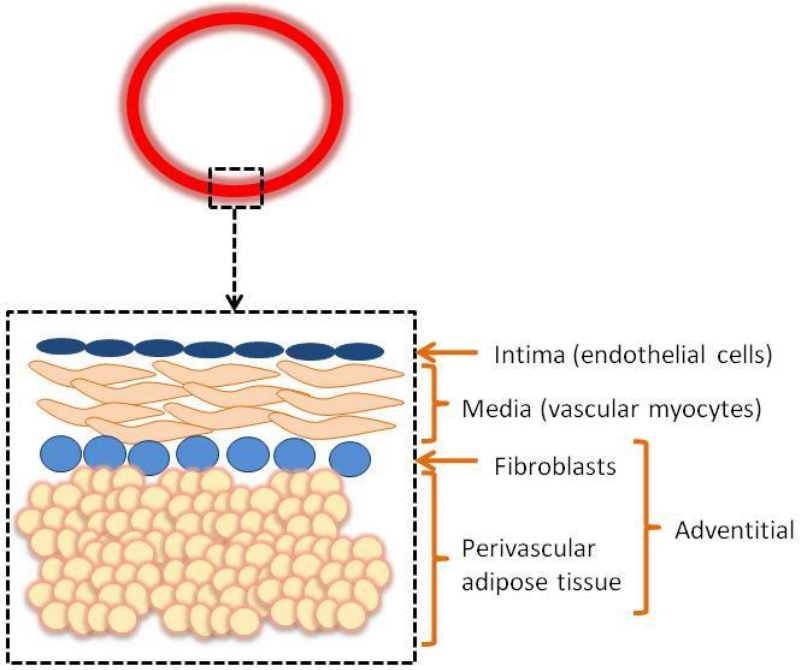

Figure 1.01. The three different layers of a blood vessel (excluding capillaries). The layer of endothelial cells that line the luminal side of the blood vessel is the intima. The media layer consists of circumferentially arranged smooth muscle cells. The outer adventitial layer has two components: fibroblast and perivascular adipose tissue.

1.1.2 Endothelial cells

The vascular endothelium is the single layer of cells that line the luminal side of all blood vessels. The importance of endothelial cells to the control of vascular functions was first appreciated in 1980s when it was realized that the relaxant effect of acetylcholine was inhibited with endothelium removal (Furchgott & Zawadzki 1980). It was proposed that endothelial cells are able to release a diffusible factor that contributes to vascular relaxation (Furchgott & Zawadzki 1980). Since then, endothelium has been the centre of attention for many studies and the area has advanced dramatically. Now, the endothelium is known to release a range of different factors and is involved in almost all aspects of vascular functions, such as vessel constriction/dilation, blood clotting, inflammation and angiogenesis (as reviewed by Deanfield et al. 2007).

1.1.3 Perivascular adipose tissue

There are two types of fat tissue in the human body: white and brown adipose tissue (see review by Smorlesi et al. 2012). White adipose tissue is responsible for storing energy and releasing this energy in the form of lipids. Brown adipose tissue dissipates energy to provide metabolic heat. There are also regional differences in the fat tissues. Generally, subcutaneous adipose tissue is found under the skin whereas visceral adipose tissue is found in close vicinity to body organs. Apart from the cerebral vessels and capillaries, abundant amount of adipose tissue can be found surrounding most of the blood vessels. This adipose tissue is known as perivascular adipose tissue (PVAT). PVAT is a mixture of both brown and white adipose tissue, and the exact composition of the two varies with different depots. While rodent aortic PVAT has been found to contain adipocytes similar to brown adipocytes (Chang et al. 2012), rodent mesenteric PVAT mostly comprises white adipocytes (Hausman 1985a). The brown and white adipocytes have very distinct morphologies. First, white adipocyte contains one single (uniocular) large lipid droplet which takes up the majority of the cytoplasm. Brown adipocytes are multiocular, with lipid droplets scattered around the cell cytoplasm (see review by Cinti 2011). Second, brown adipocytes are more abundant with cristae-rich mitochondria. Third, white adipose tissue is less densely vascularised, giving the white adipose tissue a paler appearance than the brown fat. Similar to endothelial cells, PVAT can also release many different factors to affect vascular tension (see later sections).

PVAT is composed of more than just adipocytes, but is a collection of different cell types including: macrophages; multipotent cells; preadipocytes; pericytes; endothelium

stem cells from microvessels and lymphatic vessels as well as infiltrating immune cells (Hausman 1985b; Zuk et al. 2002). Multipotent stem cells have multilineage potential and are able to differentiate into myogenic, adipogenic and neurogenic cell types (Zuk et al. 2002). The PVAT is also enriched with nerve endings, which release neurotransmitters to regulate adipocyte functions.

1.1.3.1 Lipolysis

White adipocytes store energy as triacylglycerols which form the large lipid droplet observed in every mature adipocyte. Under fasting conditions, triacylglycerol is broken down to free fatty acids and glycerol and released into the blood stream; this process is known as lipolysis. The most common known mechanism that causes lipolysis is the cAMP (cyclic adenosine monophosphate)-mediated pathway (Bojanic et al. 1985). Adrenergic stimulation (see Section 1.5.1.1) triggers the β adrenoceptors on the adipocytes to activate the coupled the G-protein Gαs leading to production of cAMP by adenylyl cyclase. Intracellular accumulation of cAMP results in activation of cAMP-dependent protein kinase (PKA) which can stimulate adipose triglyceride lipase and hormone-sensitive lipase (HSL). Both adipose triglyceride lipase and HSL are the rate limiting enzymes in the lipolysis and catalyses the hydrolysis of tri- and diacylglyceride, respectively. For more details on the lipolysis pathways, refer to review Chaves et al. 2011.

1.2 Mechanism of vascular myocyte contractility

Like many other myocytes, vascular smooth muscle cell contraction is triggered by an increase in intracellular Ca^{2+} concentration. This is usually the result of the opening of voltage-gated Ca^{2+} channels caused by membrane depolarisation. The intracellular Ca^{2+} can interact with calmodulin, a highly conserved protein that contains E-F motifs for Ca^{2+} binding (see review Chin & Means 2000). Ca^{2+}-bound calmodulin then causes activation of myosin light chain kinase (MLCK) and phosphorylation of myosin light chain (MLC), leading to smooth muscle contraction. Spasmogens such as norepinephrine and endothelin can also increase intracellular Ca^{2+} level by activating phospholipase C, resulting in formation of inositol 1,4,5-trisphosphate (IP_3) to trigger Ca^{2+} release from the intracellular Ca^{2+} stores (sarcoplasmic reticulum) through IP_3 receptors. Smooth muscle relaxation is initiated when intracellular Ca^{2+} concentration is reduced, leading to MLC phosphatase activation. This causes the removal of the phosphate on the MLC kinase. The activity of MLC phosphatise is deactivated by small GTPase Rho and its downstream effector Rho-

dependent kinase (for more information on the Rho/Rho kinase pathway, refer to reviews Fukata et al. 2001 and Webb 2003). The Rho/Rho kinase pathway forms the basis of the Ca^{2+}-sensitising mechanism within vascular myocytes and is particularly important for persistent contraction within these cells.

When the global Ca^{2+} concentration rises in the cell, Ca^{2+} removal mechanisms are activated to return the myocyte back to its quiescent state. Plasma membrane and sarcoplasmic reticulum Ca^{2+} ATPases as well as the Na^{+}/Ca^{2+} exchanger are all parts of the Ca^{2+} removal system in the myocytes. Plasma membrane and sarcoplasmic reticulum Ca^{2+} ATPases use ATP (adenosine-5'-triphosphate) as energy whereas Na^{+}/Ca^{2+} exchanger uses electrochemical gradient of Na^{+} to remove Ca^{2+} from the cytosol. This See Figure 1.02 for the mechanism of contraction in vascular myocytes.

1.2.1 Voltage-gated Ca^{2+} channels

The voltage-gated Ca^{2+} channels are important for the myocyte contractility as their opening allow Ca^{2+} entry from the extracellular space into the cytosol to elicit contraction pathways. To date, there are six different types of voltage-gated Ca^{2+} channels identified (L-, T-, N-, P/Q and R-type; see review Godfraind & Govoni 1995). As any other voltage sensitive channels, these Ca^{2+} channels open by a depolarisation in the plasma membrane. However, different Ca^{2+} channels have varying voltage threshold for activation; depending on the voltage required the Ca^{2+} channels can be divided into either high or low voltage activated channels. All Ca^{2+} channels, apart from the T-type, are high voltage activated; the T-type is a low voltage activated Ca^{2+} channel. In vascular smooth muscle cells, the predominant voltage-gated Ca^{2+} channels are the L-type channels. T-type channels, although have recently drawn much attention, will not be discussed here.

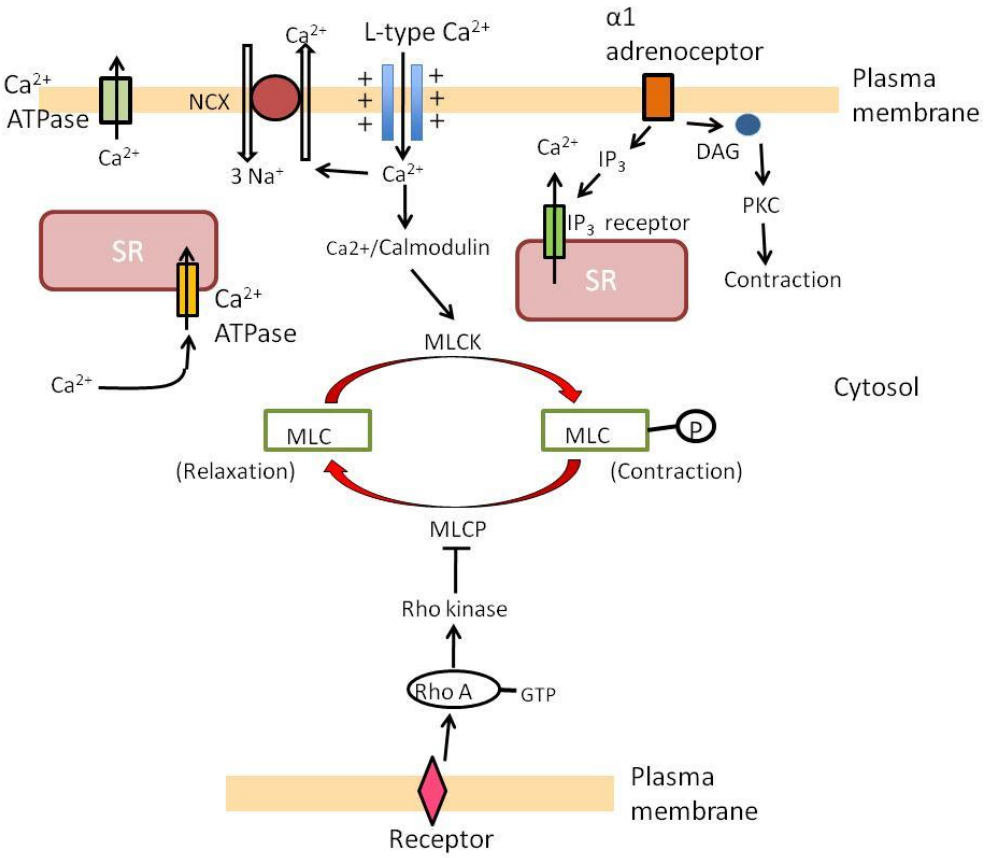

Figure 1.02. Mechanisms of contraction in a vascular smooth muscle cell. Membrane depolarisation triggers the opening of voltage-gated L-type Ca^{2+} channels, leading to influx of Ca^{2+} into the cell which results in Ca^{2+}/calmodulin dependent activation of myosin light chain kinase (MLCK). MLCK then phosphorylates myosin light chain (MLC), causing the myocyte to contract. Ca^{2+} is removed from the cytosol by Ca^{2+} ATPase on the plasma membrane and sarcoplasmic reticulum (SR), as well as the Na^{+}/Ca^{2+} exchanger (NCX) on the plasma membrane. The myosine light chain kinase phosphotase (MLCP) can phosphorylate MLC, which initiates cell relaxation. However, the activity of MLCP is inhibited by certain agonists via activation of Rho A and Rho-dependent kinase. Sympathetic nervous system can also increase myocyte contraction by activating the α1 adrenoceptors to release second messenger inositol triphosphate (IP_3) and diacylglycerol (DAG). IP_3 activates IP_3 receptors on the SR to cause Ca^{2+} to be released from the SR, an intracellular Ca^{2+} store. DAG can activate protein kinase C and phosphorylation of other protein. Both mechanisms cause myocyte contraction.

The L-type Ca^{2+} channels is one of the high-voltage activated channels as it can activate at relatively high membrane potentials, of around -40 mV (full activation at 0 mV; Orallo 1996). The α1 subunit is the pore-forming structure of the channels; although it is known to associate with four other subunits (α2, β, γ and δ) which can regulate channel activity (Catterall 1991). Once activated, the relatively large conductance of these L-type Ca^{2+} channels causes a rise in the intracellular Ca^{2+} concentration leading to myocyte contraction. As such, L-type Ca^{2+} channel blockers (such as nifedipine) are classic antihypertensive treatments (Kochegarov 2003).

1.3 Novel functions of adipose tissue

One of the most interesting scientific advances recently is the discovery of adipose tissue as an endocrine organ. Adipocytes can release adipokines (originally termed adipocytokines by Funahashi et al. 1999) which are a group of highly diverse molecules ranging from the classic cytokines (e.g. the interleukins 6 and 8 and tumour necrosis factor-α) to those only released by adipocytes (such as leptin and adiponectin). These molecules can act in autocrine, paracrine and endocrine manners to have functions in metabolism, inflammation and pro-angiogenic processes (Deng & Scherer 2010). As more comprehensive reviews on the adipokines can be found elsewhere (Deng & Scherer 2010; Scherer 2006), the following sections will briefly introduce two of the adipokines that are of particular interest: adiponectin and leptin.

1.3.1 Adiponectin

Adiponectin is a 30 kDa protein first discovered in the mid-1990s to be expressed exclusively in adipocytes (Scherer et al. 1995). Adiponectin molecules can undergo extensive post-translational modifications and can be secreted as trimers, low molecular weight entities (two trimers linked by covalent bonds) or high molecular weight complexes (consist of six trimers; Tsao et al. 2002). It has been proposed that these three forms may have different biological functions (Pajvani et al. 2004) but this is an area undergoing intensive research. The biological effects of adiponectin are via binding onto the adiponectin receptors, two of which have been identified: AdipoR1 and AdipoR2. AdipoR1 and AdipoR2 are found predominantly in skeletal muscle and liver, respectively, but are also ubiquitously expressed in peripheral tissues (Yamauchi et al. 2003; Kadowaki & Yamauchi 2005). Both of these receptors are seven-transmembrane spanning molecules, but are distinct from G-protein coupled receptors as no G proteins are coupled to the

intracellular side of the receptors (Yamauchi et al. 2003). AdipoR1 and AdipoR2, although exert similar physiological effects, have distinct coupling pathways. AdipoR1 activation tends to cause phosphorylation and activation of AMPK, whereas AdipoR2 is more prominent in activation of peroxisome proliferator-activated receptor α (Yamauchi et al. 2007). The pathways which connect adiponectin receptor activation to downstream effectors are currently unclear. It is believed that recruitment of adapter molecules, such as APPL-1 (adapter protein containing pleckstrin homology domain phosphotyrosine binding domain and leucine zipper motif), was suggested (see review Buechler et al. 2010).

Adiponectin concentration varies greatly within the plasma (3 to 30 µg/ml) and is altered by many different factors including gender and disease states (Combs et al. 2003). In general, patients with obesity, insulin resistance, metabolic syndrome and hypertension have lower concentrations of adiponectin in their blood (Arita et al. 1999; Yamauchi et al. 2001; Chow et al. 2007). High plasma levels of adiponectin have been reported to suppress development of atherosclerosis in apolipoprotein E-deficient mice by inhibiting the expression of receptors that are essential for atherosclerosis initiation (Okamoto et al. 2002). Maeda et al. (2002) also showed that adiponectin knockout mice developed diet-induced insulin resistance. Furthermore, the group illustrated that by reducing the expression of TNF-α (a factor that participates in insulin resistance) adiponectin could prevent insulin resistance (Maeda et al. 2002). In addition, adiponectin can also protect against many other cardiac diseases such as cardiac hypertrophy and myocardial injury (reviewed by Shibata et al. 2009).

Adiponectin is also important in blood pressure regulation. Adiponectin produced vasodilation in porcine retina arterioles and some of its effect are endothelium-dependent (Omae et al. 2013). Since adiponectin receptors are found on endothelial cells (Kadowaki & Yamauchi 2005) and activation of these receptors increases production of NO via increased AMPK and eNOS activity (Chen et al. 2003; see section 1.4.1 for the NO vasodilation pathway). Indeed, the importance of adiponectin in regulation of blood pressure was demonstrated in adiponectin knockout mice which display elevated blood pressure (Ouchi et al. 2006). However, whether adiponectin has any directly effects on the vascular myocytes is currently unknown.

1.3.2 Leptin

Another adipokine currently undergoing intense study is leptin. This hormone, discovered in 1994 (Zhang et al. 1994), is a highly conserved 16 kDa polypeptide. It is

expressed in adipocytes and is released in response to high triglyceride uptake (Halaas et al. 1995). Leptin is transported into the central nervous system via a selective and saturable transport uptake system in the brain-blood barrier (Banks et al. 1996). This selective uptake mechanism enables adipocytes to communicate with the central neuroendocrine systems to inhibit food intake (Halaas et al. 1995). Leptin has dual effects on vascular tone. By acting in the central nervous system, leptin can cause vasoconstriction by increasing the sympathetic stimulation. However, leptin also has direct vasodilator effect on the vasculature, both by endothelium-dependent and -independent mechanisms. The endothelium-dependent mechanism involves increasing the production NO from endothelial cells. The exact mechanism is still very much in debate, although it is claimed that leptin can activate intracellular protein kinase B (Akt) and AMPK which can in turn phosphorylate and activate eNOS (Procopio et al. 2009). Others have suggested that it is the nNOS subtype which is activated (Benkhoff et al. 2012). The endothelium-independent mechanism may be caused by leptin activating iNOS in vascular myocytes (Rodríguez et al. 2007).

1.4 PVAT and vascular contractility

PVAT (the adipose tissue that surrounds the majority of the blood vessels) was believed to have no effect on the arterial tone but likely to absorb drugs, so was essentially always removed during pharmacological experiments involving the vasculature. It was later found that the presence of PVAT reduced vessel contraction in rat aorta segments (Solti & Cassis 1991), an effect similarly observed in human systemic vessels (Greenstein et al. 2009). As described above, both adiponectin and leptin can regulate vascular tone. PVAT can also release a range of other molecules, such as nitric oxide, hydrogen sulphide, hydrogen sulphide, to reduce vascular tone (Sarzani et al. 1996; Canová et al. 2006; Gao et al. 2007; Lee et al. 2009; Nishikimi et al. 2009; Schleifenbaum et al. 2010). In addition to anticontractile factors, adipocytes have reported to promote vasocontractility by release of reactive oxygen species and angiotensin II (Gao et al. 2006; Lu et al. 2010). The following sections will introduce each of the PVAT-derived anticontractile and contractile factors in turn, concentrating on the functions of these factors in regulation of vascular tone. Since all of these factors can also be released from the endothelium (most of these are in fact originally described in the endothelium), the involvement of endothelial cells will also be introduced.

1.4.1 Nitric oxide

Nitric oxide (NO) was originally identified to be the endothelium-derived relaxing factor (Furchgott et al. 1987; Palmer et al. 1987). The synthesis of NO is by a group of enzymes known as NO synthases (NOS) which converts amino acid L-arginine to NO and L-citrulline (as reviewed by Francis et al. 2010). There are three isoforms of NOS that have currently been identified: endothelial (eNOS); inducible (iNOS) and neuronal NOS (nNOS). The names for NOS isoforms were given based on the tissues from which they were initially discovered from: eNOS was found from vascular endothelial cells and plays a key role in regulation of the vascular tone; iNOS is an inducible NOS expressed by a large number of cells especially within the immune and cardiovascular system and participates in inflammation; nNOS was first found in neuronal cells where NO acts as a neurotransmitter. However, expression of the NOS isoforms is not restricted within these cell types. Adipocytes, for example, express both eNOS and iNOS (Elizalde et al. 2000). Functional NOS is dimeric in structure consisting of two NOS monomers but is usually associated with two calmodulins, which determine the Ca^{2+}-dependent activation of all three NOS (Bredt & Snyder 1990). NOS activity can also be regulated by phosphorylation which enables Ca^{2+}-independent activation of NOS in endothelial cells by fluid sheer stress (as reviewed by Alderton et al. 2001).

1.4.1.1 The NO/cGMP/PKG pathway

NO is a vasodilator and once released, is freely diffusible to act in a paracrine manner. The vasodilator effect of NO is by forming complexes with cytosolic NO-activated guanylyl cyclase, which has two isoforms: soluble and particulate. The soluble guanylyl cyclase is activated by NO whereas the particulate form is activated by natriuretic peptide (see section 1.5.2.1). Binding of NO to soluble guanylyl cyclase increases the enzyme activity by 100 to 200 folds (see review Francis et al. 2010), to mediate the conversion of guanosine triphosphate (GTP) to cyclic guanosine monophosphate (cGMP), a second messenger responsible for regulating several downstream effectors. PKG (cGMP-dependent protein kinase), for one, is the main protein that is responsible for vasodilation of NO. There are currently two isoforms of PKG, PKGI and PKGII. PKGI is the predominant isoform (Hofmann et al. 2006) and therefore all subsequent PKG refers to PKGI. The vasodilatory mechanism of PKG is rather complicated (see review Lincoln et al. 2001), but includes: phosphorylation of Ca^{2+} pumps to increase the removal of Ca^{2+} from the cytosol; inhibition of L-type Ca^{2+} channels to minimize Ca^{2+} entry; direct activation of

BK_{Ca} channels to cause myocyte hyperpolarisation (thus reduces the opening of the L-type Ca^{2+} channels). These processes reduce the intracellular Ca^{2+} concentration, and therefore prevent Ca^{2+}-dependent activation of MLCK. Additionally, PKG also phosphorylates and activates MLC phosphatase, which opposes the action of Rho/Rho kinase in the process of myocyte Ca^{2+} sensitization. Figure 1.03 summarizes the NO/cGMP/PKG pathway within the vascular myocyte.

1.4.1.2 Phosphodieasterase

Under physiological conditions, cGMP is constantly broken down by a large family of enzymes – cyclic nucleotide phosphodiesterases (PDE). PDE is responsible for the breakdown of cyclic nucleotides, such as cAMP and cGMP and therefore controls the cellular levels of these second messengers. The level of cGMP is determined by the balance between the activity of guanylyl cyclase and PDE – reduced level of guanylyl cyclase activity leads to reduced levels of cGMP which terminates the actions of PKG. To date, eleven different members of PDEs have been recognized (PDE1-11), each with a different affinity for cyclic nucleotides and tissue distribution (reviewed by Omori & Kotera 2007). PDE 1, 2, 3 10 and 11 have dual efficacy for both cAMP and cGMP; PDE 4, 7 and 8 are more selective for cAMP and PDE5, 6 and 9 are specific for cGMP (Bender & Beavo 2006). PDE3 is the predominant phosphodiesterase in adipocytes (Miki et al. 1996), and has high affinity for both cAMP and cGMP. However, in the presence of cGMP, the breakdown of cAMP by PDE3 is inhibited; thus PDE3 is also known as the cGMP-inhibited PDE. Since cAMP is particularly important for the process of lipolysis within the adipocytes (see Section 1.1.3.1), PDE3 activation may inhibit this pathway. Indeed, insulin is believed to activate PDE3 to exert antilipolytic actions on the adipocytes (Shakur et al. 2001). PDE5 is well established for its role in hydrolysis of cGMP in vascular smooth muscle cells and inhibition of which can potentiate the cGMP/PKG pathway leading to vasorelaxation. In penis cavernosal smooth muscle cells, PDE5 inhibition enhances the cell relaxation which is the mechanism of action for sildenafil, a drug to treat erectile dysfunction (Webb et al. 1999).

1.4.2 Hydrogen peroxide

Hydrogen peroxide (H_2O_2) is a reactive oxygen species (ROS), but unlike other ROS (see Section 1.4.6 on ROS), H_2O_2 has been shown to be a vasodilator (Iesaki et al. 1999). Similar to NO, H_2O_2 activates the soluble guanylyl cyclase and cGMP/PKG pathway. In addition, H_2O_2 also causes vascular myocyte hyperpolarisation, possibly due to opening of

large conductance Ca^{2+}-activated K^+ channels (BK_{Ca} channels; Barlow & White 1998; Hayabuchi et al. 1998; Liu et al. 2011). H_2O_2 is synthesized from (other) ROS by superoxide dismutase (SOD) and three different SOD subtypes have known to exist (SOD1-3). In the vasculature, both SOD1 and SOD3 are expressed in myocytes, endothelial cells and adipocytes (Luoma et al. 1998). Indeed, H_2O_2 from adipocytes can exert anticontractile effects in the vascular myocytes as proposed by Gao et al. (2007). The action of H_2O_2 is terminated by catalase which decomposes the molecule to H_2O and O_2.

1.4.3 Hydrogen sulphide

Hydrogen sulphide (H_2S) is a toxic gas well known for its 'rotten egg' smell. It has also been found, more recently, to be a novel gasotransmitter. H_2S is a cell membrane permeable molecule, produced by three enzymes: cystathionine β-synthase (CBS); cystathionine γ-lyase (CSE) and 3-mercapro-sulphurtransferase (MST) (Stipanuk & Beck 1982). All three enzymes use L-cysteine as the main substrate, although CBS and CSE are the enzymes responsible for the majority of the endogenous production of H_2S (Stipanuk & Beck 1982; Erickson et al. 1990).

Expression of CBS and CSE is tissue specific. CBS is found mainly in the brain and nervous system (see review by Szabó 2007) but is not present in human and rat arteries (Bao et al. 1998; Chen et al. 1999). CSE, on the other hand, is the predominant subtype found in the vasculature (Hosoki et al. 1997; Zhao et al. 2001). Both endothelial cells and PVAT have been found to express CSE (Yang et al. 2008; Köhn et al. 2012). The physiological cardiovascular effects of H_2S involve vasodilation and a reduction in arterial blood pressure (Zhao et al. 2001; Schleifenbaum et al. 2010; Köhn et al. 2012). The exact mechanism behind this vasodilator effect of H_2S is still unknown. Vascular myocyte ATP-sensitive K^+ channels (K_{ATP}; Zhao et al. 2001) and voltage-gated K^+ (K_V) channels (K_V7 channels; Schleifenbaum et al. 2010) have both been reported to be activated by H_2S, leading to membrane hyperpolarisation and thus vessel relaxation.

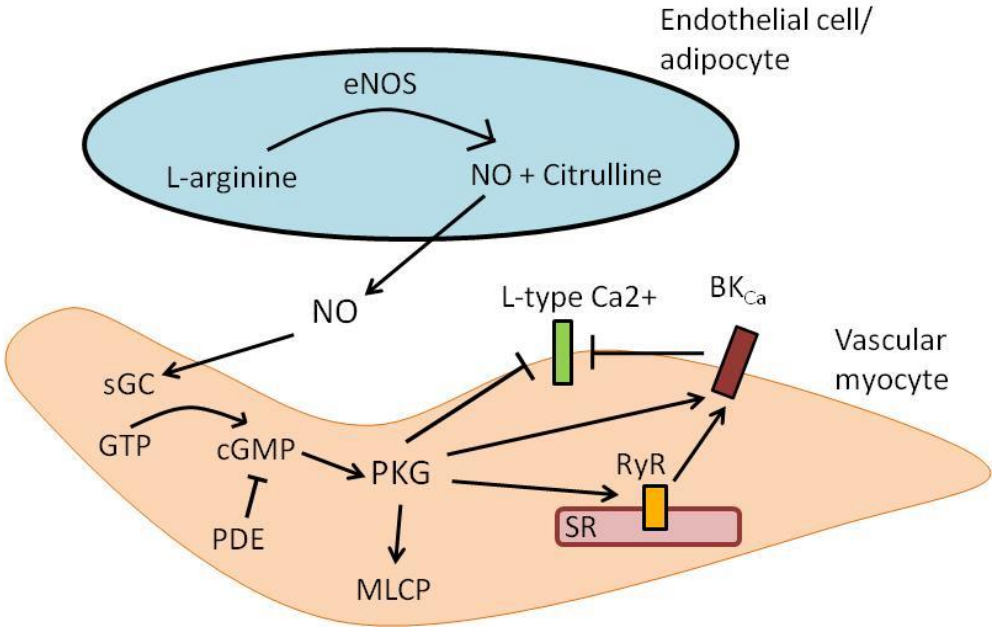

Figure 1.03. The nitric oxide (NO), cyclic guanosine monophosphate (cGMP) and cGMP-dependent protein kinase pathway in the vascular myocyte leading to cell relaxation. In both endothelial cell and adipocytes, the endothelial form of NO synthase (eNOS) is expressed which can convert L-arginine to NO and citrulline. NO is released and diffuses to the vascular myocyte to activate soluble guanylyl cyclase (sGC), which converts guanosine triphosphate (GTP) to cGMP to activate PKG. PKG can inhibit the voltage-gated L-type Ca^{2+} channels to prevent influx of Ca^{2+} required for cell contraction. Additionally, PKG can activate the large conductance Ca^{2+}-activated K^{+} channels, ryanodine receptors (RyR) on the sarcoplasmic reticulum (SR) and myosin light chain phosphatase (MLCP), all of which lead to myocyte relaxation. cGMP is hydrolyzed by phosphodieasterase (PDE) which terminates the cGMP/PKG pathway.

1.4.4 Angiotensin 1-7

Angiotensin 1-7 (Ang 1-7) is a bioactive heptapeptide of the renin-angiotensin system and is important for regulation of blood pressure. The starting point of the renin-angiotensin system is the production and secretion of angiotensinogen mainly by the liver. Renin, an enzyme secreted by the juxtaglomerular apparatus in kidney, cleaves angiotensinogen to an inactive decapeptide angiotensin I (Ang I). Ang I is further converted to angiotensin II (Ang II) or angiotensin 1-9 (Ang 1-9) by angiotensin-converting enzyme (ACE) or ACE2, respectively. Ang II and Ang 1-9 can be further catalyzed by ACE2 and ACE, respectively, to Ang 1-7 (for further details of the pathway, refer to review by Santos et al. 2013). Ang 1-7 can also be produced from Ang I directly, by many different peptidases, such as prolyl-endopeptidase and neutral endopeptidase. The renin-angiotensin pathway is summarized in Figure 1.04. Although Ang 1-7 and Ang II are both produced by the same system, they have opposing effects. Ang II, by binding mainly onto the angiotensin type-1 receptors (AT-1) causes vasoconstriction and increases vascular myocyte proliferation (as reviewed by Brede & Hein 2001). Ang 1-7, on the other hand, is a vasorelaxant and is anti-proliferative. The signalling of the Ang 1-7 is still poorly understood although it is believed that Ang 1-7 mediates most of its biological effects by binding to Mas (Santos et al. 2003) and possibly via the angiotensin type-2 receptors (AT-2; Bosnyak et al. 2011), both of which are G-protein coupled receptors. The importance of Mas to metabolism was demonstrated by Santo et al. (2008) who showed that Mas knockout mice displayed abnormal lipid and glucose metabolism as well as reduced insulin sensitivity.

Local renin-angiotensin systems can be found in almost all targeted tissues, including the vasculature. Adipose tissue expresses all components of the renin-angiotensin system (Schling et al. 1999). Lee et al (2009) showed positive staining for Ang 1-7 in adipocytes and demonstrated endothelium-dependent vasorelaxtion of Ang 1-7.

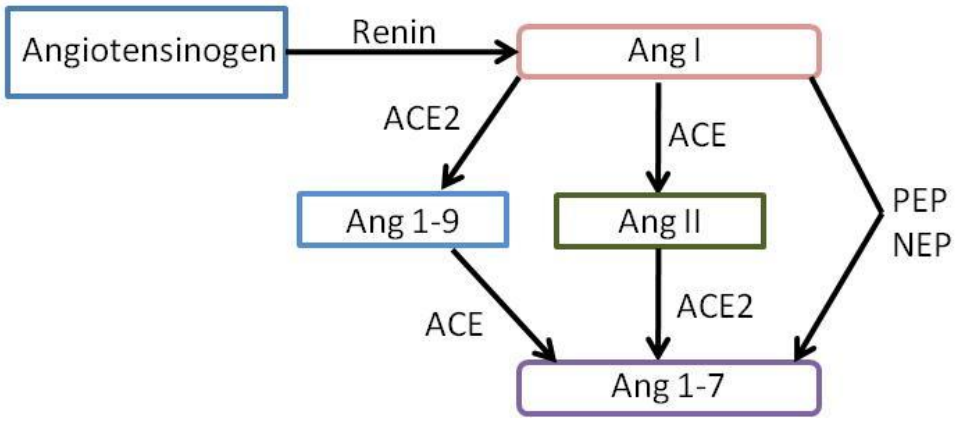

Figure 1.04. Simplified pathways of the renin-angiotensin systems leading to formation of angiotensin 1-7. Ang I: angiotensin I; Ang 1-9: angiotensin 1-9; Ang II: angiotensin II; Ang 1-7: Angiotensin 1-7; ACE: angiotensin converting enzyme; ACE2: angiotensin converting enzyme 2; PEP: prolyl-endopeptidase; NEP: neutral endopeptidase.

1.4.5 Adipocyte-derived relaxing factor

Adventitium-derived relaxing factor (or adipocyte-derived relaxing factor; ADRF) was originally describe by Löhn et al. (2002) to have a relaxant and an anticontractile effect in rat aorta. The identity of this ADRF is currently still under intense investigation and several candidates (H_2O_2, adiponectin, Ang 1-7 and H_2S) have been suggested (Gao et al. 2007; Greenstein et al. 2009; Lee et al.2009; Schleifenbaum et al. 2010). The only agreement reached by these different studies is that ADRF causes vasodilation, at least in part, by activating myocyte K^+ channels, leading to membrane hyperpolarisation. However, the concurrence stops here. Exactly which K^+ channels are opened by ADRF is very much disputed. Very recently, new evidence has emerged to support the possibility that the ADRF is adiponectin and that it can activate BK_{Ca} channels on the vascular myocytes to reduce vasoconstriction (Lynch et al. 2013; Weston et al. 2013). AMPK appears to be involved in this pathway, although the exact mechanism is unclear (Weston et al 2013). The different classes of K^+ channels and the functions of AMPK will be described later in this chapter.

1.4.6 Reactive oxygen species

Apart from the PVAT-derived anticontractile factors, PVAT can also secrete factors that promote vessel contraction. Gao et al. (2006) first proposed that PVAT may potentiate vessel contractility by releasing superoxide anions which belong to a group of reactive molecules and free radicals known as the reactive oxygen species (ROS). ROS are by-products of several systems such as cyclooxygenase production of prostanoids and the production of NO by eNOS (Cosentino et al. 1998). Vascular smooth muscle, endothelial cells and adipocytes have all known to contain ROS (Rosen & Freeman 1984; Miller et al. 1998; Wang et al. 1998). The common ROS that can have an effect on blood vessel contractility include superoxide radicals (O_2^-), hydrogen peroxide (H_2O_2) and hydroxyl radicals (·OH; see reviews Förstermann, 2010; Wong & Huang 2009). Apart from H_2O_2 (which is a vasodilator; see section 1.4.2), ROS causes vasoconstriction via several different mechanisms. First, ROS can reduce NO bioavailability. For example, O_2^- can react with NO to form peroxynitrite ($ONOO^-$). Second, ROS can also act directly by stimulating smooth muscle cyclooxygenase and inhibiting prostacyclin synthase to increase the production of vasoconstrictor prostanoids. Furthermore, ROS can activate Rho and Rho kinase to increase sensitivity to Ca^{2+} within smooth muscle cells (see review by Wong & Vanhoutte 2010 for more details on the vasoconstrictive effects of ROS).

1.4.7 Angiotensin II

Angiotensin II (or Ang II) is an octapeptide produced from the renin-angiotensin system (see Section 1.4.4) and is well known for its regulatory effects on the vascular contractility. Generally, Ang II can bind to two different receptors AT-1 and AT-2. Although both receptors are G-protein coupled receptors, they are now believed to have opposing effects (as reviewed by Iwai & Horiuchi 2009). The hypertensive, proliferative effects of Ang II is mediated mainly by binding onto the AT-1 receptors, which causes an increase in intracellular Ca^{2+} concentration leading to vasoconstriction or activation of protein kinases (such as mitogen-activated kinase) causing myocytes to proliferate (Iwai & Horiuchi 2009). In addition, Ang II may also increase the production of reactive oxygen species via activation of NADPH oxidase (see review Garrido & Griendling 2009). PVAT-derived Ang II has been demonstrated by Lu et al. (2010) and was proposed to promote PVAT-mediated vascular contraction.

1.5 Blood pressure regulation by other mechanisms

1.5.1 Neuronal hormones

1.5.1.1 Norepinephrine and epinephrine

Blood pressure is regulated by the autonomic nervous system, which has two subsystems: the sympathetic and parasympathetic nervous system. The sympathetic nervous system innervating the blood vessels causes vasoconstriction by releasing chemical mediators norepinephrine and epinephrine, which bind to adrenoceptors expressed on the vasculature. The roles of adrenoceptors were demonstrated as early as 1894 by Oliver and Schäfer that adrenal gland extract caused an increase in blood pressure (Oliver & Schäfer 1894).

Adrenergic receptors can be classified into two main groups: α and β, each of which can be further divided into subtypes (reviewed by Guimarães & Moura 2001). Both the α and β adrenoceptors are G-protein coupled receptors, which elicit intracellular signalling pathways by recruiting and activating the coupled G-proteins. There are two groups within the α adrenoceptor subfamily: α1 and α2. The α1 adrenoceptors play crucial roles in the regulation of vascular tone. Agonists binding onto the α1 adrenoceptors activate Gαq, which stimulates phospholipase C (PLC). PLC can then dissociate phosphatidylinositol bisphosphate (PIP_2), located at the plasma membrane, to release second messengers inositol triphosphate (IP_3) and diacylglycerol (Helliwell & Large 1997). IP_3 is able to

diffuse away from the plasma membrane and activate IP_3 receptors on the sarcoplasmic reticulum, resulting in the release Ca^{2+} from these intracellular stores (see Figure 1.02). Diacylglycerol can also activate protein kinase C to phosphorylate and activate other contractile proteins. Thus, activators of α1 adrenoceptors (i.e. phenylephrine and cirazoline) are vasoconstrictors. There are three groups of β adrenoceptors: β1-3. All β adrenoceptors are coupled to Gαs proteins; stimulation of these receptors activates adenylyl cyclase and increases intracellular cAMP. Norepinephrine and epinephrine can activate both subtypes of adrenoceptors, although the vasoconstrictive effect is mediated by activating the α1 adrenoceptors; β adrenoceptor activation can cause relaxation (Starke 1972; Guimarães & Moura 2001). Since vascular myocytes express both α and β adrenoceptors, the net effect of norephinephrine or ephinephrine is therefore determined by which of the adrenoceptors are predominately expressed by the particular vasculature. Adrenoceptors are also found to be expressed on the endothelium and both the α and β adrenoceptors are important for the regulation of vascular tone.

In adipocytes, β3 adrenoceptors are expressed at high levels on adipocytes and activation of which leads to an increase in lipolysis (Umekawa et al. 1997; see Section 1.1.3.1). Nerve endings have found to be extended into the adipose tissue, enabling the central nervous system to regulate adipocyte function via the release of norepinephrine and epinephrine.

1.5.1.3 Acetylcholine

By acting on the muscarinic receptors, acetylcholine causes endothelium-dependent vasodilation (Furchgott & Zawadzki 1980). Five muscarinic receptors have been identified (M1-5), the relaxation effect of acetylcholine is mainly via binding to the muscarinic receptor type 3 (M3) on the endothelial cells (Jaiswal et al. 1991). M_3 is a G-protein couple receptor, activation of which by acetylcholine leads to PLC-dependent release of IP_3 within the endothelial cells causing Ca^{2+} to be released from the intracellular stores (Adams et al. 1989). The increase in intracellular concentration results in activation eNOS and increases NO release from the endothelial cells. Acetylcholine is commonly used in the vascular studies to test for the presence of intact endothelium.

1.5.1.4 5-Hydroxytryptamine

5-Hydroxytryptamine (5-HT; also known as serotonin) is a central and peripheral nervous system neurotransmitter playing roles in the regulation in many systems including respiratory, gastrointestinal and immune systems. There are currently seven major subtypes

of 5-HT receptors (5-HT_{1-7}), different 5-HT receptor subtypes are found on vascular myocytes and endothelial cells. In the majority of blood vessels, the constrictive action of 5-HT is mediated via the 5-HT_2 receptors (G protein Gαq to activate phospholipase C) expressed by vascular myocytes. While activating the 5-HT_1 receptors on the endothelial cells stimulate the release of vasodilators (e.g. NO), causing vasorelaxation (Schoeffter & Hoyer 1990). The net effect of 5-HT is complicated and depends on the targeted vasculature (see review Watts et al. 2012).

1.5.2 Endogenous hormones

1.5.2.1 Natriuretic peptides

Depending on the source, there are three different forms of natriuretic peptide, atrial (ANP), brain (BNP), both secreted primarily by the heart, and C-type (CNP), secreted by a wide range of tissues including the vascular endothelium (Stingo et al. 1992). The general biological effects of ANP and BNP are mediated by binding to the natriuretic peptide receptor A (NPR-A), expressed by adipose tissue, endothelial cells and vascular myocytes (Wilcox et al. 1991). Activating NPR-A can reduce blood pressure via several different mechanisms including natriuresis, diuresis and vasorelaxation (Nishikimi et al. 2009). Both NPR-A and B are coupled to particulate guanylyl cyclase which is a membrane-bound guanylyl cyclase. Similar to the soluble form, particulate guanylyl cyclase is able to catalyse cGMP leading to subsequent activation of PKG (Leitman et al. 1988). The importance of natriuretic peptide in maintaining blood pressure has been illustrated by the development of hypertension in natriuretic peptide knockout mice (Melo et al. 1998). NP receptor C (NPC) is not couple to particulate guanylyl cyclase and may participate in natriuretic peptide clearance. Although interestingly, NPR-C receptors have been proposed to be linked to G protein (Gαi) and demonstrated to cause smooth muscle cell hyperpolarisation leading to vasodilatation (Chauhan et al. 2004). Natriuretic peptides are also known to be effective lipolytic agents via the cGMP/PKG pathway (Sengenès et al. 2000).

1.5.3 Endothelium-derived relaxing factors

1.5.3.2 Carbon monoxide

Vascular myocytes and endothelial cells have both been found to express hemeoxygenase, an enzyme that breaks down heme to produce biliverdin, iron and carbon monoxide (Christodoulides et al. 1995; Naik et al. 2003). Carbon monoxide has a

vasodilatory effect by a mechanism similar to NO, via activating the soluble guanylyl cyclase/cGMP/PKG pathway (Wang et al. 1997).

1.5.4 Endothelium-derived contraction factors

1.5.4.1 Endothelin

Endothelin, discovered in the late 1980s (Yanagisawa et al. 1988), are currently the most potent vasoconstrictive peptides and are particularly important for the regulation of systemic blood pressure. In the vasculature, endothelin is synthesized and released primarily by the endothelial cells as a response to many different stimuli such as hypoxia, cytokines and shear stress (as reviewed by Russell & Davenport 1999). There are three isoforms of endothelin, endothelin-1, -2 and -3, endothelin-1 being the most well studied isoform. Endothelin-1 acts by binding onto its receptors (ET_A and ET_B) which are expressed ubiquitously on all cells types. In blood vessels, ET_A is mainly expressed by smooth muscle cells and ET_B on endothelium as well as smooth muscle cells. The actions of the two endothelin receptors are rather complicated and generally have opposing effects. Stimulation of ET_A causes vasoconstriction via G-protein coupled pathways that increase the intracellular Ca^{2+} (from both extracellular space and intracellular stores; refer to review Ivey et al. 2008); ET_B stimulation, on the other hand, mediates the vasodilatation by increasing the production of NO (reviewed by Bohm & Pernow 2007). As ET_A is more widely distributed and in much higher numbers than ET_B, endothelin-1 causes vasoconstrictive effects.

1.5.4.2 Prostanoids

Similar with adipocytes, endothelium cells can also secrete other mediators that can trigger smooth muscle contraction and a reduction in blood pressure. Prostanoids are a group of lipid molecules which include prostaglandins and thromboxane A_2. Prostanoids are generated by cyclooxygenases (COX) which are either constitutively active (COX-1) or inducible (COX-2). COX-1 plays a major role in the endothelium-dependent vessel contraction and converts arachidonic acid to prostaglandins H_2 (PGH_2) which is then made to other molecules such as prostacyclin (PGI_2), thromboxane A_2 (TXA_2) and prostaglandins D_2 (PGD_2) and E_2 (PGE_2) by subsequent, respective synthases. Apart from the PGI_2 (a vasodilator) and PGE_2, all other mediators cause smooth muscle cells to contract (as reviewed by Wong & Vanhoutte 2010). Under basal conditions, prostacyclin synthase is the dominant enzyme within the endothelium. However, under certain states

(i.e. in disease states), when prostacyclin synthase is inhibited, other synthases become more active resulting in endothelium producing mainly constrictive prostanoids.

1.6 Vascular K^+ channels

It has been proposed, by several studies, that PVAT-dependent vessel relaxation effect is due to opening of K^+ channels on the myocytes by ADRF (Section 1.4.5). The following sections will therefore introduce some of the K^+ channels that have previously been proposed to be activated by ADRF.

Vascular myocyte contraction is closely linked to myocyte membrane potential. Depolarisation of the myocyte resting membrane causes opening of L-type voltage-dependent Ca^{2+} channels leading to an influx of Ca^{2+} into the cell and cell contraction; hyperpolarisation, however, reduces L-type Ca^{2+} channel opening and the cell remains relaxed. Tonic vascular myocytes have negative membrane potentials (Nelson & Quayle 1995) that are close to the activation threshold for voltage-gated K^+ channels. Opening of cell membrane K^+ channels allows K^+ efflux, keeping the myocyte hyperpolarised. Thus, K^+ channels act as 'off switches' in excitable vascular smooth muscle cells and are particularly important for maintaining low basal vascular tone. There are generally 4 different classes of K^+ channels in the vasculature: Ca^{2+}-activated (K_{Ca}); voltage dependent (K_V); ATP-sensitive (K_{ATP}) and inward rectifying (K_{ir}) channels. The following sections will introduce some of the K^+ channels of particular interest.

1.6.1 Ca^{2+}-activated K^+ channels

Ca^{2+}-activated K^+ (K_{Ca}) channels are a class of K^+ channel with sensitivity to increase in intracellular Ca^{2+} concentration. To date, there are three sub-families of K_{Ca}, commonly distinguished by their different unitary conductance as small (SK_{Ca}), intermediate (IK_{Ca}) and large (big; BK_{Ca}).

1.6.1.1 Small and intermediate conductance Ca^{2+}-activated K^+ channels

SK_{Ca} and IK_{Ca} channels have small (10-20 pS; Köhler et al. 1996) and intermediate (30-39 pS; Jensen et al. 1998) unitary conductance, respectively, and are voltage-independent channels activated by an increase in intracellular Ca^{2+}. Their Ca^{2+} sensitivity is due to their association with calmodulin (Köhler et al. 1996; Xia et al. 1998). SK_{Ca} and IK_{Ca} channels do not appear to have a functional role in healthy, non-proliferating vascular myocytes (reviewed by Coleman et al. 2004). In endothelial cells, however, IK_{Ca} and SK_{Ca} are essential for endothelium-dependent myocyte hyperpolarisation (Busse et al. 1988;

Edwards & Weston 1998). Physiological functions of IK_{Ca} and SK_{Ca} channels in the vasculature are investigated mostly by using both specific and non-specific channel blockers. Tetraethylammonium is a non-selective inhibitor of K_{Ca} channels. More selective inhibitors include apamin (SK_{Ca} channels) and charybdotoxin and 1-[(2-chloroohenyl)-diphenyl-methyl]-1H-pyrazole (TRAM-4; IK_{Ca} blockers; Wulff et al. 2000). See Wulff et al. (2007) for further details of the pharmacology of the SK_{Ca} and IK_{Ca} channels. In rat aortic PVAT, ADRF have been suggested to act by opening SK_{Ca} and IK_{Ca} channels (Gao et al. 2007).

1.6.1.2 Large conductance Ca^{2+}-activated K^+ channel

Both Lynch et al. (2013) and Weston et al. (2013) have suggested the importance of BK_{Ca} channels in the anticontractile effects of PVAT. BK_{Ca} channels have a high unitary conductance (100 – 300 pS; Marty 1981) and are functionally distinct from the other two K_{Ca} channels. Structurally, BK_{Ca} channels are formed from four pore-forming α subunits, either alone or with regulatory β-subunits in a 1:1 stoichiometry (Knaus et al. 2006). The α subunit of BK_{Ca} consists of seven transmembrane domains (S0-S6) and four hydrophobic domains located on the cytoplasmic tail. The S0 domain is unique to the BK_{Ca} channels and allows interaction with, and channel modulation by β subunits. The S4 domain possesses abundant positively charge residues (Papazian et al 1991), a characteristic shared by all voltage-dependent K^+ channels. Depolarisation of the membrane causes positive residues to move which leads to a channel conformational change and results in channel opening. BK_{Ca} is the only K_{Ca} channel that has this voltage-dependent property. SK_{Ca} and IK_{Ca} have S4 domains which contain fewer positively-charges residues and thus, lack voltage sensitivity (Latorre & Brauchi 2006). The S5 and S6 domains, together with the re-entrant pore-loop region in between, form the gating region of the channel. The long cytoplasmic tail (the C-terminus) is highly conserved and contains regulatory domains (Wei et al. 1994) – regulator of conductance for K^+ 1 (RCK1), RCK2 and a Ca^{2+} bowl (located in RCK2). Ca^{2+} can interact with the Ca^{2+} bowl as well as parts of RCK2 to assist in channel opening. The presence of β-subunits can influence Ca^{2+} sensitivity, channel kinetics and pharmacological properties (McManus et al. 1995; Meera et al. 1996; Hanner et al. 1997).

Opening of BK_{Ca} channels hyperpolarises the cell membrane to ‘turn off’ excitable cells. Dysfunction of BK_{Ca} channels has been shown to be the basis of many different diseases, such as hypertension, epilepsy and urinary incontinence (Meredith et al. 2004;

Grimm & Sansom 2010; N'Gouemo 2011). Thus, BK_{Ca} channel activators have potential therapeutic uses in these illnesses. BK_{Ca} channel openers include synthetic benzimidazolone derivatives (e.g. NS004 and NS1619), the biarylureas (e.g. NS1608) and mefenamic and flufenamic acids. NS1619 has been demonstrated to cause hyperpolarisation in aortic myocytes (Olesen et al. 1994) and is now commonly used in patch clamp experiments. BK_{Ca} channel blockers are often used in studies to examine the functions of the channel at different physiological conditions. Iberiotoxin is a highly specific BK_{Ca} channel blocker that can bind directly onto the external pore region of the channel (Giangiacomo et al. 1992). Other less selective channel blockers include charybdotoxin and tetraethylammonium.

1.6.1.3 Large conductance Ca^{2+}-activated K^+ channels and spontaneous transient outward currents

Spontaneous transient outward currents (STOCs) are the result of simultaneous and brief openings of clusters of BK_{Ca} channels (up to a hundred). A STOC lasts about 100 ms and is triggered by the opening of a localized group of ryanodine receptors in the sarcoplasmic reticulum, leading to a local increase in Ca^{2+} (this is known as a Ca^{2+} spark). The occurrence of Ca^{2+} sparks can be either spontaneous or induced by an increase in global Ca^{2+} concentration, pharmacological activation of the ryanodine receptors (i.e. caffeine) or an increase in sarcoplasmic reticulum Ca^{2+} content (as reviewed by Wellman & Nelson 2003). The ryanodine receptors are found in close proximity to BK_{Ca} channels and this increase in Ca^{2+} triggers the opening of BK_{Ca} channel, thus limiting membrane depolarisation. The link between Ca^{2+} sparks and cell membrane hyperpolarisation were first observed in 1983 by Brown and colleagues who saw a transient increase in membrane hyperpolarisation on addition of caffeine (Brown et al. 1983). They hypothesized that this membrane hyperpolarisation was due to opening of K_{Ca} channels – these transient currents, conducted by BK_{Ca} channels, were later termed STOCs (Benham & Bolton 1986). STOCs are important for smooth muscle relaxation and can act as a negative feedback to the global increase in Ca^{2+} concentration (Nelson et al. 1995).

1.6.2 Voltage-gated K^+ channels

K_V channels are a large group of proteins that can be divided into 12 subfamilies (K_V1-12; for full details of the K_V channels subfamilies, refer to Gutman et al. 2005). K_V channels are well known for their diversity. One of the features of the channel is heteromultimerization of the α subunits, meaning α subunits from different subfamilies can

form functional channels with varying channel characteristics (see review Mckeown et al. 2008). Depending on their current phenotypes, K_V channels can be divided into two types, those that are rapidly activating/inactivating (e.g. K_V4.2 and 4.3; reviewed by Amberg et al. 2003) and others that activate more slowly, the delayed rectifiers (e.g. K_V7 channels). The following section introduces K_V7 channels.

1.6.2.1 K_V7 channels

K_V7 channels consist of five subtypes: K_V7.1-7.5, encoded by KCNQ1-5 genes; therefore, K_V7 channels are sometimes referred to as KCNQ channels. Functional K_V7 channels are hetero- or homotetramers with very distinct tissue localisation. The hetero-tetramer K_V7.2/K_V7.3 is believed to be the molecular structure responsible for the M-current in the brain. Mutation in KCNQ genes in the brain can lead to benign familial neonatal convulsion (a form of general epilepsy; see review Gribkoff 2008). K_V7 channels have been demonstrated in other various parts of the body such as the heart, inner ear and vascular smooth muscle cells. In the vasculature, K_V7.1, K_V7.4 and K_V7.5 have been found in rat aortic and mesenteric artery smooth myocytes (Brueggermann et al. 2007; Mackie et al. 2008). The pore-forming α subunit is co-assembled with ancillary subunits encoded by KCNE genes. There are five different ancillary subunits (MinK (minimal K^+ channel protein) and MinK-related peptides), each with a single transmembrane domain (Figure 1.05). The presence of these ancillary proteins alters the biophysical properties of the K_V7 channels (for more information, refer to review McCrossan & Abbott 2004).

In general, functional K_V7 channels conduct a current that is slowly activating with activation threshold of -60 mV and is non-inactivating (Xiong et al. 2008). The hyperpolarised voltage of activation suggests that the K_V7 channels could remain open at the resting membrane potential, to conduct the resting K^+ current in vascular myocytes. Flupirtine, a marketed drug used for its centrally-acting analgesic effects (Gribkoff 2008), and retigabine, an anticonvulsant (Faulkner & Burke 2013), are both K_V7 channel openers. Flupirtine and retigabine have been shown to have vasorelaxation effect in tissue studies (Yeung et al. 2007). KCNQ channel blockers XE991 and linopirdine have been used as cognitive enhancers (Gribkoff 2008). By blocking the K^+ channels expressed in the central nervous system, these compounds can enhance neurotransmitter release and thus improve learning and memory abilities (Elmedyb et al. 2007). Both are valuable tools for examining the K_V7 channel functions.

1.6.3 ATP-sensitive K^+ channels

ATP-sensitive K^+ (K_{ATP}) channels are weakly inwardly rectifying – they pass inward current more easily than outward. Unlike the other strong inward rectifiers, such as Kir2.x and Kir3.x, they can still carry a significant amount of outward current at positive potentials (Nichols & Lopatin 1997). Functional K_{ATP} channels are octameric, comprised of 4 pore-forming Kir6 subunits and 4 regulatory sulphonylurea receptors (SUR) (as reviewed by Cole & Clément-Chomienne 2003). There are currently two different subtypes of pore forming subunits, Kir6.1 and Kir6.2 (Teramoto 2006). Each of these subunits has two transmembrane domains bridged by an ion selectivity loop (Nichols 2006). The sulfonylurea receptors belong to the ATP-binding cassette protein family, and to date three subtypes of SUR have been identified – SUR1, SUR2A and SUR2B. SUR takes no part in pore-forming, but is essential for surface expression of K_{ATP} and nucleotide dependent activation of the K_{ATP} channel (Ammälä et al. 1996; see Figure 1.05C). K_{ATP} are activated by a reduction in intracellular ATP/ADP concentration ratio, which enable the cells to control K^+ conductance depending on their metabolic states.

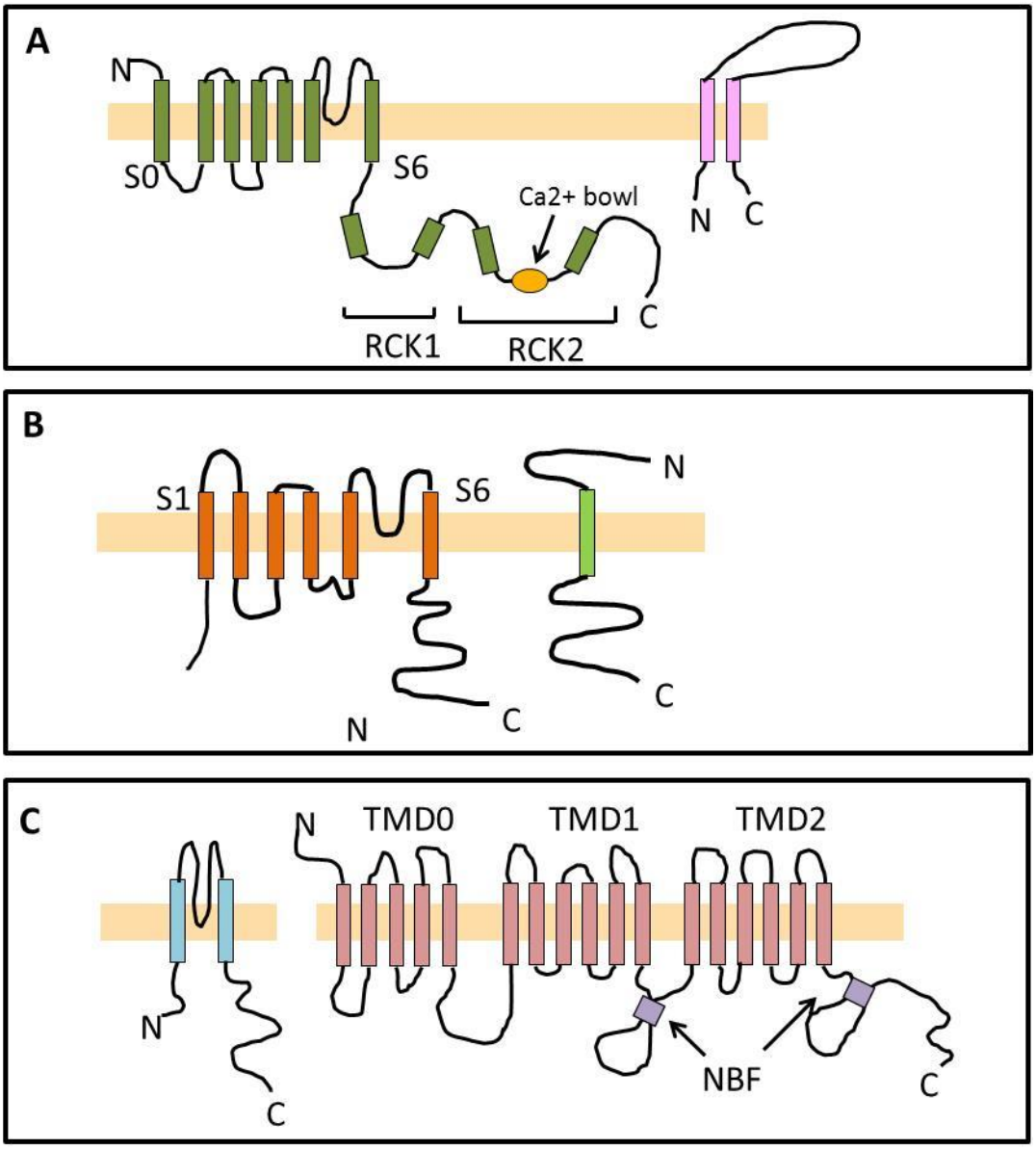

Figure 1.05 A. Transmembrane topology of large conductance Ca^{2+}-activated K^+ (BK_{Ca}) channel pore forming α subunit and regulatory β subunit. The BK_{Ca} channel α subunit possesses seven transmembrane domains (S0-S6). The C-terminus of the α subunit contains regulatory domains regulator for conductance for K^+ 1 and 2 (RCK1 and 2) as well as a 'Ca^{2+} bowl' to which Ca^{2+} can bind. The β subunit has two transmembrane domains. **B.** Topology of the delayed rectifier K_V7 pore-forming α subunit which consists of six transmembrane domains and the regulatory ancillary subunit with a single transmembrane domain. **C.** Topology of K_{ATP} the pore-forming α subunit and the regulatory SUR subunit. The K_{ATP} α subunit has two transmembrane domains bridged by the pore-forming selectivity loop. The SUR is much bigger in structure, and consists of three transmembrane domains (TMD1-3). TMD0 is responsible for interacting with the $K_{ir}6$ subunits for proper assembly and surface expression of the K_{ATP} channel. The interaction of MgADP with the nucleotide binding folding (NBF) domains is vital for activation of the K_{ATP} channel.

K_{ATP} channels are expressed at low density on both vascular myocytes and endothelial cells (Dart & Standen 1993; Janigro et al. 1993) when compared with cardiac myocytes (Nichols & Lederer 1990). In vascular myocytes, the K_{ATP} current is both time- and voltage-independent and is inhibited by sulphonylurea compounds such as glibenclamide. The molecular composition of K_{ATP} channels in pancreatic β-cells and cardiac cells is accepted to be SUR1/Kir6.2 and SUR2A/Kir6.2, respectively (Teramoto, 2006). In contrast, the molecular entities responsible for K_{ATP} current conduction in the vasculature is less clear. The predominant K_{ATP} channel conductance in native vascular myocyte is relatively small (20-50 pS) and is activated by nucleotide diphosphates in the presence of magnesium (Beech et al. 1993; also reviewed by Flagg et al. 2010). The molecule entities that have similar characteristics with the native K_{ATP} channels are Kir6.1/SUR2B and hence been proposed to be the predominant K_{ATP} channel in the vascular myocytes (see review Flagg et al. 2010). However, in some vessels, such as the rat portal vein, two different K_{ATP} channels were described (Zhang & Bolton 1996). Zhang and Bolton observed that apart from the K_{ATP} channels with a lower conductance and activated by nucleotide diphosphate, the vein myocytes also express other K_{ATP} channels with a larger conductance (50 pS) and were inhibited by ATP (similar with cardiac K_{ATP} channels; Zhang & Bolton 1996). Thus, it seems likely that more than one type of K_{ATP} channels exist in the vasculature.

1.7 AMP-activated protein kinase

AMP-activated protein kinase (AMPK) is a key protein for regulation of intracellular homeostasis. It is activated by an increase in the AMP/ATP ratio caused by exercise or metabolic stress; thus, AMPK can serve as a metabolic switch to coordinate metabolism and synthesis of ATP to cellular demands. Functional AMPK is a heterotrimeric complex consisting of three subunits: α; β and γ. The α-subunit contains a serine/threonine catalytic site. Two different α-subunit isoforms exist (α1 and α2) and they are not evenly distributed in the vasculature. Current evidence shows that α_1 is the dominant isoform expressed within the endothelium layer (Davis et al. 2006); and both α1 and α2 isoforms are present in the vascular smooth muscle cell layer, although their relative proportions may differ depending on the different arteries (Rubin et al. 2005). There are two isoforms of β subunits (β1 and β2). The β-subunit contains a central conserved domain to which glycogen can bind and inactivate AMPK (McBride et al. 2009). This enables AMPK also

to monitor the status of energy availability in the form of glycogen. The γ-subunits contains tandem regions that bind AMP or ATP in a competitive manner. Binding of AMP promotes phosphorylation at position Thr-172 on the activation loop of the α-subunit by an upstream kinase of AMPK, whereas binding of ATP allosterically antagonizes phosphorylation. High concentrations of AMP can also inhibit dephosphorylation of AMPK (Davies et al. 1995). There are now three recognized upstream kinases that are known to phosphorylate AMPK – liver kinase B1 (LKB1; Woods et al. 2003), Ca^{2+}/calmodulin dependent protein kinase kinase β (CaMKKβ; Hurley et al. 2005) and transforming growth factor-β (TGF-β)-activated protein kinase 1 (TAK1; Xie et al. 2006). LKB1 is constitutively active in vascular myocytes, but requires prior binding of AMP to the γ-subunits (Hawley et al. 2003). CaMKKβ is activated by an increase in intracellular Ca^{2+} and can phosphorylate AMPK independent of AMP (Hawley et al. 2005). Thus, AMPK activity can be regulated both by the ratio of adenine nucleotides and by Ca^{2+} levels. TAK1 has been shown to activate mammalian AMPK in cell-free assays (Momcilovic et al. 2006). However, its physiological functions in the AMPK pathways remain unclear. AMPK activation is reversed by dephosphorylation of the α-subunit by protein phosphatase 2A and 2C (PP2A and PP2C; Davies et al. 1995).

AMPK activity is essential for regulation of metabolic processes. Activated AMPK can phosphorylate and inhibit several metabolic proteins such as acetyl-coenzyme A (CoA) carboxylase (ACC), 3-hydroxy-3-methylglutaryl (HMG)-CoA reductase to prevent ATP-consuming processes and, in adipose tissue, hormone sensitive lipase and adipocyte triglyceride lipase. ACC is the rate-limiting enzyme in the process of fatty acid synthesis. There are currently two subtypes of ACC (ACC1 and ACC2) with unique expression profiles. ACC1 is found in lipogenic tissues, such as liver and adipose tissue whereas ACC2 is more commonly associated with skeletal muscle, heart and liver (Ha et al. 1996; Abu-Elheiga et al. 1997). ACC catalyzes the carboxylation of acetyl CoA to malonyl-CoA, which (in lipogenic cells) is the source of fatty acid synthesis. Thus, AMPK activation results in an increase in lipolysis (due to phosphorylation and inhibition of ACC) and was mimicked by an ACC knockout mouse model (Oh et al. 2005). HMG-CoA reductase, a rate limiting enzyme for synthesis of cholesterol, is also inhibited by AMPK, resulting in a reduction of cholesterol levels (Henin et al. 1995). Other inhibited enzymes include HSL (hormone-sensitive lipase; see Section 1.1.3.1) and glucose synthase (for glycogen synthesis).

AMPK can also activate proteins to increase biosynthesis of ATP. For example, glucose transporter 4 on the skeletal muscle can be activated by AMPK to increase uptake of glucose (Kurth-Kraczek et al. 1999). Other catabolic pathways, such as lipid oxidation and glycolysis can be activated by AMPK (as reviewed by Hardie et al. 2012).

1.7.1 Pharmacology of AMPK

The effect of AMPK activation is generally to switch on energy conservation pathways and to switch off high energy consuming processes. AMPK is activated in several physiological and pathological conditions including hypoxia and exercise (see a review by Wang et al. 2012). There are several groups of pharmacological agents known to work on AMPK and a few have clinical uses. One of the oldest and the most used AMPK activators is 5-aminoimidazole-4-carboxamide ribonucleoside (AICAR; Corton et al. 1995). AICAR is an adenosine analogue and therefore can be taken up into cells by binding onto the adenosine receptors. It is then converted to the active analogue ZMP (monophosphate AICAR) by adenosine kinase. ZMP has a very similar mechanism of action to AMP, in that it can interact with the γ-subunit and can promote phosphorylation of the α-subunits which stabilizes this active state of AMPK. Metformin (and its analogues) is a member of a group of anti-type 2 diabetic drugs collective known as biguanides. Both AICAR and metformin, have other cell metabolism effects not related to AMPK activation. A-769,662 was discovered in 2006 by compound library screening followed by lead optimization (Cool et al. 2006). A-769,662 has a very poor oral availability, which limits its potential as clinical medication. However, its selectivity and potency makes it a useful tool in AMPK research.

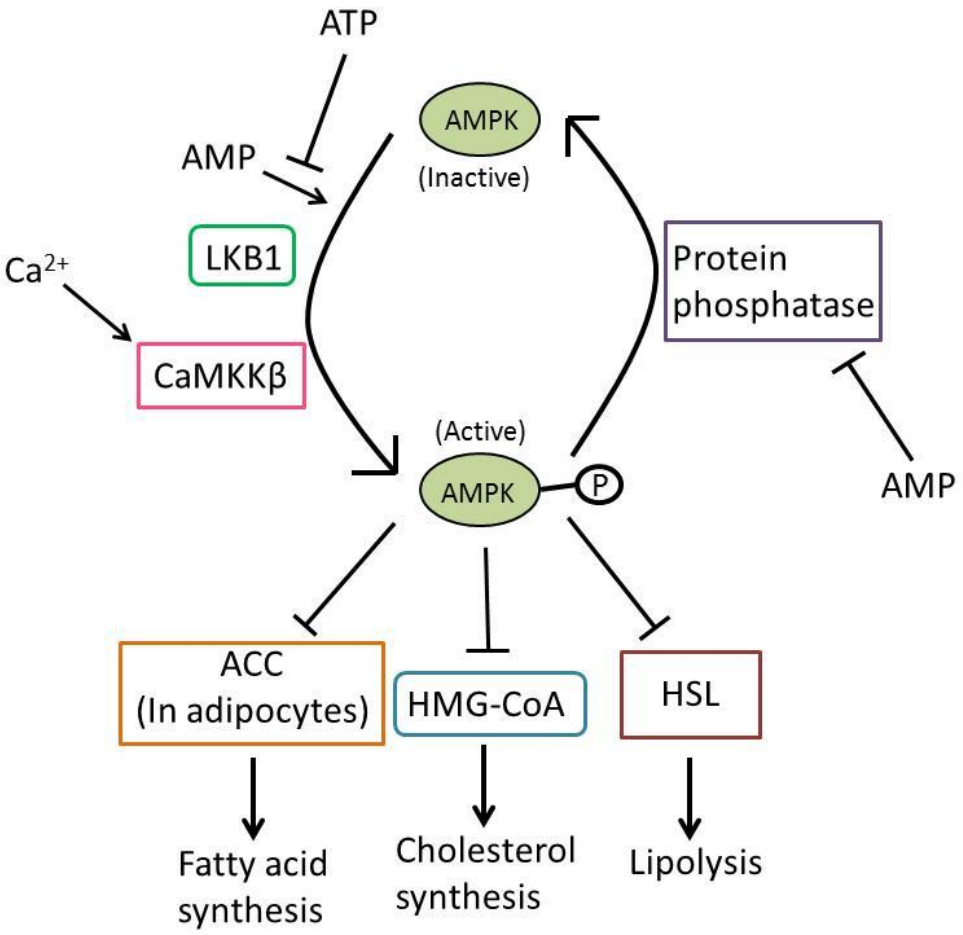

Figure 1.06. The mechanism of AMP-dependent protein kinase (AMPK) activation and a few of the downstream target proteins inhibited by AMPK. An increase in AMP concentration can bind to AMPK which promotes phosphorylation and activation of AMPK by LKB1 (liver kinase B1) which is active at basal conditions. Alternatively, AMPK can also be activated by CaMKKβ (Ca^{2+}/calmodulin dependent protein kinase kinase β) which is stimulated by an increase in intracellular Ca^{2+} concentration. ATP prevents the activation of AMPK by acting as an allosteric antagonist to AMP. The AMPK activation is reversed by protein phosphatase which is inhibited by AMP. Activated AMPK can phosphorylate and inhibit numerous downstream proteins, including ACC (acetyl-coenzyme A carboxylase), HMG-CoA (3-hydroxy-3-methylglutaryl coenzyme A reductase) and HSL (hormone-sensitive lipase). ACC, HMG-CoA and HSL are important enzymes for fatty acid synthesis, cholesterol and lipolysis, respectively. Thus, AMPK activation inhibits these processes.

AMPK is inhibited by several biological molecules such as glucose and glycogen, but currently there is only one commercially-available, pharmacological inhibitor – dorsomorphin (also known as compound C). Discovery of dorsomorphin was very similar to A-769,662 by high-throughput *in vitro* assay (Zhou et al. 2001). Unlike A-769,662, dorsomorphin is very unselective and has a range of different targets other than AMPK. Bain et al. (2007) has shown dorsomorphin to inhibit a range of kinases with a potency similar to or even greater than that to AMPK.

1.8 Obesity and PVAT functions

Obesity is the build-up of fat inside the body to an extent that could lead to health risks to the individual (World Health Organisation, 2013). Patients are diagnosed as obese based on their body mass index (BMI; higher than 30 kg/m^2) and, in relation to normal individuals, have a higher waist-to-hip ratio. In 2008, it was estimated that 35% of the world adult population was overweight, while 11% were classified as clinically obese (World Health Organisation, 2013). Obesity is a huge threat to the health of the patient as it is closely associated with hypertension, diabetes, cardiovascular diseases and atherosclerosis; the exact link remains un-identified.

In obese patients, the anticontractile effect of PVAT is lost (Greenstein et al. 2009). In addition, the total mass of PVAT with adipocyte hypertrophy are often observed in these patients (Greenstein et al. 2009). Similar adipocyte hypertrophy was also observed in obese mice (Marchesi et al. 2009) and rats (Ma et al. 2010). Since an increased blood supply is not associated with the increase in PVAT mass (Coppack et al. 1992), local hypoxia may occur within the adipose tissue leading to inflammation and impaired release of adipokines from the adipocytes. *In vitro*, inflammatory cytokines (tumour necrosis factor-α and interleukin-6) seem able to attenuate the anticontractile effects of adipocytes in healthy arteries, thus mimicking the phenotypes of obesity (Greenstein et al. 2009). The group (Greenstein et al. 2009) further showed that the cytokine effects could be reversed by enzymes that scavenge free radicals, suggesting that oxidative stress, at least in part, participate in inflammation and disrupt normal adipocyte function. Thus, it seems that inflammation as a result of obesity could lead to a loss of adipocyte functions which may result in reduced anticontractile factors (e.g. NO and adiponectin) and increased contractile factors (e.g. ROS and leptin) to be released. This is observed in obese mice, where obesity induced PVAT secretion of ROS whereas adiponectin levels were reduced (Marchesi et al.

2009). Thus, it seems that obesity is likely to be linked to a dysfunction of adipocytes, resulting in a loss of protective roles of PVAT within the cardiovascular system.

1.9 Project aims

Adipose tissue plays an important part in vascular pressure control. While healthy PVAT has an anticontractile effect on the underlying vasculature, this effect is lost in obesity. The anticontractile mechanism of PVAT is still far from clear, although it is generally proposed that PVAT can release a variety of anticontractile factors including nitric oxide and ADRF (a factor with an unknown identity). For this thesis, the main area of interest is therefore to investigate the mechanism responsible for the anticontractile effects of PVAT from two different aspects. The first aspect is to determine the functions of PKG in the anticontractile effect of PVAT. To achieve this aim, wire myograph experiments will be carried out with rat mesenteric arteries to determine if sildenafil (an indirect activator of PKG) could potentiate the anticontractile effects of PVAT. The release of NO from rat mesenteric PVAT would also be assessed using a chemical analysis test (Griess reagents) and whether pharmacological agents, such as sildenafil and β3 adrenoceptor activator CL-316,243, would enhance it.

ADRF is an unknown anticontractile factor released by PVAT with an unknown mechanism of action. Several recent studies have suggested that this factor causes vasodilation by activating the BK_{Ca} channels expressed by the vascular myocytes, possibly via AMPK activation. Therefore, the second aspect is this project aims to determine if activation of AMPK can lead to activation of BK_{Ca} channels.

Additionally, adiponectin is a known AMPK activation via activation of AdipoR1 receptors. There are speculations that the unknown ADRF is in fact adiponectin. The third aim is to find out whether adiponectin can mimic the effect of ADRF and increase BK_{Ca} currents; if so, whether AMPK is involved. Both the second and the third aim will be achieved by patch clamp electrophysiology using freshly isolated vascular myocytes as well as wire myograph with whole vessels.

Chapter 2

Methodology

2.1 Animals

Male Wistar Han (200-300 g; Harlan, UK) and Sprague-Dawley (200-300 g; Charles River, UK) rats were housed in a 12-hour light-dark cycle with food and water available ad libitum. Rats were killed either by carbon dioxide asphyxiation or stunning, followed by cervical dislocation. C57BL/6J control mice (Harlan, UK) and adiponectin-deficient ($Adipo^{-/-}$) mice (B6.129-$Adipoq^{tm1Cham}$/J; Jackson Laboratory Repository, USA) were killed by cervical dislocation. Both rats and mice were killed in compliance with Schedule 1 of the Animals (Scientific Procedures) Act 1986. The mesenteric bed (rats and mice) or aorta (rats) were removed and placed immediately in ice-cold physiological saline solution (PSS). Tissues were kept in PSS at 4 ºC until required and were used within 6 hours of isolation.

2.2 Tissue histology staining

2.2.1 Tissue embedding

The rat mesenteric bed was pinned out on a sylgard base of a petri dish and approximately 1 cm long segments of arteries and vein together with the surround PVAT were dissected free and placed in periodate-lysine-paraformaldehyde (PLP) fixative. After 30 min of fixation at room temperature, the tissue segments were briefly washed with phosphate buffered saline (PBS; prepared fresh from PBS tablets from Sigma-Aldrich, UK) for 5 min. PBS was then replaced with 30 % sucrose solution (weight/volume) in which the tissues were kept at 4 °C overnight. On the following day, tissue segments were placed in an aluminium-foil boat containing optimum cutting temperature fluid (OCT®; Raymond A Lamb, UK), which was frozen by immersion in isopentane (cooled with dry ice). This tissue-containing OCT® block was sliced transversely as 50 μm sections using a Leica CM3050S cryostat (Leica Microsystems, UK) and the sections transferred onto SuperFrost® Plus slides (Menzel-Glaser, Thermo Scientific, UK). The slides were stored at -80 °C and were used within one week.

2.2.2 Puchtler's Picro-Sirius Red staining

Slides with tissue sections were retrieved from -80 °C and allowed to thaw at room temperature before fixing for 30 min with 10 % formalin solution (ready prepared by Sigma-Aldrich, UK). Any excess fixative was removed by washing the slides in excess PBS for 10 min three times. Picro-Sirius Red solution was then applied and the tissue

sections stained for 30 min at room temperature. Following staining, 0.5 % acetic acid water was used to wash the tissue section twice for 2 min each. The tissue slices were then dehydrated with various ethanol solutions as follows: 1 min in 70 % ethanol; 1 min in 90 % ethanol; followed by 2 min in absolute ethanol. The tissue slices were then bathed in a clearing solvent (HistoChoice®; Sigma-Aldrich, UK) twice for 5 min each time. The stained tissue slices were visualised using a Zeiss LSM 5 PASCAL microscope (Carl Zeiss, UK).

2.3 Multi-wire myography

The wire myograph is a device for *in vitro* investigation of the dynamic mechanical response of arterial resistance vessels and was first introduced by Mulvany & Halpern in 1976. Blood vessels of different arteries (i.e. mesenteric, pulmonary and aorta) and from a variety of species (from mouse to human) can be studied with this technique. In this project, three different vessels types (rat mesenteric arteries, rat aortas and mouse mesenteric arteries) were isolated and their contractility was studies with wire myograph 610M with four 8 ml chambers (Danish Myo Technology A/S, Denmark).

2.3.1 Rat and mouse mesenteric artery

Experiments were performed on second order rat mesenteric arteries or first order mouse mesenteric arteries. Depending on the experimental requirements, PVAT was either left intact or carefully removed using dissection scissors. To minimized vessel variability, PVAT-intact and PVAT-free vessels were two branches of the same vessel. Vessel segments of approximately 1-2 mm in length were cut out and mounted on two 40-µm wires, which were each then attached to separate jaws of a wire myograph in a chamber containing 6 ml of Krebs solution (continually gassed with 95 % air/5 % CO_2) at 37 ºC (Figure 2.01). Within each myograph chamber, one jaw is fixed and the other is attached to a transducer to detect changes in tension, enabling vessel tone to be determined and recorded by a computer.

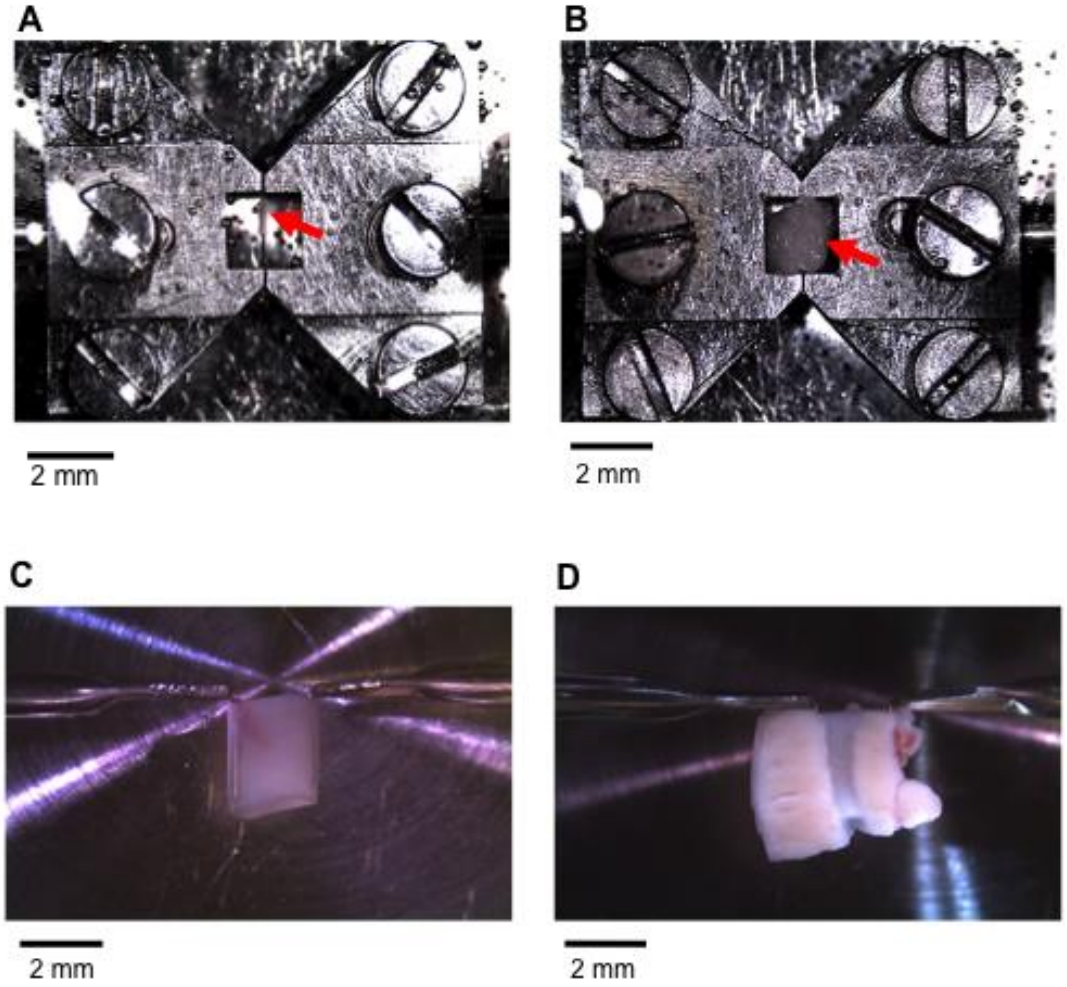

Figure 2.01. Rat mesenteric arteries without (A) and with (B) surrounding fat mounted onto the jaws of the wire myograph using two wires of 40 µm in diameter. The red arrows point to the mounted blood vessels. **Rat aorta without (C) and with (D) surrounding fat mounted onto the two pins of the wire myograph.**

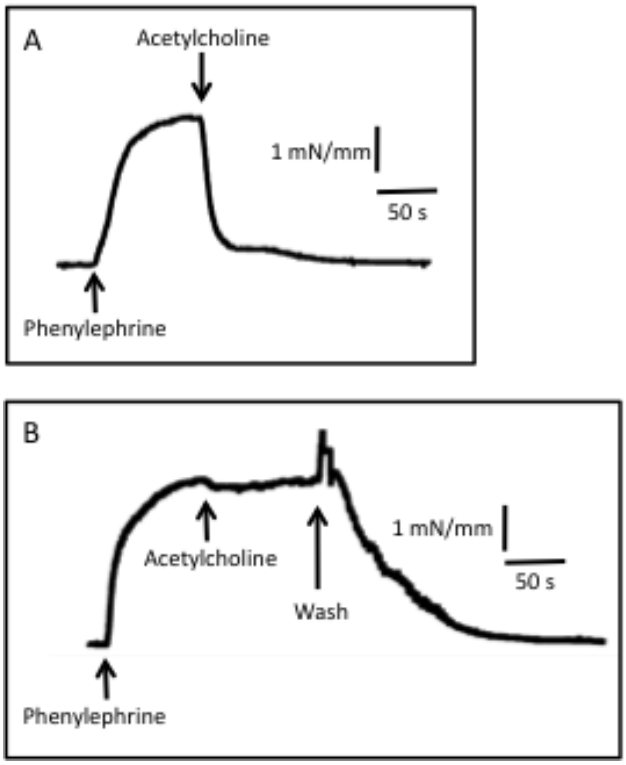

Figure 2.02. Myograph traces illustrating the rat PVAT-denuded mesenteric artery contraction responses to 10 µM phenylephrine followed by relaxation caused by 10 µM acetylcholine. A. Addition of acetylcholine caused a large vasorelaxation response (reduced the contraction by approximately 80 %). Hence, this vessel was classified as with endothelium. **B.** Acetylcholine produced a relaxation less than 10 % of the original contraction. Thus, this vessel was classified as endothelium-denuded.

After successfully mounting the vessels onto the myograph jaws, (where necessary) the endothelium was removed by gently rubbing the vessel lumen with a piece of human hair. No attempts were made to remove endothelium from mouse mesenteric arteries. The mounted vessel segments were then incubated in Krebs solution for 30 min to stabilize, then blood vessel wall tension was normalized using the standardized method (Mulvany & Halpern 1977).

2.3.1.1 Vessel wall tension normalisation

The rat mesenteric arteries normally have an *in vivo* transmural pressure of 100 mmHg (equivalent to a wall tension of 13.3 kPa). However, artery drug sensitivity and active force are both at the maximum when the vessel internal circumference is 90 % of that *in vivo*. Thus, the normalization process aims to standardize the tension of the mounted vessels by stretching the vessel internal circumference to that of 90 % the circumference at 100 mmHg. This was done by using the Normalization Module on the Chart software (version 5; ADInstruments, UK).

The first step was to determine the length of the vessel segments (in mm) by using an eyepiece reticule. The distance between the two jaws was increased in a stepwise manner by increasing micrometer readings on that of the free jaw. This produced force which was detected by the force transducer and was converted to tension by: Tension = Force / (Vessel length $\times$ 2). An internal circumference was calculated by the Chart software according to the Laplace equation: Pressure = Tension / [Internal circumference / (2 $\times$ π)]. The stepwise increase in the distance between the two jaws was stopped when the pressure reached 13.3 kPa. A micrometer reading was then given which corresponded to the optimum internal circumference to which vessel was equilibrated to and the resulting equilibrated tension was expressed as mN/mm (tension/length of the vessel segment).

2.3.2 Rat aorta

Since the rat aorta has a large lumen, the vessel rings (with the length of approximately 3 mm) were mounted in the myograph chamber on two pins rather than the two jaws (see Figure 2.01). Aorta segments were either dissected clean of surrounding PVAT or left with PVAT intact. Endothelium was removed by gently rubbing the vessel lumen with a piece of rolled notepaper. The tension on the aorta wall was increased to 1 g.

2.3.3 Experimental design

After the initial mounting, vessels (both aortas and mesenteric arteries) were left in 6 ml Krebs solution, maintained at 37 ºC and continually gassed with 95 % air/5 % CO_2, for 30 min to stabilize vessel wall tension. The vessels were then challenged with 60 mM KCl (by adding a highly concentrated KCl solution (4 M) to the Krebs solution) which was washed off by replacing myograph chambers twice with fresh Krebs solution. The tissues were then contracted by the addition of 10 μM phenylephrine followed by 10 μM acetylcholine to detect the presence of endothelium. The tissue was considered to have an endothelium when acetylcholine reduced the phenylephrine-induced contraction by at least 50 %; lack of endothelium was indicated by less than 10 % relaxation (see Figure 2.02). The vessels that did not meet the criteria for endothelium were excluded from further analysis. The myograph chambers were then washed three times at 5 min intervals with Krebs solution so that the tension returned back to the baseline level. Cumulative concentrations of relevant spasmogens were added to construct concentration-response curves (following pre-incubation with, and in the continued presence of modulators where appropriate). Time-matched control experiments were performed concurrently, following a similar protocol, but with the equivalent volumes of solvent added in place of the drugs. For each vessel segment, contraction responses to spasmogens were expressed as a percentage of the initial contraction to 60 mM KCl.

2.4 Nitric oxide assay

The release of nitric oxide was measured indirectly using the Griess Reagent System for nitrite determination (Promega Ltd, UK). The assay relies on the chemical reaction which utilizes NO_2^- and N-1-napthylethylenediamine dihydrochloride (NED) to convert sulfanilamide to an azo compound which can be quantified spectrophotometrically (Figure 2.03).

Figure 2.03. Chemical reactions involved in the nitrite detection Griess Reagent System. NED: N-1-napthylethylenediamine dihydrochloride.

There are two main metabolites of NO: nitrite (NO_2^-) and nitrate (NO_3^-). To avoid underestimating the amount of NO released, additional steps were taken to convert any NO_3^- within the samples to NO_2^- prior to addition of Griess Reagent. Nitrate reductase was used for this reaction with nicotinamide adenine dinucleotide phosphate (NADPH) as a co-factor (Reaction 1). High concentrations of NADPH and NADP- can interfere with formation of the azo compound. Thus, to minimize the concentration of NADPH required, glucose-6-phosphate dehydrogenase (G6P-D; which uses glucose-6-phosphate (G6P) as a substrate and forms 6-phosphoglucolactone (6-PG) as a by product) was used to recycle NADPH (Reaction 2; Verdon et al. 1995).

$$NO_3^- + NADPH + H^+ \Rightarrow NO_2^- + NADP^+ + H_2O \qquad \text{(Reaction 1)}$$

$$H_2O + NADP^+ + G6P \Rightarrow 6\text{-}GP + NADPH + H^+ \qquad \text{(Reaction 2)}$$

To determine the effect of drugs on NO release, white PVAT was dissected from rat mesenteric beds and incubated with PSS (2 µl/mg PVAT), containing the appropriate concentration of drug, for 30 min at 37 °C. The bath solution was then kept frozen at -20 °C until use.

Immediately before assay, samples were thawed and were added as duplicates into a 96-well plate (150 µl of sample per well). On the same plate, two different standards (NO_2^- and NO_3^-) were added at increasing concentrations, also in duplicates: (0, 1.56, 3.13, 6.25, 12.5, 25, 50 and 100 µM; 150 µl per well). To the wells containing NO_3^- and samples, 15 µl of G6P, 5 µl of nitrate reductase, 5 µl of G6P-D and 1 µl of NADPH were added per well; the final concentrations were 500 µM, 10 U/ml, 250 U/ml and 1.67 µM, respectively. Deionized H_2O (104 µl) was finally added per well to make the final volume of 280 µl. All drugs/enzymes, apart from nitrate reductase (Roche, UK), were purchased from Sigma-Aldrich Ltd, UK. To NO_2^--containing wells, 130 µl of deionized H_2O was added instead of the drugs/enzymes. The 96-well plate was then left for 3 h at room temperature in the dark for the reaction to take place. Following this incubation period, 10 µl of sulfanilamide (provide in the Griess Reagent kit; Promega, UK) was added to each of the wells and left for 15 min in the dark at room temperature. The same volume of NED was added followed by the same incubation time, before absorbance at 550 nm was measured with an EL 800 plate reader (BioTek Instruments, UK). The absorbance readings from the NO_2^-/NO_3^- standard wells were used to construct linear concentration-absorbance lines to determine NO_2^-/NO_3^- concentration in the samples (see Figure 2.04).

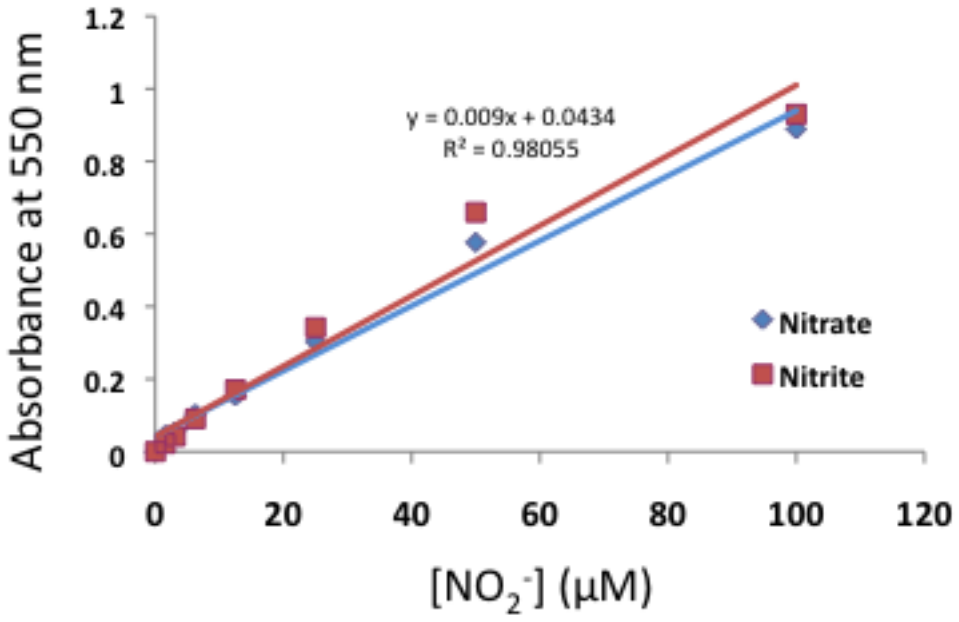

Figure 2.04. Concentration-absorbance lines for nitrite (NO_2^-) and nitrate after conversion to nitrite. The lines shown are lines of best fit and the equation was used to determine the nitrite/nitrate concentration depending on the measured absorbance. R^2 value represents line correlation.

2.5 Smooth muscle cell isolation

2.5.1 Aorta

A segment of aorta of approximately 1 cm in length was dissected from the rat (Sprague-Dawley) and placed immediately in ice-cold PSS. The aorta was cleaned of surrounding fat and connective tissue and transferred to taurine solution (see Solutions section below) containing Collagenase II (1200 U/ml; Worthington, USA). After 10 min incubation at 37 °C, the aorta was cut transversely into 2 mm rings and placed in taurine solution containing 8 U/ml of papain (Sigma-Aldrich, UK) for 1-2 h at 4 °C. Dithiothreitol (DTT at 6 mM; Sigma-Aldrich, UK) was then added to the papain/tissue mixture and further incubated for 4 min at 37 °C, after which tissue was immediately transferred to some fresh taurine solution containing collagenase II (1100 U/ml) and kept at 37 °C for 10 min. The digested vessel segments were washed in fresh taurine solution several times before gentle trituration with a wide-bore glass pipette to release single cells. Cells were maintained at room temperature and used within 5 h.

2.5.2 Mesenteric arteries

The steps of myocyte isolation from Sprague-Dawley rat mesenteric arteries were similar to those of aorta. Mesenteric arteries were carefully cleaned of surrounding PVAT under a dissection microscope and placed in some taurine solution containing Collagenase II (1500 U/ml; as above). The mixture was then incubated at 37 °C for 15 min, after which the arteries were transferred immediately to some taurine solution containing papain (8 U/ml; same as above) and left for 1 h at 4 °C. Following this incubation period, 6 mM of DTT was added to the papain mixture and the enzyme allowed to digest the artery segments for 20 min at 37 °C. The arteries were then washed in plenty of fresh taurine solution (at least twice with a total of approximately 10 ml) to remove any remaining enzyme before gentle trituration with a wide-bore pipette to release single cells. These cells were maintained at room temperature and were used within 6 h.

2.6 Electrophysiological methods

The patch clamp electrophysiology technique, developed in the 1970s by Edwin Neher and Bert Sakmann (Neher & Sakmann 1976), measures ionic currents under a voltage clamp. The system is sensitive enough to detect currents from a single channel, but is frequently used to measure currents across the entire experimental cell (whole-cell patch

clamp). The patch pipette electrode is used continuously for both voltage recording and for current passage. Thus, currents flow across the cell membrane (i.e. between the patch pipette and the bath electrode, a silver chloride wire placed in the bath solution to serve as ground electrode) stimulated by different voltage commands can be amplified by the patch clamp amplifier and recorded by a computer.

2.6.1 Whole-cell configuration

All electrophysiological experiments were carried out at room temperature (20-25 °C). Freshly isolated myocytes were added to the cell chamber and allowed to settle for a few minutes before superfusing the cells with fresh PSS (at a rate of 2 ml/min). In a two-step procedure, patch pipettes were pulled from barosilicate glass (1.5 mm outside diameter; 1.17 mm internal diameter; Harvard Apparatus, UK). New pipettes were pulled on each day of experiments and had resistances ranging from 2.5 to 4.0 MΩ when filled with pipette solution. The micropipette was then manoeuvred onto the cell membrane. After the micropipette had made gentle contract with the cell membrane, negative pressure was applied to enable the formation of a high resistance seal (a gigaseal; > 1 gigaohm (GΩ)) between the pipette and the membrane. A sudden suction was then required to disrupt the membrane while leaving the high resistance seal intact. A large and rapid capacitative transient indicated that the patch of membrane within the micropipette was successfully ruptured. The pipette solution inside the micropipette mixes with the cytoplasm and over a short period, will replace the cytoplasm. The whole-cell configuration is now achieved.

After the whole-cell configuration was achieved, the cells were given three minutes to allow full mixing between pipette solution and cell cytoplasm. Two different voltage protocols were then applied to the subject cells. The first protocol held the cells at a potential of -10 mV for 200 ms from a holding potential of -60 mV; then stepped to various voltages (ranging from -40 to 50 mV) for 500 ms. The second protocol was very similar to the first, but the cells were maintained at the holding potential of -60 mV before stepping to different voltages which ranged from -90 to 50 mV. Under control conditions, PSS was perfused continually through a gravity-fed perfusion system. Where appropriate, drugs were perfused directly onto the cells. Whole-cell currents were amplified with an Axopatch 200B amplifier (Molecular Devices LLC, USA), filtered at 2 kHz (4-pole Bessel filter) and sampled at 10 kHz. Recordings were digitized with a Digidata 1322A and data

acquisition and storage were both done using Axon pClamp v9.12 (Molecular Devices, USA) in conjunction with a computer running on Windows XP (Microsoft, USA).

2.6.2 Perforated patch configuration

A disadvantage to the whole-cell configuration, formed by disrupting the patch of membrane within the tip of the microelectrode by suction, is the replacement of the cell cytoplasm by the pipette solution. This alters the physiological condition of the cell and when intracellular signalling is the subject of investigation, displacement of the cytoplasm is undesirable. Hence, a variant of the whole-cell recording, termed perforated-patch configuration, is more appropriate. Antibiotics, added to the intracellular pipette solution, can form small perforations on the cell membrane. The perforations have a distinct size and are permeable to smaller monovalent ions, but not larger molecules such as adenosine-5'-triphosphate (ATP), and multivalent ions. The perforated-patch configuration enables STOCs to be detected.

In order to perform perforated patch clamp, a different intracellular pipette solution (which contained amphotericin B; see Solutions section below) was used to fill the micropipette. After the gigaseal was achieved, the cell/micropipette was left for 30 to 40 minutes to allow perforations to form. Successful access to the cell was observed as progressively faster capacitive transients. The cells were then held at -20 mV for the whole duration of the experiment. Under control conditions, cells were continually superfused with PSS using a gravity-fed system. Recordings were amplified, digitized and acquired as described above (Section 2.6.1).

2.7 Statistical Analysis

Data were illustrated as mean ± SEM (standard error of the mean). When comparing data from two different groups, non-parametric paired (Wilcoxon matched-paired signed rank tests) or unpaired (Mann-Whitney U) tests were performed. When comparing three or more data groups, two-way ANOVA (analysis of variance) tests followed by Bonferroni post-hoc tests were used. When the mentioned tests failed to reveal a significance difference, repeated t-tests (to compare for two groups of data) or two-way ANOVA tests (to compare for three or more groups of data) were then performed to compare for differences at each data point. Repeated t-test comparisons were corrected by Holm-Sidak tests. Repeated-measures two-way ANOVA tests were followed by Bonferroni post-hoc tests. For NO assay data, one-way ANOVA Kruskal-Wallis tests, followed by Dunn's

multiple comparison post hoc tests were performed. Differences were considered significant when $p < 0.05$.For analysis of STOCs, events were counted when the spike magnitude exceeded 15 pA. Wilcoxon matched-paired signed rank tests were performed to compare for changes in STOCs.

To calculate pEC_{50} values of the dose response curves, non-linear regression lines were fitted based on the equation: Y = Bottom + (Top - Bottom)/(1 + 10^((LogEC_{50} - X))). All data analysis (apart from repeated t-tests) and graphs were performed and generated using Prism 5 (GraphPad Software, USA); repeated t-test comparisons were performed using Prism 6 (GraphPad Software, USA).

2.8 Drugs

Unless otherwise stated, all drugs were obtained from Sigma-Aldrich (UK) and were dissolved in deionized H_2O.

- **Acetylcholine hydrochloride:** stock solution 10 mM; kept at 4 °C for up to 4 weeks.
- **Adiponectin** (BioVendor, Czech Republic): stock solution 500 µg/ml; aliquoted and stored at -20 °C for up to 4 weeks.
- **AICAR** (*N*1-(β-D-Ribofuranosyl)-5-aminoimidazole-4-carboxamide; Tocris Bioscience, UK): stock concentration of 50 mM; freshly prepared.
- **A-769,662** (4-hydroxy-3-(2'-hydroxybiphenyl-4-yl)-6-oxo-6,7-dihydrothieno[2,3-b]pyridine -5-carbonitrile; Tocris Bioscience, UK): stock concentration of 10 mM; stored at 4 °C.
- **Cirazoline hydrochloride** (Tocris Bioscience, UK): stock concentration of 10 mM; diluted to different concentrations (1 mM, 100 µM, 10 µM, 1 µM); all stored at 4 °C.
- **CL-316,243** (5-[(2R)-2-[[(2R)-2-(3-chlorophenyl)-2-hydroxyethyl]amino]-propyl]-1,3-benzodioxole-2,2-dicarboxylic acid disodium salt; Tocris Bioscience, UK): stock concentration of 10 mM; stored at 4 °C for up to 2 months.
- **Catalase**: stock concentration of 40,000 units/ml; aliquoted and stored at -20 °C.
- **Dorsomorphin dihydrochloride** (Tocris Bioscience, UK): stock concentration of 2 mM; freshly prepared.

- **Glibenclamide** (Tocris Bioscience, UK): stock concentration of 10 mM in DMSO; freshly prepared.
- **Iberiotoxin** (Tocris Bioscience, UK): stock concentration of 100 μM; aliquoted and stored at -20 °C.
- **L-NMMA** (NG-monomethyl-L-arginine; Tocris Bioscience, UK): stock concentration of 100 mM; freshly prepared.
- **Norepinephrine (or noradrenaline)**: stock concentration of 10 mM; kept at 4 °C for up to 4 weeks.
- **NS1619**: stock concentration of 20 mM in DMSO; stored at 4 °C.
- **Phenylephrine hydrochloride**: stock concentration of 10 mM; stored at 4 °C for up to 4 weeks.
- **PT1** (Tocris Bioscience, UK): stock concentration of 20 mM; aliquoted and stored at -20 °C.
- **Serotonin (5-HT) hydrochloride**: stock concentration of 100 mM; diluted to 10 mM, 1mM, 100 μM and 10 μM; all freshly prepared.
- **Sildenafi**l: stock concentration of 10 μM in DMSO; aliquoted and stored at -20 °C.
- **XE991 dihydrochloride** (Tocris Bioscience, UK): stock concentration of 30 mM; freshly prepared.

2.9 Solutions

All solutions were prepared fresh (unless otherwise stated) and at room temperature. All compounds used for making solutions were obtained from Thermo Fisher Scientific UK, unless otherwise stated.

- **Krebs solution** (in mM): NaCl 118; KCl 3.4; $MgSO_4$ 1.2; $CaCl_2$ 1; KH_2PO_4 1.2; $NaHCO_3$ 25; glucose 11.1.
- **Perforated-patch pipette solution** (solution pH adjusted to 7.2 with KOH and filtered through 0.22 μm filters twice before aliquoted and stored at -20 ºC), in mM: KCl 110; NaCl 10; HEPES 10; EGTA 10; $CaCl_2$ 0.5 and amphotericin B (Sigma-Aldrich, UK) 100 mg/ml.
- **Picro-Sirius Red solution**: Direct Red 80 (Sigma-Aldrich, UK) 0.73 mM in aqueous picric acid.
- **PLP fixative**, prepared the day before and store at 4 ºC:

  - Solution 1: 3.7 g Lysine-HCl (Sigma-Aldrich, UK) in 100 ml H_2O
  - Solution 2: 3.58 g $Na_2HPO_4 \cdot 2H_2O$ (BDH, UK) in 100 ml H_2O
  - Solution 3: 1.56 g $NaH_2PO_4 \cdot 2H_2O$ (BDH, UK) in 100 ml H_2O and pH adjusted to 7.4 with NaOH
  - Solution 4: 2 g paraformaldehyde (BDH, UK) in 50 ml H2O
  - Solution 5: solution 1 but with pH adjusted to 7.4 with solution 2
  - Solution 6: solution 5 mixed with solution 3 in a 1:1 ratio
  - Solution 7: solution 6 mixed with solution 4 in a 3:1 ratio
  - Sodium-m-periodate (Sigma-Aldrich, UK) was added to solution 7 at 50 mM to give PLP fixative.
- **PSS** (prepared from a ten-times concentrated solution and added glucose, Ca^{2+} and adjusted pH on the day of use), in mM: NaCl 122; KCl 5; HEPES 10; KH_2PO_4 0.5; NaH_2PO_4 0.5; $MgCl_2$ (BDH, UK) 1; glucose 11; $CaCl_2$ (Sigma-Aldrich, UK) 1. pH adjusted to 7.3 using NaOH.
- **PSS with altered Ca^{2+} levels:** same as above, but with $CaCl_2$ of 0.5, 1.6 or 2.0 mM.
- **Taurine solution**, in mM: NaCl 115; KCl 4; HEPES 10; NaH_2PO_4 1.2; $MgSO_4$ 1.2; taurine (Sigma-Aldrich, UK) 50; glucose 11.1; $CaCl_2$ 0.1. pH adjusted to 7.34 with NaOH.
- **Whole-cell pipette solution** (solution prepared, pH adjusted to 7.2 with KOH and filtered through 0.22 μm filters twice before aliquot and stored at -20 ºC), in mM: KCl 110; NaCl 10; $MgCl_2$ 5; HEPES 10; EGTA 10; $CaCl_2$ 5. This solution contained 200 nM free [Ca^{2+}] (calculated using the Maxchelator, Stanford University USA).
- **Whole-cell low Ca^{2+} pipette solution** (prepared in the same way as above), in mM: KCl 110; NaCl 10; $MgCl_2$ 5; HEPES 10; EGTA 10; MgATP 5; $CaCl_2$ 0.5. This solution contained 8 nM free [Ca^{2+}] (calculated using the Maxchelator, Stanford University USA).

Chapter 3

Sildenafil and perivascular adipose tissue anticontractile mechanism

3.1 Introduction

Perivascular adipose tissue (PVAT), the adipose tissue that surrounds most of the arteries, is now recognized as one of the major contributors to vascular tone control. PVAT can act as an endocrine organ to release adipokines and various other vasoactive factors which affect the underlying smooth muscle cells to regulate vessel contractility. The anticontractile effect of PVAT was first demonstrated by Soltis and Cassis (1991) with rat aorta, but can also be observed in other vascular beds (Gao et al. 2005; Greenstein et al. 2009). There are two different type of PVAT: brown and white PVAT. While both have anticontractile effects (Löhn et al. 2002; Greenstein et al. 2009), the mechanisms are unclear for either of them. In all subsequent sections of this chapter (and in chapters 4 and 5), the anticontractile mechanism of white PVAT will be at the centre of attention.

Adipocytes express eNOS (Giordano et al. 2002) although there is some dispute about how they increase NO bioavailability. Canová and colleagues (2006) found that, similar to endothelial cells, primary cultures of rat adipocytes isolated from epididymal adipose tissue can directly release NO. In contrast, Gao et al. (2007) suggested that aortic PVAT does not release NO *per se*, but stimulates the endothelium to increase endothelium-derived NO. Greenstein et al. (2009) later showed that the anticontractile effect of human (subcutaneous artery) PVAT was reversed by a NO synthase inhibitor, suggesting the involvement of NO in the anticontractile effect of PVAT in man, although the source of this NO was not identified. Apart from NO, adipocytes can also reduce artery contractility via a different, transferable adipocyte-derived relaxing factor (ADRF; Löhn et al. 2002). Despite the growing amount of research on identifying this ADHF, no agreement has yet been reached (ADRF will be described more in details in Chapter 4 and 5).

The intracellular pathways that are important for the normal functioning of adipocytes are far from clear. Preliminary data from our laboratory showed that PVAT isolated from PKG knockout mice had reduced anticontractile activity (Withers et al. 2011), which implied that PKG could be important for the anticontractile effects of adipocytes. In support of this, natriuretic peptides increased adiponectin release from cultured human adipocytes (Tsukamoto et al. 2009). Additionally, PKG activators promote adipogenesis (Zhang et al. 2010) and lipolysis (via the cGMP/PKG pathway) in isolated human adipocytes (Sengenès et al. 2000) and cultured rat adipocytes (Nishikimi et al. 2009). Thus, it seems that PKG may have important functions in the regulation of adipocyte differentiation and lipolysis and the release of anticontractile factors.

On the other hand, the cAMP/protein kinase A pathway may also be important. β3 adrenoceptors are expressed by adipocytes (Berkowitz et al. 1995; Collins et al. 2004) and stimulation of these receptors is positively coupled to adenylyl cyclase which converts ATP to cAMP. Accumulation of intracellular cAMP causes activation of protein kinase A (PKA) which then increases lipolysis and adipogenesis via activation of cAMP-responsive element binding protein (CREB) and lipase (Langin et al. 1992; Reusch et al. 2000). Furthermore, stimulation of these β3 adrenoceptor with a specific agonist CL-316,243 (Bloom et al. 1992) increased the anticontractile effects of PVAT (Egner 2012) and caused myocyte hyperpolarisation (but only in the presence of PVAT; Weston et al. 2013). Interestingly, the CL-316,243-induced hyperpolarization was blunted in the PKG1 knockout mouse (unpublished data), suggesting that the PKG pathway, at least partially, mediates the hyperpolarisation observed. Even though PKA and PKG pathways appear to be separate, cross-talk can occur between the two due to the high degree of sequence homology between the two kinases (Shabb et al. 1990). Therefore at high levels of cAMP, PKG can be activated and *vice versa* (Shabb et al. 1990).

Sildenafil (more commonly known as Viagra) is an agent used to prolong the effects of cGMP by selectively inhibiting PDE (phosphodiesterase) type 5 (PDE5). It was initially developed as an antihypertensive agent (Webb et al. 1999), but was later found to promote penile erection as a side effect which lead it to be remarketed in 1998 for the treatment of erectile dysfunction. Since then, sildenafil was demonstrated to have beneficial effects against other diseases such as pulmonary hypertension (Sastry et al. 2004) as well improving right heart failure (Chen et al. 2003). In the adipocytes, the predominant type of PDE is PDE type 3 subtype B (PDE3B; Taira et al. 1993), also known as the cGMP inhibited phosphodiesterase, which has affinity for both cAMP and cGMP; in adipocytes, PDE3B primarily controls the concentration of cAMP (see review Armani et al. 2011). More recently, functional roles of PDE5 in adipocytes (i.e. adipogenesis and lipolysis) have emerged (reviewed by Armani et al. 2011). Thus, this chapter aims to investigate the importance of PKG in the anticontractile mechanism of adipocytes by testing the differential effects of sildenafil in PVAT-intact and PVAT-denuded rat mesenteric arteries. Given the importance of PKG in adipocytes, by inhibiting PDE5 in adipocytes, sildenafil indirectly activates PKG and should theoretically enhance the anticontractile effects of PVAT. All of the tissues used in this chapter were taken from male Wistar rats.

3.2 Results

3.2.1 Morphology of the PVAT

Following staining of the PVAT with Puchtler's Picro-Sirius Red, connective tissue, myocytes and cell nuclei were clearly distinguished in transverse sections of mesenteric artery (Figure 3.01).

The adipocytes had elongated nuclei (as observed by the blue staining) with single large lipid stores typical of white adipose tissue adipocytes. They varied greatly in size, although most adipocytes had diameters less than 100 μm.

3.2.2 PVAT slows KCl-induced vessel contraction

For each vessel segment, its contractile response to the various spasmogens was expressed as a percentage of its contraction to 60 mM KCl. Initial experiments confirmed that PVAT did not affect vessel contraction to KCl. Figure 3.02 shows the KCl-induced vessel contraction in PVAT-denuded and PVAT-attached vessels.

The magnitudes of the KCl-induced vessel contractions were similar in the presence or absence of PVAT (Figure 3.02A). PVAT-free vessels contracted 2.9 ± 0.1 mN/mm (n = 54) versus 2.8 ± 0.2 mN/mm for vessels with intact PVAT (n = 54). The time for PVAT-free vessels to reach their KCl-induced contraction maximum (22 ± 3 s (n = 38) was significantly longer than for PVAT-intact vessels (105 ± 7 s (n = 38); Figure 3.02B) ($p < 0.0001$).

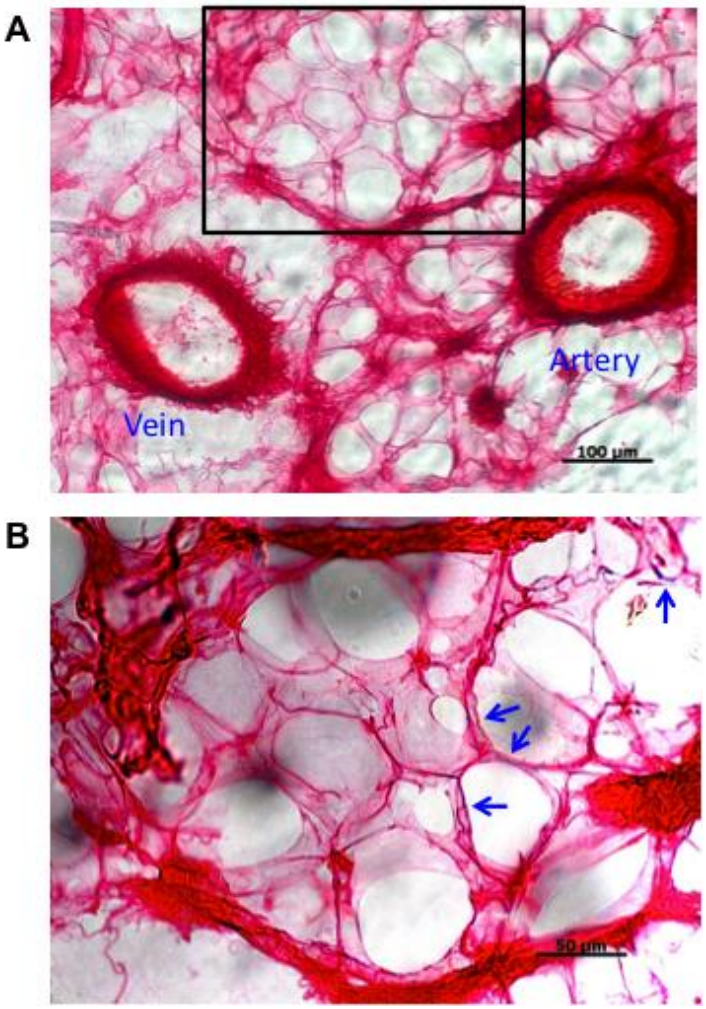

Figure 3.01. Puchtler's Picro-Sirius Red staining of rat mesenteric arteries and perivascular adipose tissue. The tissue was frozen, sliced at 50 µm and then stained. The connective tissue was stained red, smooth muscle yellow and cell nuclei blue. **A.** Images captured at ×20 magnification. An area of interest highlighted with a black box and re-imaged in **B.** at ×40 magnification. The blue arrows point to blue staining indicating the elongated nuclei of adipocytes.

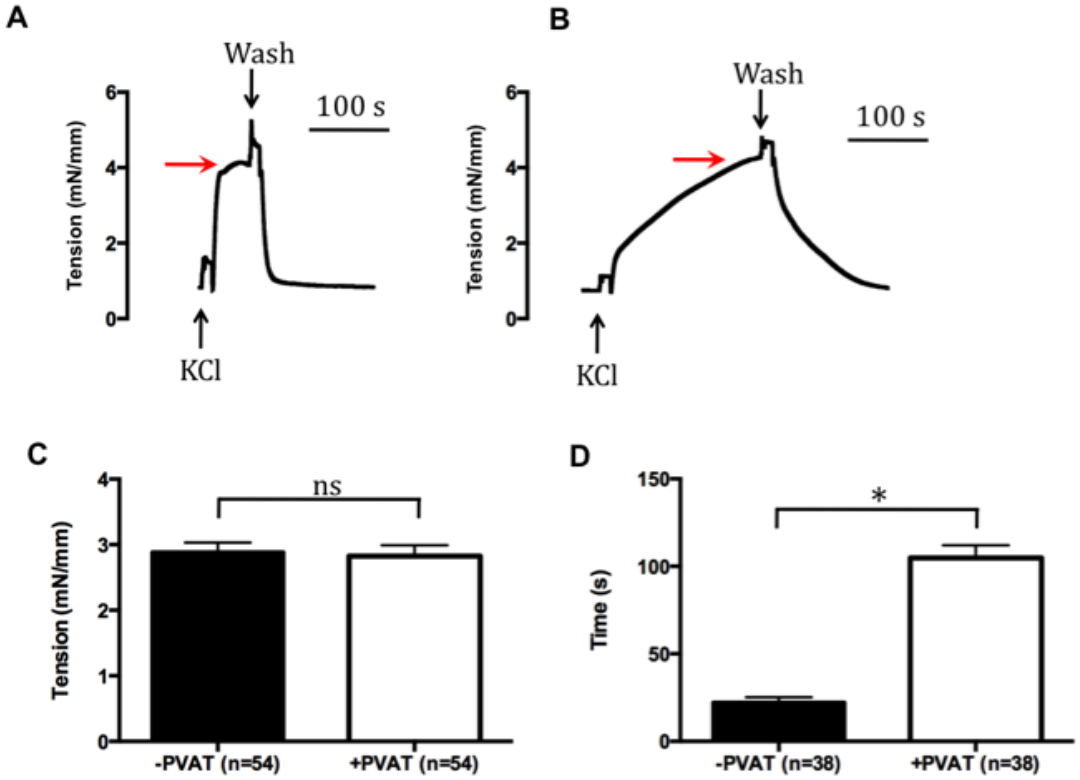

Figure 3.02. The effect of perivascular adipose tissue (PVAT) on KCl-induced rat mesenteric artery contractions. Vessels were first equilibrated in physiological saline solution (PSS) before addition of a concentrated KCl solution to increase the PSS K^+ concentration to 60 mM. When contractions reached plateau, the myograph chambers were drained and refilled with PSS. In the recorded traces of KCl-induced contraction in a PVAT-denuded vessel (**A**) and a PVAT-intact vessel (**B**), the red arrows represent the plateau levels. The inflections that occur at each of the point labelled 'wash' are artefacts due to draining and replacing solution in the baths. Tensions are represented as mN per mm of mounted blood vessel. **C.** Averaged magnitudes of KCl-induced contractions of PVAT-free (-PVAT) and PVAT-attached (+PVAT) vessels. **D**. Averaged time required for PVAT-free and PVAT-intact vessels to reach their contraction plateaus. * Significant different $p < 0.05$ using the non-parametric t-test. Ns: non-significance observed by the same test.

3.2.3 Changing extracellular Ca^{2+} concentration did not alter vessel contraction

The possible effects of altering extracellular Ca^{2+} concentration on the mesenteric artery contractile response to norepinephrine in the presence or absence of PVAT was investigated by using PSS with four different Ca^{2+} concentrations (0.5, 1.0, 1.6 and 2.0 mM; Figure 3.03). All of the vessels were de-endothelialised. The vessel incubated in PSS with the lowest Ca^{2+} concentration (0.5 mM) displayed the highest contractile responses to norepinephrine in both PVAT-free and PVAT-intact configurations. There were no significant differences in contractility when vessels were incubated in 1.0, 1.6 or 2.0 mM Ca^{2+} PSS (Figure 3.03B). Thus, in all subsequent sections, all experiments were performed in the presence of PSS with 1.0 mM Ca^{2+}.

3.2.4 The anticontractile effect of PVAT

To observe the PVAT anticontractile effects, norepinephrine was added sequentially to the vessel segments over a concentration range of 0.1 to 30 μM. The norepinephrine-induced contractions were analyzed and used to construct the concentration-response curves for the PVAT-free and PVAT-attached vessels (Figure 3.04).

The presence of PVAT shifted the concentrations-response curve significantly to the right ($p < 0.01$; Mann-Whitney U tests) and pEC_{50} values were reduced from 5.79 ± 0.04 to 5.21 ± 0.10 ($n = 3$-5). In PVAT-denuded vessels, 5.6 μM norepinephrine caused the maximum contraction (121 ± 7 % of KCl-induced contraction; $n = 5$); but a sub-maximal contraction when PVAT was intact (57 ± 14 %; $n = 3$). In the presence of PVAT, the maximum contraction occurred at 30 μM of norepinephrine (114 ± 8 %; $n = 3$).

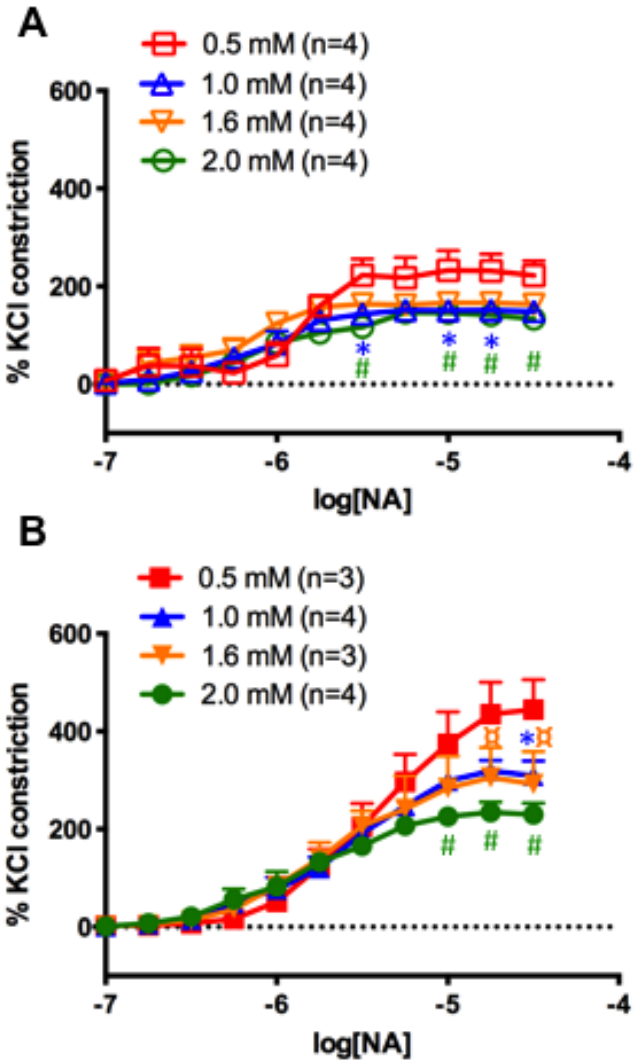

Figure 3.03. Norepinephrine (NA) concentration-response curves to show the effect of altering physiological saline solution Ca^{2+} concentrations on mesenteric artery contraction. A. Mesenteric artery without perivascular adipose tissue; **B.** arteries with PVAT. All vessels were without endothelium. Physiological saline solution with four different Ca^{2+} was used: 0.5; 1.0; 1.6; and 2.0 mM. Significant difference at the corresponding data points: between 0.5 M and 1.0 mM curves (*); between 5 mM and 1.6 mM curves (¤); between 0.5 mM and 2.0 mM curves (#) by repeated measures two-way ANOVA followed by Bonferroni post-hoc tests; $p < 0.05$.

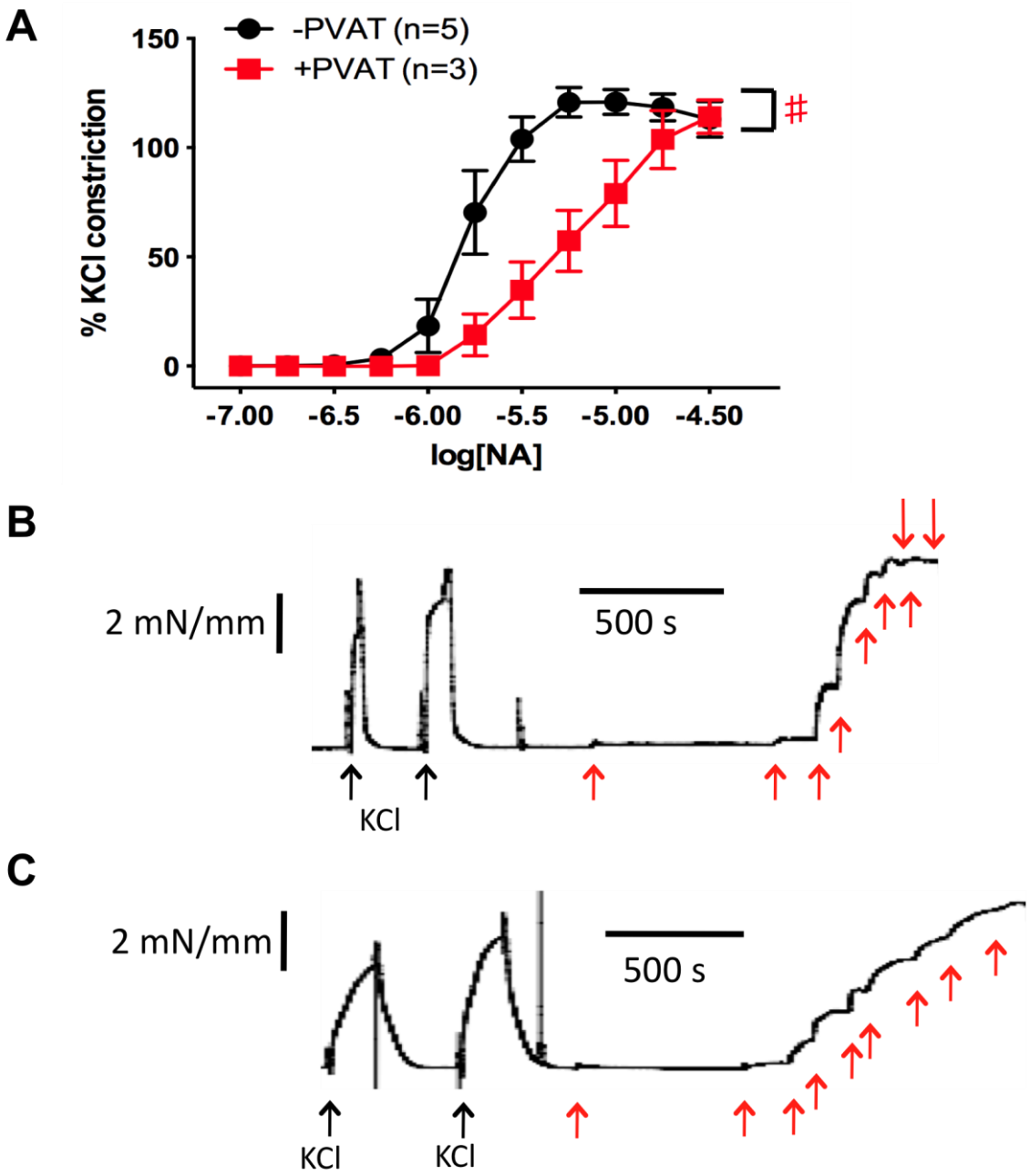

Figure 3.04. Norepinephrine (NA) concentration-response curves to show the anticontractile effects of perivascular adipose tissue (PVAT) in rat mesenteric arteries. A. The vessels used were either PVAT-free (-PVAT) or PVAT-intact (+PVAT), with intact endothelium layer. ♯ Presence of PVAT significantly shifted the curve to the right by Mann-Whitney U tests ($p < 0.05$). **B and C.** Typical myograph traces to show norepinephrine-triggered increase in tension in PVAT-free and PVAT-intact vessels, respectively. Red arrows represent each cumulative addition of norepinephrine.

3.2.5 Sildenafil is a vasorelaxant

Sildenafil at 5 nM induced vasodilation in endothelium-intact mesenteric arteries with or without PVAT (Figure 3.05). In PVAT-denuded vessels, norepinephrine concentration response curves were significantly shifted to the right by sildenafil (norepinephrine pEC_{50} value was reduced from 5.79 ± 0.04 to 5.35 ± 0.06 (n = 5). Sildenafil also reduced the maximum vessel contractility (relative to 60 mM KCl contraction) from 113 ± 8 % to 66 ± 10 % (n = 5). The sildenafil vasodilator effect was similarly observed in PVAT-intact vessels, where pEC_{50} was reduced to 5.05 ± 0.06 and the maximum contraction was reduced to 60 ± 4 % (n = 3). The sildenafil effect was statistically significant by two-way ANOVA tests ($p < 0.001$) for both PVAT-denuded and PVAT-intact vessels.

3.2.6 The presence of PVAT did not enhance the sildenafil vasorelaxant effects

To investigate a possible role of PKG in PVAT, the sildenafil vasorelaxant effect on PVAT-intact vessels was investigated in further detail (Figure 3.05 and 3.06).

In Figure 3.05, sildenafil appeared to have a greater effect in PVAT-intact vessels. The norepinephrine concentration-response curve was shifted to the right when PVAT was present (norepinephrine pEC_{50} reduced from 5.35 ± 0.06 to 5.05 ± 0.06 when PVAT was present; n = 3-5). However, these changes were not statistically significant (by repeated measures t-tests).

Sildenafil seemed to have enhanced the PVAT anticontractile effects, although the presence of endothelium may have complicated the system by releasing vasoactive factors.

Thus, to observe the effects of sildenafil more clearly, sildenafil concentration-response curves were constructed for four different vessel combinations: +/- PVAT and +/- endothelium. A series of increasing concentrations of sildenafil was added to the vessels and each concentration was allowed 15 min of incubation, after which 30 μM of norepinephrine was added to elicit vessel contraction. In between each sildenafil addition, several PSS washes were applied to allow recovery from the drug effects. Figure 3.06 shows the sildenafil concentration-response curves and corresponding DMSO (vehicle) controls for endothelium-intact (A) and de-endothelialised vessels (B).

The data demonstrated that, of the four different vessel configurations, sildenafil displayed the greatest vasorelaxant effect on the PVAT-free, endothelium-intact vessels. The presence of PVAT significantly reduced vessel sensitivity to sildenafil and shifted the response curve rightwards. For endothelium-attached vessels, PVAT reduced pEC_{50} value from 8.47 ± 0.08 to 7.59 ± 0.17 (n = 4); for de-endothelialised vessels, the presence of PVAT reduced pEC_{50} from 8.16 ± 0.15 to 7.81 ± 0.22 (n = 5). The process of endothelium removal appeared to have reduced the sildenafil effect only in PVAT-free vessels (no reduction in PVAT-attached vessels); but this was not statistically significant (non-parametric unpaired t-tests; p = 0.06).

3.2.7 The sildenafil vasorelaxant effect was endothelium-dependent only in PVAT-free vessels

Norepinephrine is a non-selective adrenoceptor agonist – it can activate the α1 adrenoceptors on the vascular myocytes to induce contraction as well as activating the β3 adrenoceptors expressed by the adipocytes. Since β3 adrenoceptor activation in adipocytes may increase the anticontractile effects of PVAT, it is desirable to use a spasmogen to induce vessel contraction without any β3 adrenoceptor-related effects. Hence, cirazoline, a selective α1 adrenoceptor activator (Gellai & Ruffolo 1987), was employed. A β3 adrenoceptor agonist CL-316,243 (Bloom et al. 1992) was also added, where appropriate, to stimulate adipocytes for any further effects of PVAT.

In endothelium-intact vessels lacking PVAT, 5 nM sildenafil caused a rightward shift of the cirazoline concentration-response curve (cirazoline pEC_{50} value was reduced from 7.27 ± 0.18 to 6.61 ± 0.13; n = 3-4) with no further shift in the presence of PVAT (Figure 3.07). In endothelium-denuded vessels, sildenafil also produced a rightward shift in the concentration-response curve in the absence of PVAT (from pEC_{50} of 7.35 ± 0.22 to 6.85 ± 0.14), but the curve was further shifted by the presence of PVAT (cirazoline pEC_{50} value of

6.14 ± 0.21). In the presence of PVAT (and sildenafil), CL-316,243 produce no further effects, irrespective of the presence or absence of the endothelium (Figure 3.07).

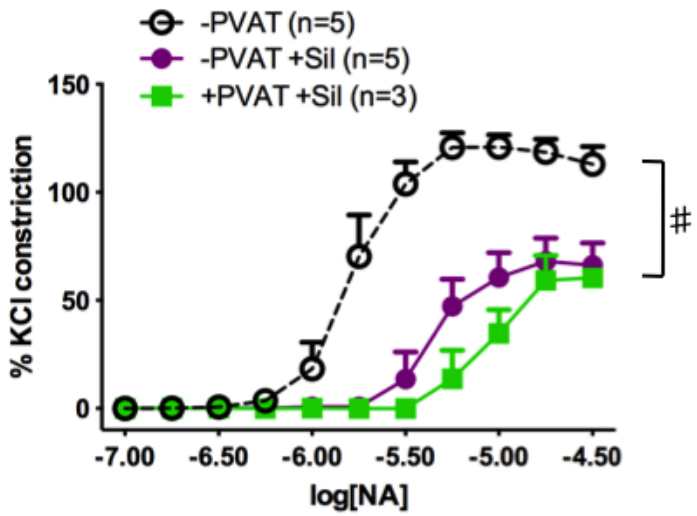

Figure 3.05. Norepinephrine (NA) concentration-response curves to show the effect of 5 nM sildenafil on endothelium-intact mesenteric artery segments without (-) or with (+) perivascular adipose tissue (PVAT). ♯ Sildenafil had vasorelaxant effects on both PVAT-denuded and PVAT-intact vessels (in comparison with control; $p < 0.05$; two-way ANOVA with Bonferroni post-hoc tests). The presence of PVAT did not significantly enhance the sildenafil vasorelaxant effect.

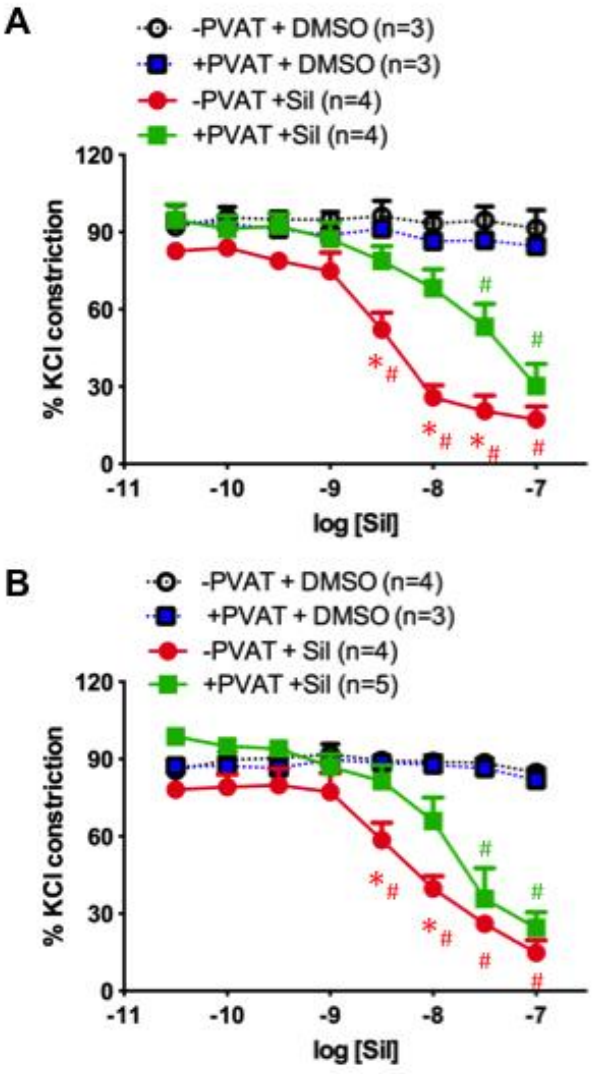
A
-PVAT + DMSO (n=3)
+PVAT + DMSO (n=3)
-PVAT +Sil (n=4)
+PVAT +Sil (n=4)
% KCl constriction
120
90
60
30
0
-11
-10
-9
-8
-7
log [Sil]
B
-PVAT + DMSO (n=4)
+PVAT + DMSO (n=3)
-PVAT + Sil (n=4)
+PVAT +Sil (n=5)
% KCl constriction
120
90
60
30
0
-11
-10
-9
-8
-7
log [Sil]

Figure 3.06. Sildenafil (Sil) concentration-response curves against spasmogen norepinephrine (30 µM) in vessels without (-) or with (+) perivascular adipose tissue (PVAT), with (A) or without (B) intact endothelium. DMSO was added to the vessels as vehicle controls. The vasorelaxant effect of sildenafil was concentration-dependent on both PVAT-intact and PVAT-denuded vessels (# Repeated measures two-way ANOVA followed by Bonferroni post-hoc tests; $p < 0.05$ between sildenafil-treated vessels and DMSO controls); the presence of PVAT reduced the effects of sildenafil (* The same test as before; $p < 0.05$ between vessels with and without PVAT).

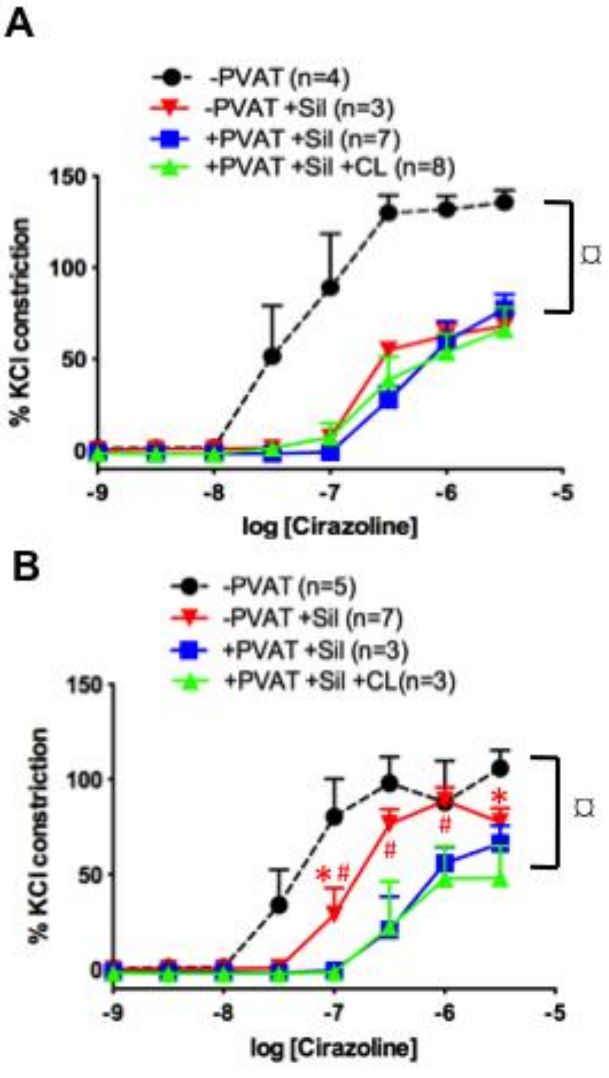

Figure 3.07. Cirazoline concentration-response curves in endothelium-intact (A) and endothelium-denuded (B) vessels without (-) and with (+) perivascular adipose tissue (PVAT). Sildenafil (sil; 5 nM) and CL-316,243 (CL; 10 μM) were added to the relevant myograph chambers and incubated with tissue for 1 hour. **A.** Sildenafil significantly reduced contractility in both PVAT-intact and PVAT-denuded vessels. ¤ Significant difference between control and the other three sildenafil-treated groups (two-way ANOVA with Bonferroni post-hoc tests; $p < 0.05$). CL-316,243 did not further shift the curves to the right. **B.** Sildenafil significantly relaxed the PVAT-intact vessels (¤ two-way ANOVA with Bonferroni post-hoc tests; $p < 0.05$) and PVAT-free vessels (* repeated measures two-way ANOVA tests with Bonferroni post-hoc tests; $p < 0.05$). Removal of PVAT significantly shifted the curve to the left (# between sildenafil-treated PVAT-free and PVAT-intact vessels; repeated unpaired t-tests followed by Holm-Sidak method to correct for multiple comparisons; $p < 0.05$).

3.2.8 L-NMMA prevented the effect of sildenafil

Both PVAT and endothelium can release factors such as NO to activate guanylyl cyclase in the myocytes leading to increased intracellular cGMP levels. The sildenafil vasorelaxant effect is dependent on the elevated levels of cGMP and is therefore dependent on the presence of endothelium or PVAT to release these factors. To determine which factor was responsible for activation of guanylyl cyclase in all of these experiments, vessels were pre-incubated with 100 μM L-NMMA (a non-selective NOS inhibitor; Rees et al. 1990) for 15 min before being exposed to sildenafil. Figure 3.08 shows the cirazoline concentration-response curves for vessels with or without PVAT, L-NMMA and 5 nM sildenafil. All vessels had intact endothelial cell layers.

Figure 3.08 shows the vasorelaxant effect of sildenafil was essentially abolished by L-NMMA. The cirazoline pEC50 value for the control was 7.3 ± 0.2 (n = 4). After L-NMMA and sildenafil, the pEC50 values remained at similar levels of 7.1 ± 0.1 and 7.1 ± 0.2 (n = 4 for both) for PVAT-denuded and PVAT-intact vessels, respectively. However, CL-316,243 shifted the curve significantly to the right ($p < 0.01$; repeated measures two-way ANOVA tests) with a lowered pEC_{50} value of 6.5 ± 0.1 (n = 4).

3.2.9 Drug-induced NO release from adipocytes

To investigate whether the release of NO from PVAT can be enhanced, PVAT was isolated from rat mesentery and incubated in PSS (control) or PSS with 5 nM sildenafil, 10

μM CL-316,243, 10 μM acetylcholine or 5 μM A-769,662 for 30 min at 37 °C. Concentration of NO released from PVAT was analyzed (as NO_2^-) by the Greiss reagents and the results are displayed in Figure 3.09.

Figure 3.09 shows that PVAT was able to release NO without any external stimulation (1.39 ± 0.17 μM of NO_2^- under control conditions; n = 6). Sildenafil appeared to have reduced NO release from PVAT (0.81 ± 0.24 μM; n = 5); but this reduction was not statistically significant. Neither CL-316,243 (0.87 ± 0.60 μM; n = 5) nor acetylcholine (0.91 ± 0.42 μM; n = 4) caused any increase in NO release from PVAT. Incubation with A-769,662, on the other hand, significantly increased PVAT-derived NO concentration to 4.29 ± 0.74 μM (n = 5; $P < 0.05$). All comparisons were made with one-way ANOVA Kruskal-Wallis tests.

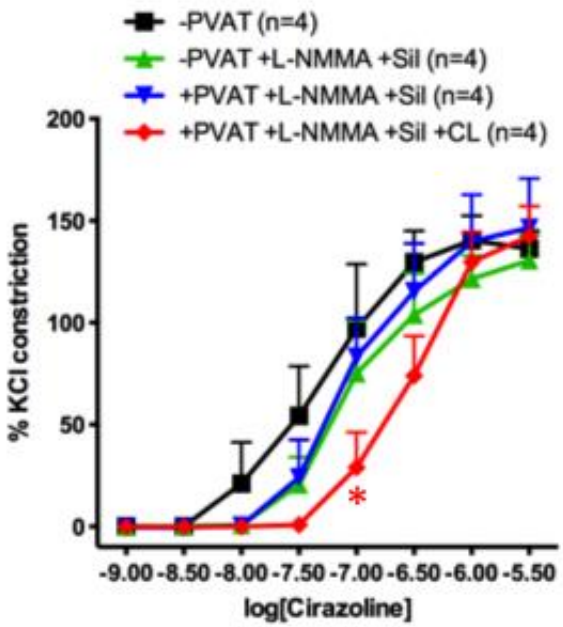

Figure 3.08. Cirazoline concentration-response curves for endothelium-intact mesenteric arteries without (-) or with (+) perivascular adipose tissue (PVAT). Where appropriate, L-NMMA (100 μM) was added first and incubated for 15 min followed by CL-316,243 (CL; 10 μM) for 15 min and finally sildenafil (Sil; 5 nM) for 1 h. L-NMMA prevented sildenafil vasorelaxant effect. However, CL-316,243 still significantly reduced vessel contractility (* Significantly different at the indicated concentration in comparison with control data by repeated measures two-way ANOVA followed by Bonferroni post-hoc tests; $p < 0.05$).

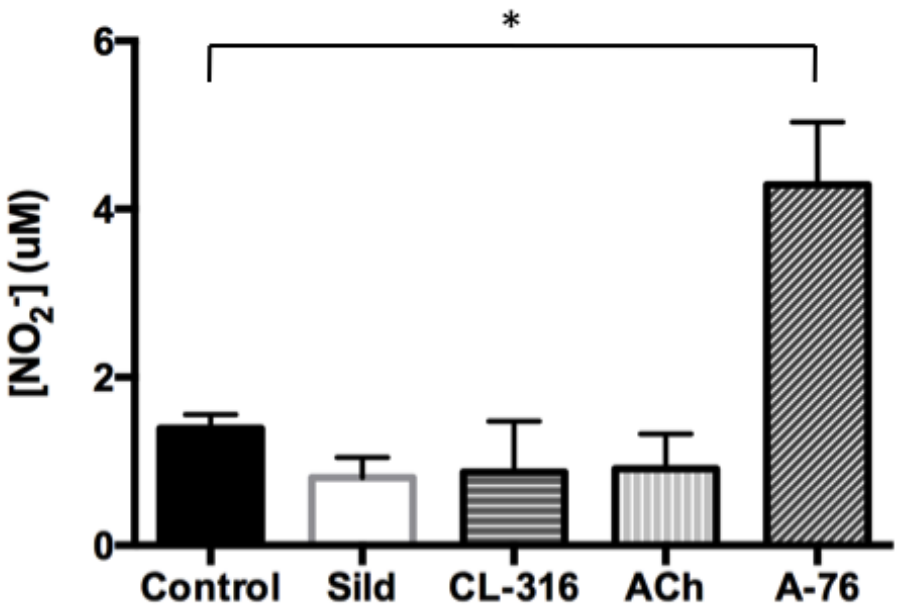

Figure 3.09. Effect of sildenafil (Sild), CL-316,243 (CL-316), acetylcholine (ACh) or A-769,662 (A-76) on the release of nitric oxide from perivascular adipose tissue. Isolated mesenteric PVAT was incubated in physiological saline solution (Control) or physiological saline solution with 5 nM sildenafil, 10 µM CL-316,243, 10 µM acetylcholine or 5 µM A-769,662 for 30 min. Nitric oxide was detected as nitrite (NO_2^-). The presence of sildenafil, CL-316,243 or acetylcholine did not affect the amount of NO released. However, A-769,662 significantly increased NO release from perivascular adipose tissues. * Significantly different by one-way ANOVA Kruskal-Wallis tests (n = 5-6).

3.3 Discussion

3.3.1 Rat mesenteric arteries are surrounded by white adipocytes

This project investigated the potential effects of PKG activation on the anticontractile effects of PVAT by using sildenafil, an indirect activator of PKG. Two types of adipocytes exist: brown and white. White adipocytes act as metabolic energy storage sites and brown adipocytes can generate heat by energy expenditure. The histology staining of rat mesenteric tissue slices showed the typical morphology of white adipocytes which surround the mesenteric arteries. In this chapter, the anticontractile effect of healthy white PVAT against norepinephrine was illustrated (the anticontractile effect of brown PVAT will be presented in Chapter 4).

3.3.2 Extracellular Ca^{2+} concentration and vessel contractility

The PSS Ca^{2+} concentration used in PVAT studies is often 1.6 mM (Löhn et al. 2002; Gao et al. 2005; Greenstein et al. 2009); whereas the Ca^{2+} concentration used in this study is 1.0 mM Ca^{2+}. Since the process by which the anticontractile factor is released by brown adipose tissue is Ca^{2+}-dependent (Dubrovska et al. 2004), it was considered important to investigate the effect of extracellular Ca^{2+} for the release of anticontractile factors in white PVAT. Apart from the lowest Ca^{2+} concentration (0.5 mM), changing the extracellular Ca^{2+} concentrations (up to 2 mM) did not change the contractility of mesenteric arteries,

regardless of whether PVAT was present or not. The increased contractility to norepinephrine in both PVAT-free and PVAT-intact mesenteric arteries due to lowering of extracellular Ca^{2+} to 0.5 mM probably results from a reduced constriction to 60 mM KCl (because of the reduced Ca^{2+} entry into the myocytes for contraction). Indeed, in PVAT-denuded vessels, contraction response to KCl was the lowest when PSS Ca^{2+} concentration was 0.5 mM (1.3 mN/mm versus 2.1, 1.9 and 2.3 mN/mm for the other three concentrations). Similar observations were also made for PVAT-intact vessels. Although it seems that at the two most used concentrations of 1.0 and 1.6 mM, the PVAT effect is not compromised.

3.3.3 PVAT is a source of NO

The effect of sildenafil on the contractility of vessels in four different configurations (+/- PVAT and +/- endothelium) was investigated. Sildenafil exerted a vasorelaxant effect on vessels in all four configurations, irrespective of the spasmogen (norepinephrine or cirazoline). When the vessel endothelium layer was intact, the vasorelaxant effect of sildenafil was not further enhanced by the presence of PVAT. In fact, as displayed by the sildenafil concentration-response curves, the presence of PVAT slightly reduced the apparent effectiveness of sildenafil. This could possibly be due to the relative lipophilic nature of sildenafil (Walker et al. 1999), with absorbance of the drug by PVAT, lowering its effective concentration.

Vasodilator effects of sildenafil are dependent on guanylyl cyclase activation by factors such as NO. Since the endothelium is a source of NO (Palmer et al., 1987), it was expected that endothelium removal would attenuate sildenafil-induced vasodilation. The results presented here, however, showed that this is only the case when PVAT was absent. When PVAT is intact, removal of the endothelium did not reduce the effects of sildenafil. A possible explanation is that PVAT can secrete an anticontractile factor which acts independently of the endothelium to activate PKG in myocytes. As PVAT expresses both eNOS and iNOS (Ribiere et al. 1996; Giordano et al. 2002), it is likely that this PVAT-derived factor is NO. The observation that L-NMMA completely reversed the effects of sildenafil supports this theory.

NO assay results showed that PVAT could indeed release NO without any external stimulation but release was further enhanced by an AMPK activator A-769,662. It is very likely that this is due to AMPK-dependent activation of eNOS within the adipocytes, since AMPK activation has been observed to increase NO release from aortic endothelial cells

(Morrow et al. 2003). In endothelial cells, acetylcholine increases production of NO via activation of muscarinic receptors (Jaiswal et al. 1991). The observation that acetylcholine did not increase NO release from the PVAT shows that the endothelium from the microvessels embedded in the adipose tissue is not the primary source of this NO. Together, these data provide evidence that PVAT can indeed release NO to reduce vascular tone. In contrast to the previous suggestion by Gao et al. (2007), this release of NO is independent of endothelium and can directly affect vascular myocytes.

3.3.4 Functions of PKG in PVAT

The initial aim of this study was to determine whether PKG activation is important for the anticontractile mechanism of PVAT. Mitschke et al. (2013) found sildenafil to increase 'browning' of white adipocytes; a phenomenon that is associated with improving obesity and glucose tolerance (Seale et al. 2011). In vivo 'browning' is a term used to describe the occurrence of adipocytes with features of those found in brown fat ('brown-like' adipocytes) in white adipose depots. The origin of these brown-like adipocytes, also known as 'brite' or 'beige' adipocytes, is very much in debate, but their appearance is frequently observed as a response to appropriate stimulation (temperature or β-adrenergic stimulation). Therefore, the observation that sildenafil increased browning in rodents suggests possible novel uses of sildenafil against obesity and obesity-linked hypertension. Furthermore, studies carried out by Zhang et al. (2010) and Mitschke et al. (2013) using cultured 3T3-L1 (a mouse embryonic fibroblast cell line that can be induced to differentiate into adipocytes; Chang & Polakis 1978) found PKG activation by either sildenafil or cGMP to increase adiponectin expression. Since adiponectin has been demonstrated to be important for the anticontractile mechanism of PVAT (Greenstein et al. 2009), it was anticipated that sildenafil would enhance the anticontractile effects of PVAT. However, short-term incubation of PVAT-attached mesenteric arteries with sildenafil did not seem to do so. Additionally, short term incubation of PVAT with sildenafil did not stimulate the further release of NO from the adipocytes. However, current results do not exclude the beneficial effect of chronic exposure to sildenafil.

PKG is a protein ubiquitously expressed in all cell types and plays vital functions in vascular myocytes (see a review by Hofmann 2005). Applying sildenafil indirectly activates PKG in both vascular smooth myocytes and adipocytes. Thus, it is impossible to conclude whether any effects observed (or lack of) are due to one or the other. One of the ways to overcome this problem is the generation of a conditional knockout mouse in which

the expression of PKG is selectively prevented in vascular myocytes without affecting the PKG gene expression in adipocytes. However, in the present study, the generation of such a mouse model failed (see the supplementary chapter 6).

3.3.5 β3 adrenoceptor stimulation and PVAT functions

The β3 adrenoceptor activator CL-316,243 has anticontractile effects against spasmogens in PVAT-intact mesenteric arteries (Porter 2011; Egner 2013). Weston et al. (2013) also reported that CL-316,243 only hyperpolarised mesenteric artery myocytes when PVAT was present. The mechanism by which β3 adrenoceptor stimulation increased adipocyte anticontractile functions is still unclear; although adiponectin has been suggested to play a part (Weston et al. 2013). The results presented in this chapter showed that, in the presence of sildenafil, CL-316,243 did not produce a further anticontractile effect on mesenteric artery contraction. However, in the presence of L-NMMA which inhibited the sildenafil effect, vessels treated with CL-316,243 showed reduced contraction and thus, indicate that CL-316,243 has anticontractile effects independent of NO. Furthermore, CL-316,243 did not stimulate PVAT to release NO which suggests that β3 adrenoceptor-dependent anticontractile effect of PVAT is not mediated via the release of NO. The possibility that CL-316,243 may have triggered the release of ADRF will be discussed in the next two chapters.

3.3.6 Conclusions

This chapter investigated the functions of PKG on the anticontractile effects of PVAT by using isolated rat mesenteric arteries and a phosphodiesterase type 5 inhibitor sildenafil. Short-term incubation with sildenafil (less than 1 h) did not seem to have triggered PVAT to release any anticontractile factors. Sildenafil-dependent vasodilation effects was reduced by the process of endothelium removal, but only in PVAT-denuded vessels suggesting that the presence of PVAT-compensated for the loss of endothelial cells. The NOS inhibitor L-NMMA reversed the effects of sildenafil in both PVAT-free and PVAT-intact vessels. Together, these results act as indirect evidence to support the likelihood of endothelium-independent release of NO from PVAT. A β3adrenoceptor activator enhanced the anticontractile effects of PVAT; this effect was not inhibited by L-NMMA. Thus, the CL-316,243-induced anticontractile effect of PVAT is possibly exerted via the stimulated release of an ADRF.

Chapter 4

Effect of AMPK activation on vascular myocyte BK_{Ca} channel current

4.1 Introduction

The previous chapter suggested that PVAT could release NO to reduce vascular tone. However, data generated from our lab showed that L-NMMA does not completely inhibit the anticontractile effects of PVAT and other adipocyte-derived factors can also contribute (Egner 2012). As mentioned briefly in Chapter 3, PVAT can also release ADRF, a term originally used by Löhn et al. (2002) to identify a transferable, anticontractile factor released from rat aortic PVAT. The authors proposed that this ADRF acts by activating the K_{ATP} channels on the myocytes to reduce membrane depolarisation (Löhn et al. 2002). Later, ADRF was also found to be release from mesenteric artery PVAT, but myocytes K_V channels were suggested to be activated instead (Verlohren et al. 2004). To add to the confusion, K_{Ca} and K_V7 channels have also been proposed to be involved in the anticontractile mechanism of ADRF in human and rat aorta, respectively (Gao et al. 2005; Schleifenbaum et al. 2010) although data recently published from our lab suggests a role for BK_{Ca} channels (Lynch et al. 2013; Weston et al. 2013). In wire myograph experiments using small resistance arteries, Lynch et al (2003) found that PVAT taken from BK_{Ca} knockout mice had lost its anticontractile effects. Additionally, by using the sharp electrode electrophysiology technique, Weston et al. (2013) have shown that adiponectin caused cell membrane potential hyperpolarisation; an effect which was reversed by iberiotoxin (a selective BK_{Ca} inhibitor; Galvez et al. 1990) and a loss of functional BK_{Ca} channels in myocytes. These results strongly support the participation of myocyte BK_{Ca} channels in the anticontractile mechanism of ADRF. To understand the anticontractile mechanism of PVAT, it is therefore important to determine exactly which K^+ channel is activated by ADRF.

In addition to the uncertainty about the mechanism underlying anticontractile effect of ADRF, its identity is also highly controversial. Several molecules (i.e. H_2O_2, H_2S, Ang 1-7, adiponectin) have been suggested to be the putative ADRF but no agreement has so far been reached (Gao et al. 2007; Greenstein et al. 2009; Lee et al. 2009; Schleifenbaum et al. 2010). It is likely that this variation of the anticontractile mechanism as well as the identity of the ADRF arises because of the differences in vascular beds (i.e. aorta verses smaller resistance arteries) and species (i.e. rats versus human) and the possibility that there is more than one contributory factor. Additionally, the conclusions drawn by several studies with respect to the K^+ channels involved relied on pharmacological agents using intact blood vessels (Löhn et al. 2002; Gao et al. 2007; Schleifenbaum et al. 2010) which

may introduce complications. Firstly, the selectivity of certain pharmacological agents (at the concentrations used) and secondly, the same K^+ channel type (i.e. K_{Ca}) may be expressed not just on myocytes, but also on endothelial cells and/or on adipocytes. Thus, to minimize the complications and to simplify the system electrophysiological experiments were performed on isolated cells.

Adiponectin is a relaxant factor which is abundantly released by adipocytes. In most tissues, the adiponectin receptor AdipoR1 signals via AMPK, an enzyme which also acts as a sensor for cellular energy status. When activated, it can switch off ATP consuming processes while switching on catabolic pathways for ATP synthesis (see review by Hardie et al. 2012). In smooth muscle cells, AMPK has been demonstrated to phosphorylate and desensitize MLCK to calmodulin, thus reducing phosphorylation of MLC which leads to cell relaxation (Horman et al. 2008). Thus, adiponectin released from adipocytes may exert its relaxant effect solely due to the modification of MLC phosphorylation. However, in endothelium-denuded segments of rat mesenteric artery, exogenous adiponectin also hyperpolarises mesenteric artery myocytes by stimulating the opening of BK_{Ca} channels via a mechanism which involves AMPK activation (Weston et al. 2013). Furthermore, application of an AMPK activator (A-769,662) causes membrane hyperpolarisation, an effect that is inhibited by iberiotoxin (Weston et al. 2013). Therefore, it seems likely that AMPK activation results in the opening of BK_{Ca} channels either directly or indirectly, although this has not yet been demonstrated.

To improve on the understanding of how PVAT can exert its anticontractile effects, the possibility that AMPK activation can lead to the opening of BK_{Ca} channels in vascular myocytes was explored. To achieve the objectives, whole-cell and perforated-patch configurations were used to record BK_{Ca} currents in two different cell types: mesenteric artery myocytes and aortic myocytes. The effect of AMPK modulators (A-769,662 and dorsomorphin) on isolated myocytes was investigated to determine whether BK_{Ca} channel currents were affected. Aortic myocytes and mesenteric artery myocytes are surrounded by different PVAT, brown and white, respectively. Although both white and brown PVAT has an anticontractile effect, the anticontractile mechanism of only the white PVAT, which surrounds the resistance arteries and thus is likely to influence blood pressure, was investigated. All of the tissue/cells used to obtain the data presented in this chapter were taken from male Sprague-Dawley rats.

4.2 Results

4.2.1 Anticontractile effect of brown PVAT

To illustrate that aortic PVAT has a similar anticontractile effect to that of mesenteric artery PVAT, aorta with its surrounding PVAT was isolated from rats. Some segments were cleaned of PVAT, whereas some were left with PVAT intact. All aorta segments were endothelium free (as confirmed by the lack of response to 10 μM acetylcholine). 5-HT was then added, cumulatively, in concentrations ranging from 0.03 to 100 μM to elicit contractions and responses were normalised by expressing as a percentage of the constriction induced by 60 mM KCl.

Figure 4.01 demonstrates the 5-HT concentration-response curves for PVAT-free and PVAT-attached aorta rings. This anticontractile effect of PVAT was only significant at the highest 5-HT concentrations employed (30 and 100 μM). At the top concentration of 100 μM, 5-HT caused 390 ± 110 % KCl contraction in PVAT-free vessels versus 104 ± 18 % in PVAT-attached vessels (n = 3). Thus, the presence of PVAT reduced contractility ($p < 0.001$; repeated t-tests). 5-HT pEC_{50} values for PVAT-free and PVAT intact vessels were -4.8 ± 0.3 (n = 3) and -5.3 ± 0.2 (n = 3), respectively.

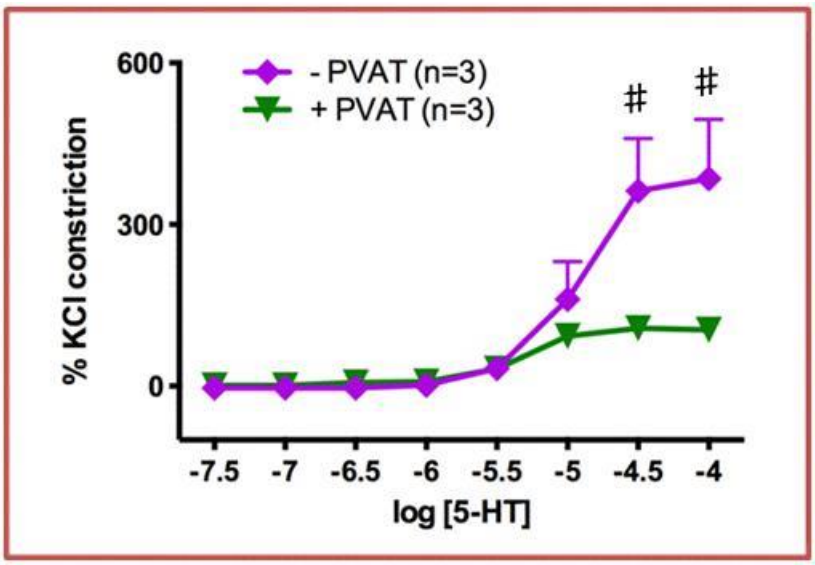

Figure 4.01. 5-HT concentration-response curves for rat aorta segments without (-) and with (+) perivascular adipose tissue (PVAT). Increasing concentrations of 5-HT were added cumulatively to de-endothelialised aorta segments. Contractile responses to 5-HT were to the initial contraction to 60 mM KCl in each segment. The presence of PVAT significantly reduced vessel contraction (# repeated t-test for each data point followed by the Holm-Sidak method to correct for repeated comparisons; $p < 0.05$).

4.2.2 Iberiotoxin did not alter PVAT-intact aortas contractility

Endothelium-denuded aorta segments with or without PVAT were then incubated with iberiotoxin (100 nM) to determine whether this selective BK_{Ca} channel blocker increased vessel contractility under either condition. Figure 4.02 shows the effect of iberiotoxin on 5-HT concentration-response curves for PVAT-intact and PVAT-denuded vessels. In vessels lacking PVAT, iberiotoxin significantly increased the maximum contraction (from 263 ± 42 to 438 ± 45 % of 60 mM KCl constriction, $p < 0.05$; $n = 3$), but 5-HT pEC_{50} values were not greatly affected (control 5.3 ± 0.1, after iberiotoxin 5.5 ± 0.1). When PVAT was intact, iberiotoxin did not significantly alter either the maximum vessel contraction (control 181 ± 39 %, after iberiotoxin 225 ± 51 %; n = 3-6) or the pEC_{50} values of 5-HT (control 5.14 ± 0.22, with iberiotoxin 5.19 ± 0.18; n = 3-6).

4.2.3 Characteristics of vascular myocyte K^+ currents

To trigger K^+ currents from the isolated vascular myocytes, two different voltage protocols were used: one in which cells were clamped at a holding potential of -60 mV and then stepped at 500 ms intervals from the holding potential to a range of test potentials from -90 mV to 50 mV in 10 mV steps; the second protocol was similar but with a holding potential of -10 mV and voltage steps ranging from -40 mV to 50 mV (see Figure 4.03). With a holding potential of -60 mV, the main outward current detected at test potentials comprised a mixture of $I_{K(V)}$ (K_V channel current), $I_{BK(Ca)}$ (BK_{Ca} channel current) and possibly K_A channel current. K_A channels activates and inactivates very rapidly within 200 ms at -20 mV, thus the peak current taken for analysis (which is the peak current detected within the final 150 ms of the voltage step) is the sum of $I_{K(V)}$ and $I_{BK(Ca)}$ (will be referred to collectively as I_K). By holding cells at a less negative potential of -10 mV, K_V channels become inactivated. Therefore the current detected using this voltage protocol is $I_{BK(Ca)}$.

Figure 4.03 and 4.04 show the currents triggered by the two different protocols using mesenteric artery myocytes and aortic myocytes, respectively. At positive potentials, the currents were large and noisy, characteristics of $I_{BK(Ca)}$ (by observation). The currents from both cell types were very similar in terms of magnitude and reversal potentials. For both cell types, the reversal potential for $I_{BK(Ca)}$ was approximately -20 mV (current at -20 mV: -0.23 ± 1 pA for mesenteric artery myocytes; -3.00 ± 4 pA for aortic myocytes; n = 12 for both). For I_K, the reversal potential was approximately -70 mV (detected current at –70 mV was 5.00 ± 1.00 pA for mesenteric artery myocytes and -0.001 ± 0.003 for aortic myocytes; n = 12 for both). The peak I_K magnitude of aortic myocytes was slight higher in aortic

myocytes than mesenteric artery myocytes, with 0.34 ± 0.06 nA for aortic myocytes versus 0.28 ± 0.03 nA (n = 12) for mesenteric artery myocytes at 50 mV.

I_K and $I_{BK(Ca)}$ have different current-voltage relationships. In between voltages of -60 and 0 mV, I_K contains larger positive (outward) current than $I_{BK(Ca)}$. The reversal potentials for $I_{BK(Ca)}$ and I_K are approximately -20 mV and -70 mV, respectively.

4.2.4 Time and vehicle controls

Before any experiments could be carried out to investigate any drug effects, it was important to determine whether myocyte $I_{BK(Ca)}$ and I_K run-up or -down with time. Any time-dependent changes were assessed by triggering the myocytes with the two different voltage protocols at 5 min intervals for a maximum of 20 min. The recorded ionic currents from both mesenteric artery myocytes and aortic myocytes are presented in Figure 4.05C and E, respectively. The data showed that neither $I_{BK(Ca)}$ nor I_K changed significantly with time.

Several drugs used were dissolved in DMSO, an excellent solvent, which may itself exert some effects on myocytes. Therefore, any DMSO effects on mesenteric artery myocytes were assessed by superfusing PSS with added DMSO (3% volume/volume; the highest level used to dissolve drugs). Figure 4.05D shows that DMSO did not have any effects on $I_{BK(Ca)}$ or I_K currents.

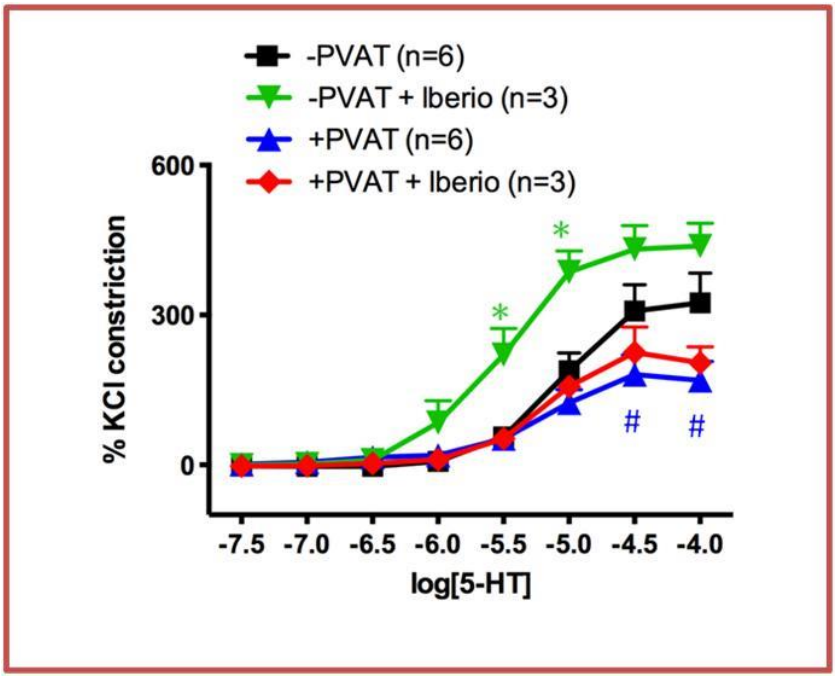

Figure 4.02. Effect of 100 nM iberiotoxin (Iberio) on 5-HT concentration-response curves for de-endothelialised aorta segments without (-) and with (+) perivascular adipose tissue (PVAT). Iberiotoxin was incubated with vessels for 30 min. Iberiotoxin significantly increased vessel contractility only in PVAT-denuded vessels (* at the corresponding data points when compared with PVAT-free control vessels; repeated measures two-way ANOVA tests followed by Bonferroni post-hoc tests; $p < 0.05$). PVAT-intact vessels have significantly lower contractility than PVAT-denuded vessels (# same as before). Iberiotoxin did not produce any significant changes in PVAT-intact vessels.

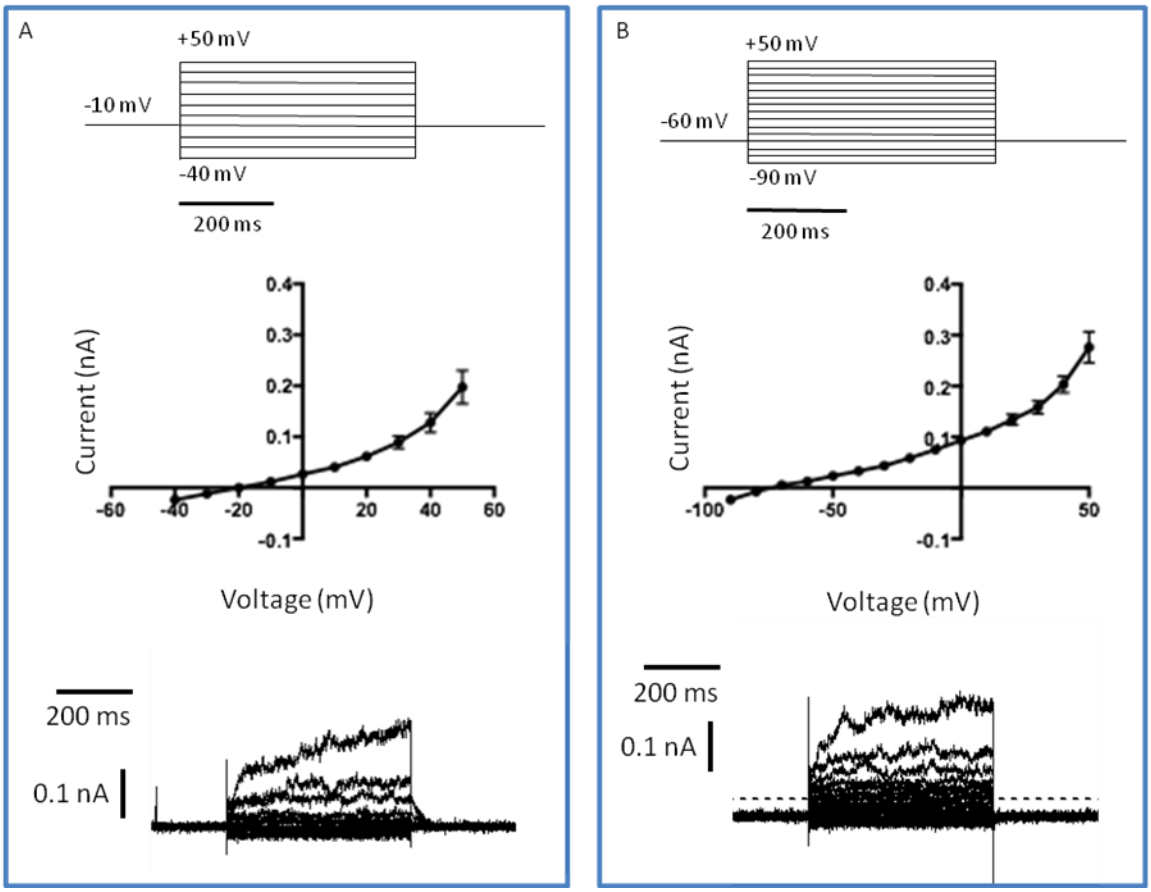

Figure 4.03. Characteristics of BK_{Ca} and whole cell K^+ currents in mesenteric artery smooth muscle cells. A. Top: the voltage protocol used to stimulate BK_{Ca} currents. **Middle**: BK_{Ca} channel current-voltage relationship curve. **Bottom**: typical BKCa channel current recording. **B**. **Top**: the voltage protocol used to stimulate whole cell K^+ current. **Middle**: whole cell K^+ channel current-voltage relationship curve. **Bottom**: typical whole cell K^+ channel current recording; dotted line represents zero current. Data from both graphs were collected with 12 myocytes from 8 rats.

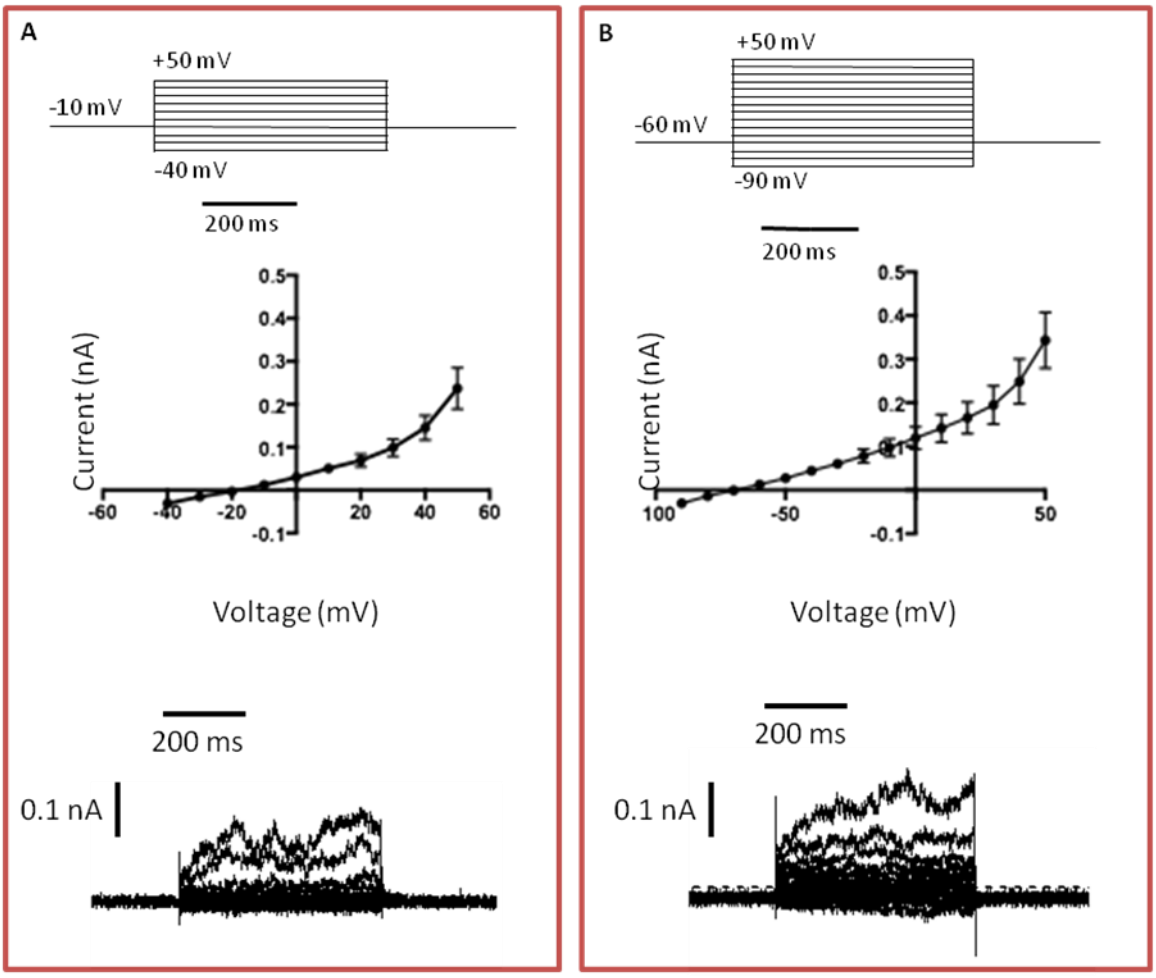

Figure 4.04. Characteristics of BK_{Ca} and whole cell K^+ currents in aortic smooth muscle cells. A. Top: the voltage protocol used to stimulate BK_{Ca} currents**. Middle**: BK_{Ca} channel current-voltage relationship curve. **Bottom**: typical BK_{Ca} channel current recording. **B**. **Top**: the voltage protocol used to stimulate whole cell K^+ currents. **Middle**: Whole cell K^+ channel current-voltage relationship curve. **Bottom**: typical whole cell K^+ channel current recording; dotted line represents zero current. Data from both graphs were collected with 12 myocytes from 12 rats.

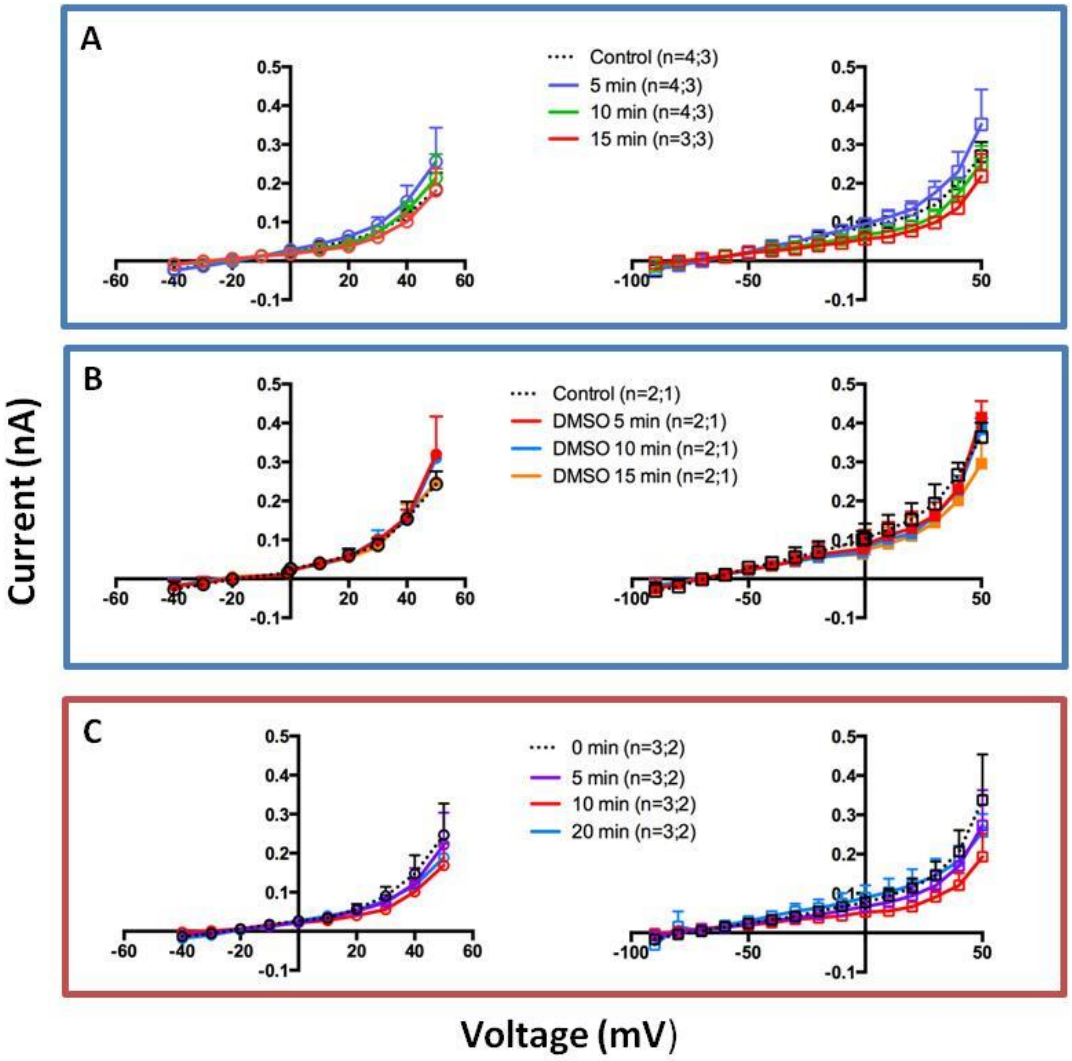

Figure 4.05. Effect of time and vehicle on rat mesenteric artery and aortic myocytes K^+ currents. For time and DMSO controls, myocytes were continuously perfused with physiological saline solution and physiological saline solution with 3 % DMSO (volume/volume), respectively. **A** and **B**. The effect of time and DMSO on BK_{Ca} current (left) and whole cell K^+ current (right) on mesenteric artery myocytes. **C**. Time control for aortic myocyte BK_{Ca} current (left) and whole cell K^+ current (right). None of the treatments caused any significant effect on the currents. n = number of myocytes; number of rats.

4.2.5 Activation and inhibition of BK_{Ca}

To confirm that $I_{BK(Ca)}$ can indeed be enhanced or inhibited by pharmacological agents under the experimental conditions, two BK_{Ca} channel modulators, NS1619 and iberiotoxin, were tested on aortic myocytes (Figure 4.06). NS1619 is a selective BK_{Ca} channel opener (Olesen et al 1994); whereas iberiotoxin, as mentioned before, is a selective BK_{Ca} channel blocker.

When aortic myocytes were superfused with NS1619, both $I_{BK(Ca)}$ and I_K were significantly increased at the two most positive test potentials (40 and 50 mV). NS1619 seemed to have a more profound effect on $I_{BK(Ca)}$ – current at 50 mV was increased from 0.28 ± 0.07 to 1.1 ± 0.2 nA (n = 4; an increase of 290 %; $p < 0.005$). I_K was also increased 200 % from 0.36 ± 0.07 to 1.1 ± 0.1 nA (n = 4).

Iberiotoxin is very potent and has an IC_{50} of 250 pM (Galvez et al. 1990). At the concentration of 100 nM, iberiotoxin seemed to have halved peak $I_{BK(Ca)}$ from 0.19 ± 0.05 to 0.10 ± 0.03 (n = 3). However, this effect was not significant (by repeated t-tests).

4.2.6 A-769,662 increased BK_{Ca} currents

The results observed with NS1619 demonstrated that $I_{BK(Ca)}$ can indeed be activated by channel openers. To investigate whether AMPK activation can lead to BK_{Ca} channel activation, the AMPK activator A-769,662 was used.

Figure 4.07 shows the effect of 5 μM A-769,662 on $I_{BK(Ca)}$ and I_K recorded from mesenteric artery myocytes. Superfusing these cells with A-769,662 caused a rapid and significant increase in $I_{BK(Ca)}$ (peak currents at 50 mV increased 150 % from 0.28 ± 0.08 to 0.71 ± 0.20 nA; n = 4; $p < 0.0001$) that was rapidly reversed (within 1 min) by washing (back to 0.29 ± 0.08 nA; n = 4).

With aortic myocytes, a larger A-769,662 effect was observed (Figure 4.08): peak $I_{BK(Ca)}$ increased 1250 % from 0.20 ± 0.03 to 2.67 ± 0.22 nA; n = 3 ($P < 0.0001$). This effect was again readily reversed by washing as well as by iberiotoxin (100 nM). Figure 4.08C shows the concentration dependent effects of A-769,662 at 1, 3 and 5 μM. All three concentrations significantly increased $I_{BK(Ca)}$; although 1 μM of A-769,662 partially increased $I_{BK(Ca)}$ at more positive testing potentials. Without A-769,662, peak current detected at 50 mV was 0.19 ± 0.02 nA (n = 4). A-769,662 at 1, 3 and 5 μM significantly increased this current to 0.56 ± 0.09 nA, 1.01 ± 019 nA and 1.38 ± 0.22 nA ($p < 0.001$ and n = 4 for all), respectively.

4.2.7 Dorsomorphin did not inhibit the effect of A-769,662

To assess the involvement of AMPK in A-769,662-induced $I_{BK(Ca)}$ increase, dorsomorphin (currently the only commercially-available inhibitor of AMPK) was used to determine whether it would reverse the A-769,662 effect. Figure 4.09 shows $I_{BK(Ca)}$ and I_K current-voltage relationship curves of mesenteric artery and aortic myocytes before and after 2 μM dorsomorphin. After the cells were incubated with dorsomorphin for approximately 10 min, 5 μM A-769,662 was applied.

In mesenteric artery myocytes (Figure 4.09B), dorsomorphin did not affect either $I_{BK(Ca)}$ or I_K by itself. Peak $I_{BK(Ca)}$ remained at similar levels: 0.15 ± 0.03 nA before to 0.17 ± 0.05 nA (n = 5) after dorsomorphin. Additionally, dorsomorphin did not appear to block the effects of A-769,662 as the latter retained its positive effect on $I_{BK(Ca)}$ and the peak current significantly increased from 0.15 ± 0.03 to 1.01 ± 0.39 nA (an increase of approximately 600 %; n = 5).

The same was observed for aortic myocytes (Figure 4.09C). $I_{BK(Ca)}$ seemed not to be altered by dorsomorphin (peak current remained similar from 0.29 ± 0.09 nA (n = 5) to 0.32 ± 0.15 nA (n = 2) after dorsomorphin). In the presence of dorsomorphin, A-769,662 increased $I_{BK(Ca)}$ from 0.29 ± 0.09 nA to 1.6 ± 0.5 nA (n = 5 for both; $p < 0.005$).

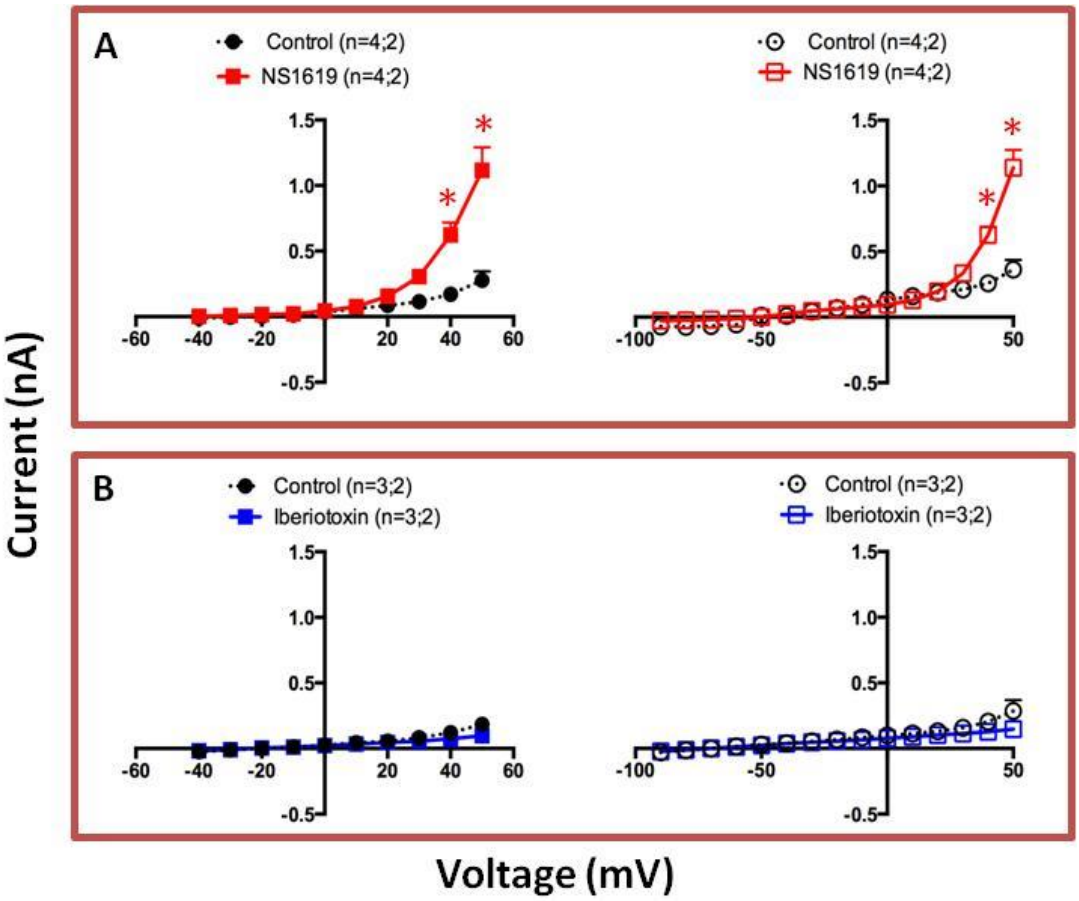

Figure 4.06. Activation or inhibition of rat aortic myocyte BK_{Ca} (left) and whole cell K^+ (right) current using 33 µM NS1619 (A) or 100 nM iberiotoxin (B), respectively. A: NS1619 significantly increased BK_{Ca} current (left) and whole cell K^+ current (right). * $p < 0.05$ repeated t-tests followed by Holm-Sidak test to correct for multiple comparisons; $P < 0.05$. **B:** Iberiotoxin did not affect BK_{Ca} or whole cell K^+ currents. n=number of myocytes; number of rats.

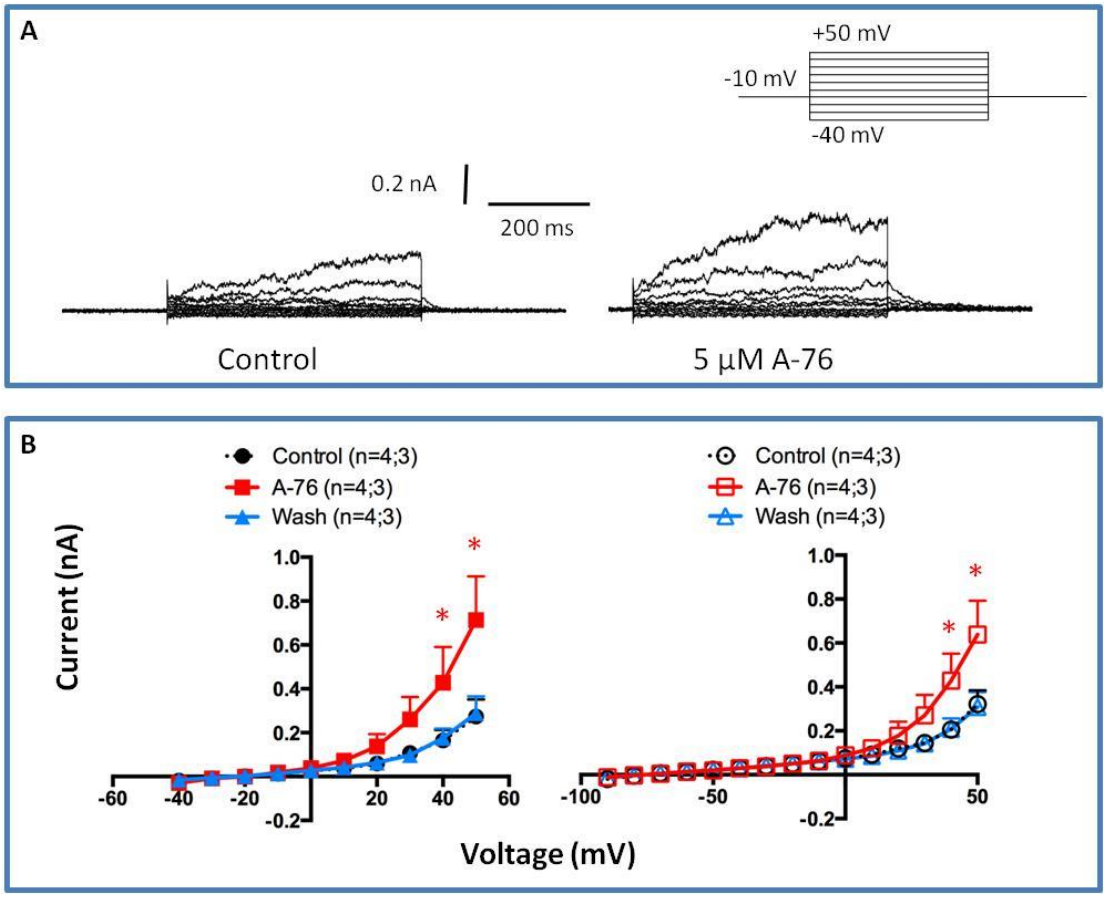

Figure 4.07. Voltage-current relationship curves for freshly isolated mesenteric artery smooth myocytes before and after A-769,662 (A-76). A. Typical myocyte BK_{Ca} current traces before and after applying 5 µM A-769,662. Inset: the voltages steps used to trigger the currents. **B.** A-769,662 significantly increased BK_{Ca} channel current (left) and whole cell K^+ channel current (Right). * Significantly different at the corresponding voltages (repeated measures two-way ANOVA followed by Bonferroni post hoc test); $p < 0.05$. The A-769,662 effect was readily reversed by wash. n = number of myocytes; number of rats.

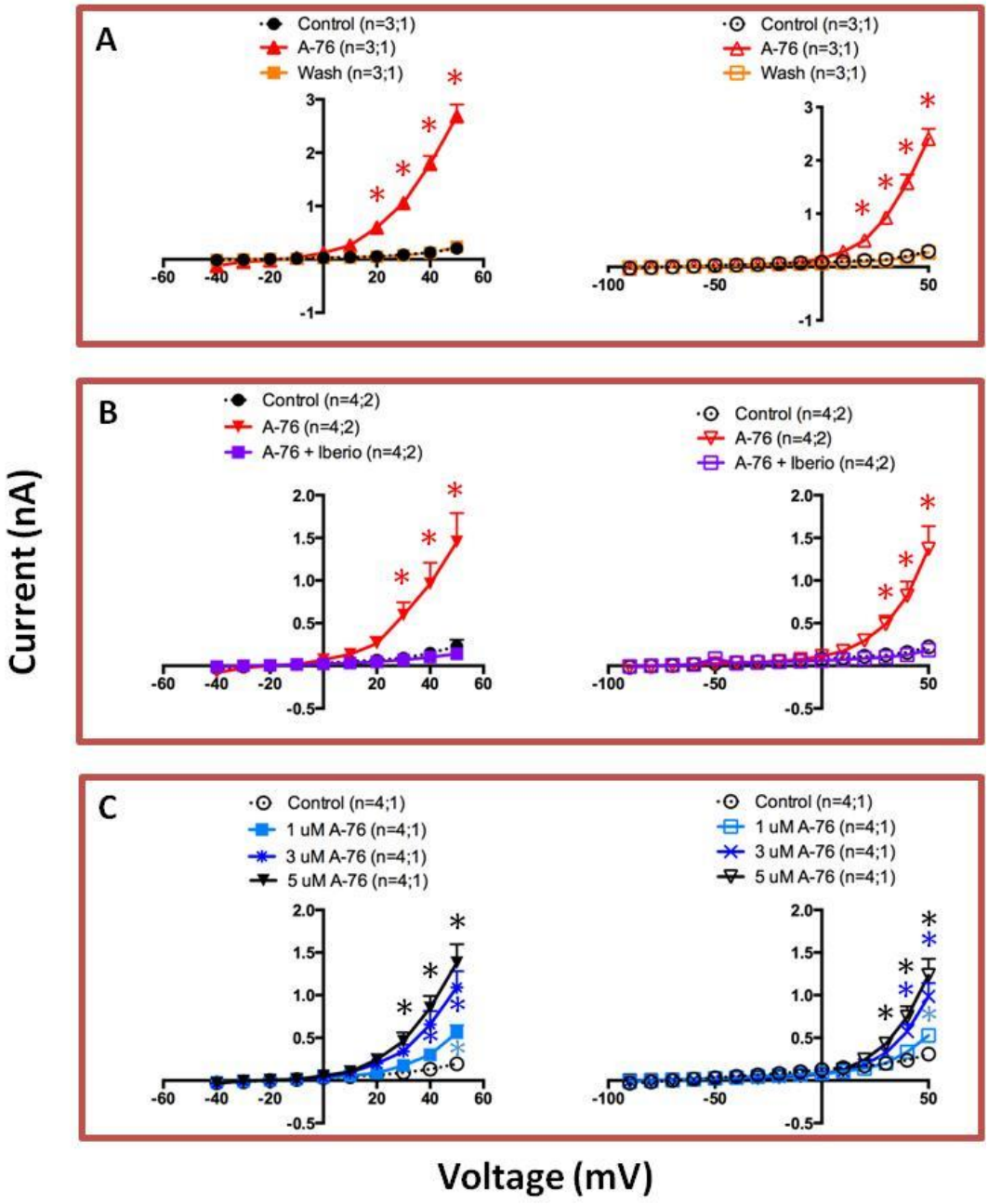

Figure 4.08. Effect of 5 µM A-769,662 (A-76) on aortic myocyte BK_{Ca} channel current (left) and whole cell K^+ channel current (right). The A-769,662 effect was reversed by wash **(A)** and 100 nM iberiotoxin (Iberio; **B**). **C**. Concentration dependent effect of A-769,662 at 1, 3 and 5 µM. * Significantly different at the corresponding voltages from the control using repeated measures two-way ANOVA followed by Bonferroni post hoc test; $p < 0.05$. N = number of myocytes; number of rats.

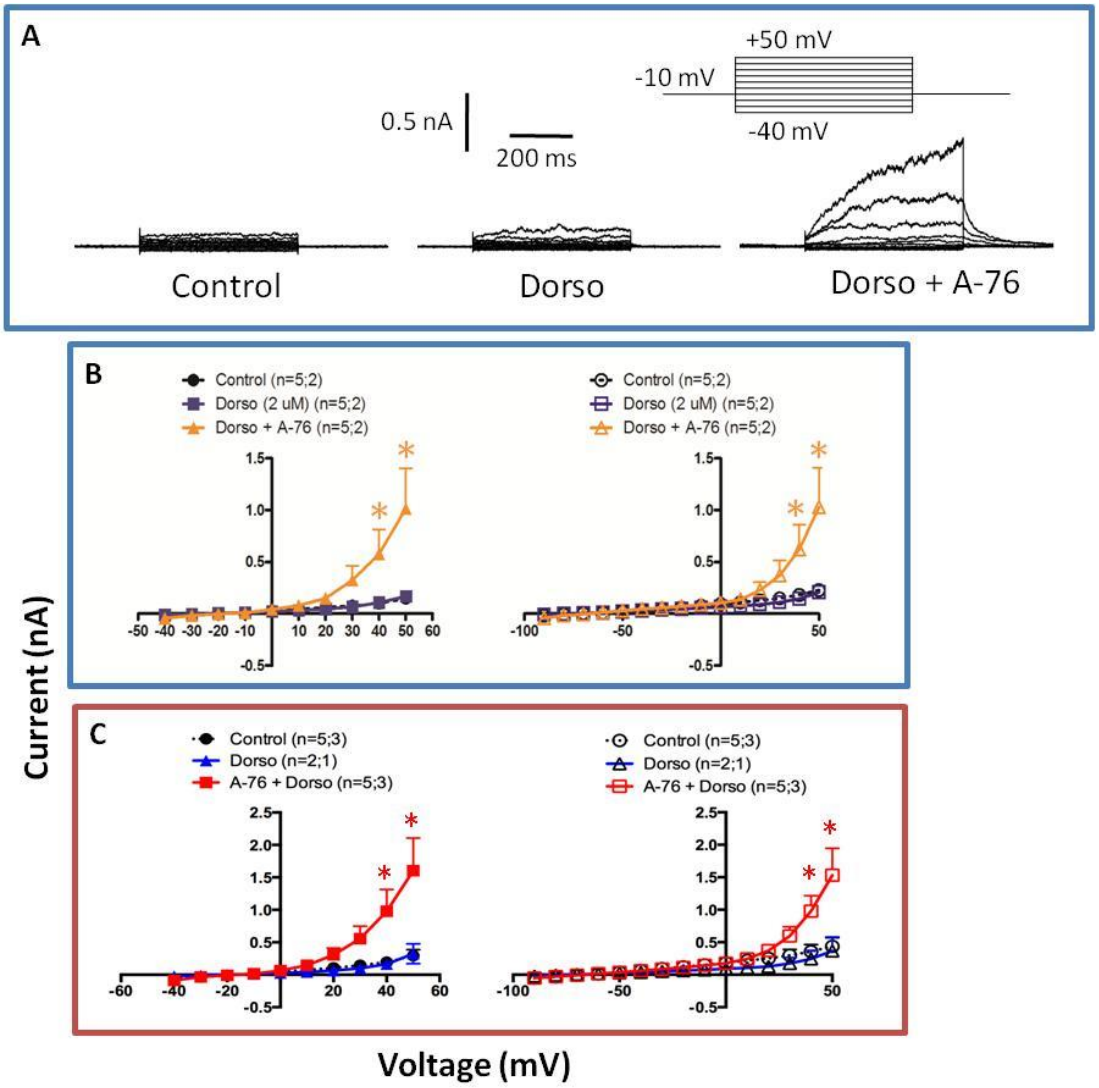

Figure 4.09. Effect of 2 µM dorsomorphin (Dorso), against 5 µM A-769,662 (A-76) using mesenteric artery myocytes (A and B) and aortic myocytes (C). A. Typical BK_{Ca} current recordings of one myocyte before and after superfusion with dorsomorphin alone or in the presence of A-769,662. Inset: the voltages steps used to trigger current. Averaged BK_{Ca} channel (left) and whole cell K^+ channel (right) currents after dorsomorphin alone or dorsomorphin with A-769,662 in mesenteric artery myocytes (**B**) and aortic myocytes (**C**). n = number of myocytes; number of rats. * Significantly different from the control using repeated measures two-way ANOVA test followed by Bonferroni post hoc test; $p < 0.05$.

4.2.8 Preincubation with glibenclamide reduced the A-769,662 effect

Weston et al. (2013) recently showed the A-769,662 hyperpolarisation to be, effectively, reversed by glibenclamide. Thus, in the present study, the ability of glibenclamide (10 μM) to inhibit the A-769,662 effect on $I_{BK(Ca)}$ was investigated. Glibenclamide was used in two different protocols: either aortic myocytes were first exposed to 5 μM A-769,662 followed by A-769,662 (5 μM) and glibenclamide or cells were incubated with glibenclamide for 30 min before the addition of A-769,662.

Figure 4.10A shows the effect of short-term exposure to glibenclamide on the A-769,662 response. As before, A-769,662 on its own caused a large increase in $I_{BK(Ca)}$ from control of 0.17 ± 0.05 to 1.56 ± 0.14 nA (n = 3). Addition of glibenclamide had no effect on the A-769,662-induced increase in $I_{BK(Ca)}$ and the detected peak current remained unchanged at 1.59 ± 0.20 nA (n = 3). However, when cells were preincubated with glibenclamide for 30 min, subsequent A-769,662 effects on both $I_{BK(Ca)}$ and I_K was markedly reduced (Figure 4.10B). Thus, in the presence of glibenclamide, $I_{BK(Ca)}$ after A-769,662 only increased $I_{BK(Ca)}$ from 0.19 ± 0.04 to 0.42 ± 0.05; n = 4; $p < 0.001$). However, A-769,662 failed to trigger a significant change to I_K, peak current at 50 mV remained at similar levels from 0.27 ± 0.05 to 0.38 ± 0.04 nA (n = 4).

4.2.9 A-769,662 increased spontaneous transient outward currents in mesenteric artery myocytes

Spontaneous opening of ryanodine receptors in the smooth muscle cells causes a local release of Ca^{2+} from the intracellular stores. The increase in Ca^{2+} can activate BK_{Ca} channels on the cell plasma membrane, resulting in STOCs, which serve to stabilize resting membrane potential in vascular myocytes (Benham & Bolton 1986; Bolton & Imaizumi 1996). To investigate if A-769,662 increased BK_{Ca} channel activity by increasing the occurrence of Ca^{2+} release/STOCs, perforated patch experiments were performed to detect any A-769,662-induced changes in STOCs. To record STOCs, mesenteric artery myocytes were held at -20 mV.

Figure 4.11A shows STOCs in three different mesenteric artery myocytes – STOC amplitude from two of which was significantly increased by A-769,662 (cell 1: from 21 ± 0.77 to 26 ± 1.21 pA ($p < 0.005$); cell 3: from 16 ± 0.58 to 20 ± 0.98 pA ($p < 0.05$)). Cell number 2 did not show any modification of STOCs by A-769,662 (STOC amplitude at control:18 ± 1 pA; to 26 ± 3 pA after 5 μM A-769,662). However, from the actual traces

recorded, both the frequency and amplitude seemed to be increased by A-769,662 (Figure 4.11B).

4.2.10 A-769,662 did not alter aorta contractility in tension studies

To investigate whether A-769,662 would affect myocyte contractility, myograph experiments were carried out using de-endothelialised PVAT-free aorta segments. After the initial vessel normalisation, either 2 μM dorsomorphin or 5 μM A-769,662 was added to the relevant myograph chamber and tissue incubated for 30 min at 37 °C. To investigate the effect of dorsomorphin on responses to A-769,662, vessels were incubated with dorsomorphin for 15 min before addition of A-769,662 (in which vessels were further incubated for 30 min). After 30 min incubation with A-769,662, in the continued presence of dorsomorphin, increasing concentrations of 5-HT were added cumulatively; 5-HT concentration-response curves are illustrated in Figure 4.12.

The 5-HT concentration-response curves show that in presence of A-769,662 and/or dorsomorphin, neither of the two AMPK modulators caused any significant changes in vessel contractility.

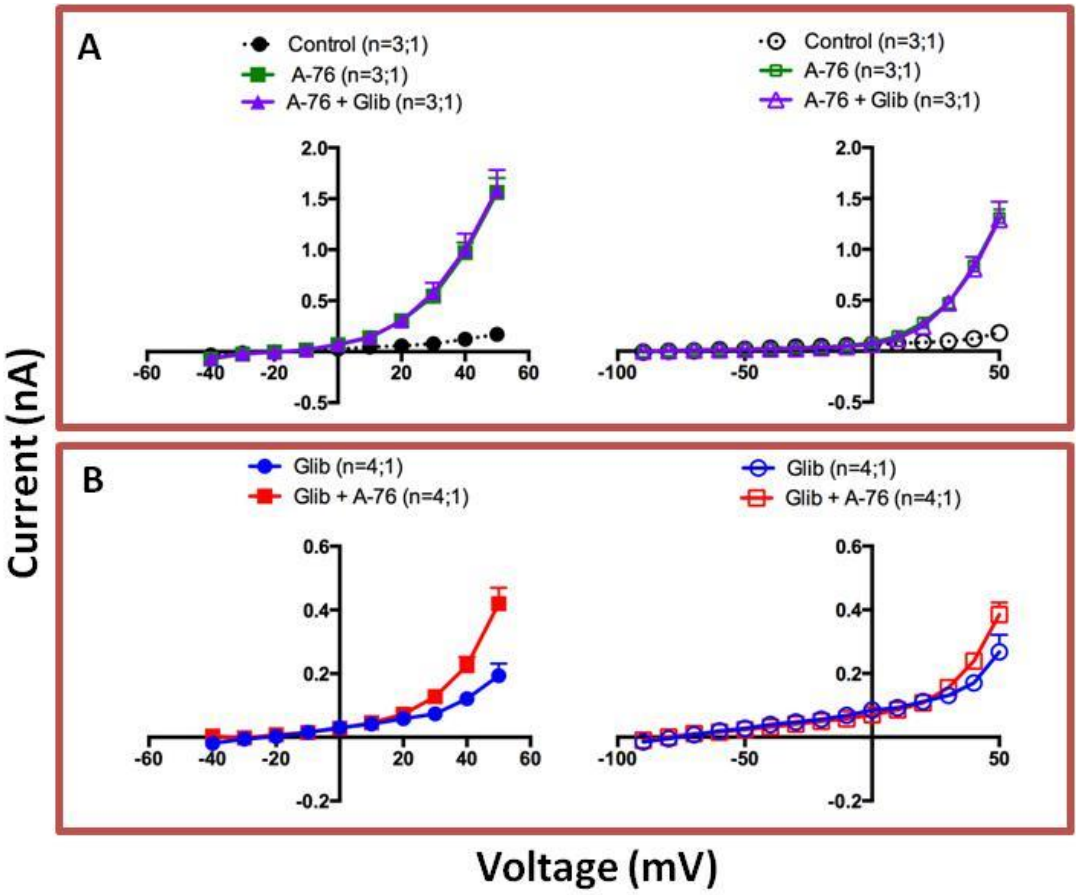

Figure 4.10. Effects of 5 µM A-769,662 and 10 µM glibenclamide (Glib) on the current-voltage relationship curves in aortic myocytes. A. Effect of short term perfusion of glibenclamide on the A-769,662 response. Myocytes were first exposed to A-769,662 followed by glibenclamide for approximately 5 min. Left: averaged BK_{Ca} current. Right: averaged whole cell K^+ current. **B.** The effect of long term incubation with glibenclamide on the A-769,662 response. Myocytes were incubated with glibenclamide for 30 min at room temperature before being exposed to A-769,662. * Significantly different from the control using repeated measures two-way ANOVA test followed by Bonferroni post hoc test; $p < 0.05$. # Significantly different using the non-parametric paired t-test ; $P < 0.05$. n = number of myocytes; number of rats.

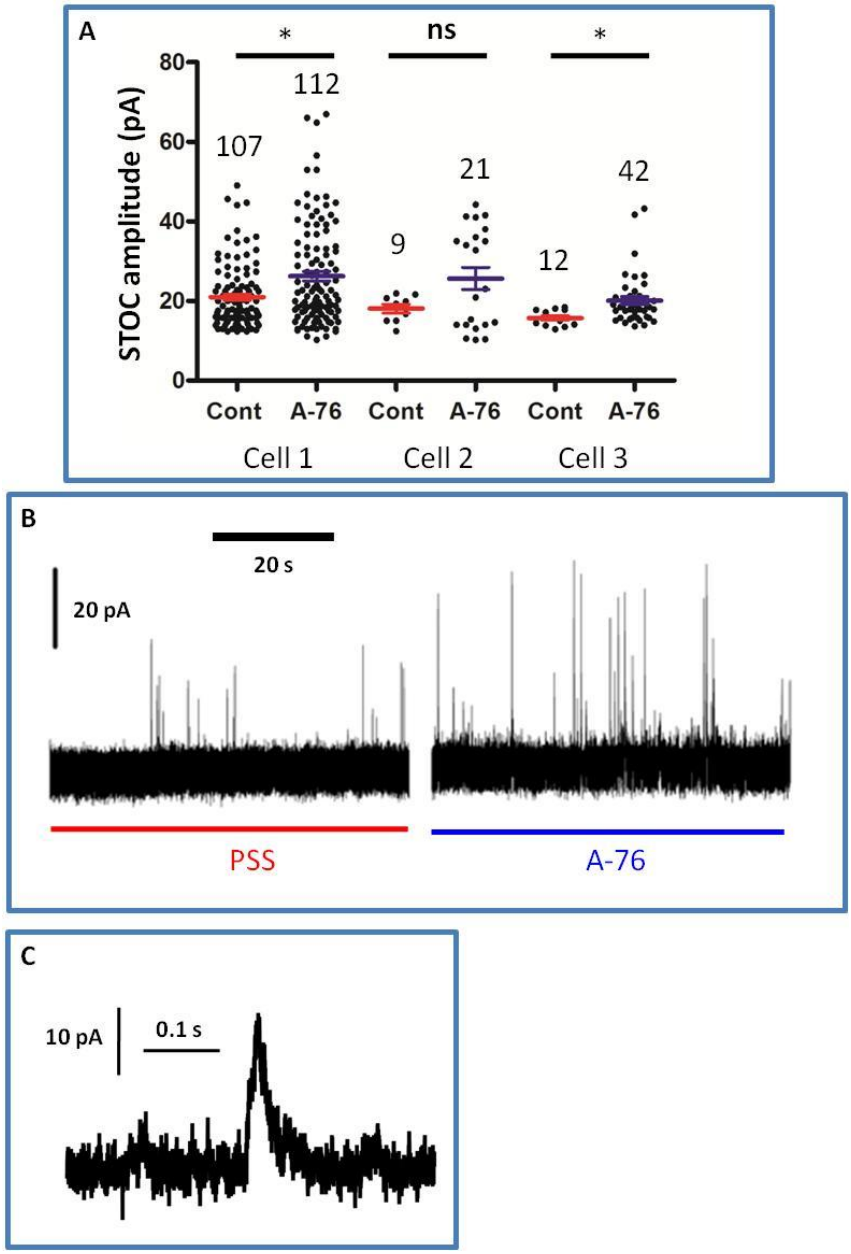

Figure 4.11. Spontaneous transient outward currents (STOCs) in mesenteric artery myocytes before and after 5 µM A-769,662 (A-76). STOCs were recorded at the holding potential of -20 mV. **A.** The STOC amplitude in three different myocytes. The dots on the scatter diagrams represent the amplitudes of individual STOCs recorded within 1 min duration. The coloured lines represent mean ± SEM. The numbers above the dots represent the total number of STOCs within the 1 min duration. **B.** Current traces recorded in Cell 2 when perfused with physiological saline solution (PSS) or A-769,662. C. Expanded view of one particular STOC under control condition. * Statistically different using non-parametric t-test; $p < 0.05$. ns: non-significantly different using the same t-test.

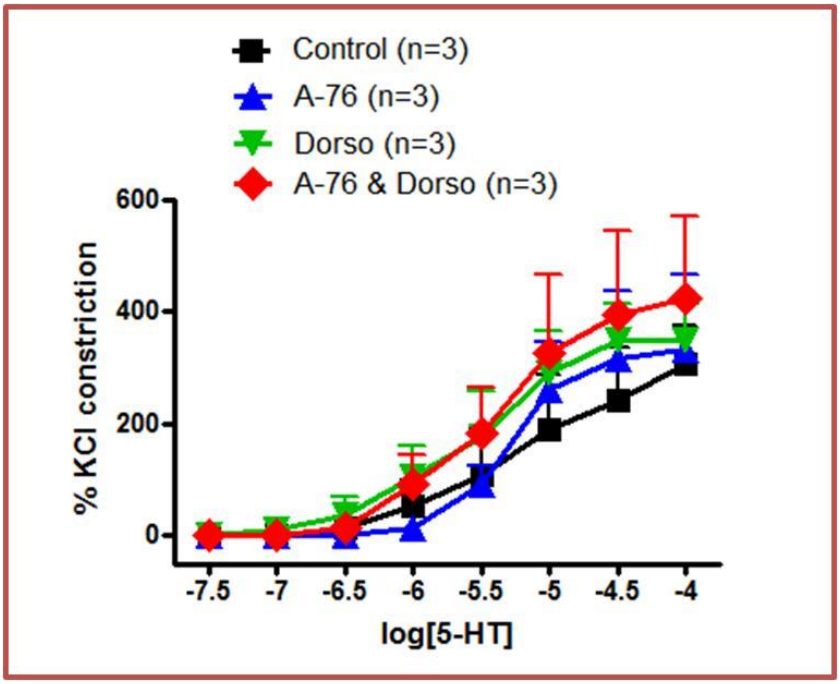

Figure 4.12. 5-HT concentration response curves to illustrate the effect of 5 µM A-769,662 (A-76) and 2 µM dorsomorphin (Dorso) on aorta tension. All vessel segments were cleaned of perivascular adipose tissue and were de-endothelialised. No significance was observed between different treatments (by two-way repeated measures ANOVA).

4.2.11 AICAR did not increase BKCa channel current

To confirm that effect of A-769,662 was really due to activation of AMPK, AICAR (an alternative AMPK activator) was used to see whether it had any effect on K^+ currents in myocytes. Figure 4.13 shows the effect of 1 mM AICAR on BK_{Ca} and whole cell K^+ channel current-voltage relationships in mesenteric artery myocytes (A) and aortic myocytes (B).

In mesenteric artery myocytes, both $I_{BK(Ca)}$ and I_K remained the same after perfusion of AICAR and the peak $I_{BK(Ca)}$ current remained similar before 0.18 ± 0.03 nA (control) and after AICAR 0.19 ± 0.03 nA (n = 3). In aortic myocytes, AICAR seemed to have reduced both $I_{BK(Ca)}$ (0.20 ± 0.03 before versus 0.151 ± 0.005 nA after; n = 3) and I_K (0.29 ± 0.03 to 0.191 ± 0.002 nA; n = 3), but only the change I_K was statistically significant (non-parametric paired t-test; $p < 0.05$).

4.2.12 PT1 activated BK_{Ca} channels

The two AMPK activators so far tested had shown mixed effects on the BK_{Ca} channels. To generate more clues as to whether AMPK activators could activate BK_{Ca} channels, a third AMPK activator was used – PT1. When PSS containing PT1 (20 μM) was superfused over mesenteric artery myocytes, $I_{BK(Ca)}$ was significantly increased after just 1 min and current at +50 mV doubled from 0.28 ± 0.10 nA to 0.57 ± 0.16 nA (n = 4; $P < 0.001$) (Figure 4.14A). After 10 min of incubation, PT1 did not further enhance the peak BK_{Ca} current (0.79 ± 0.24 nA; n = 4). The PT1 effect was reversed on washout of the drug.

Again, 2 μM dorsomorphin was superfused with 20 μM PT1 to try to reverse this PT1 effect. Cells were first exposed to PSS containing PT1 for 10 min before switching to PSS containing both dorsomorphin and PT1. Currents were recorded before and 3 min after being exposed to dorsomorphin and the results were illustrated in Figure 4.14B. Similar to its lack of effect on A-769,662-induced current, dorsomorphin did not appear to alter PT1 responses. $I_{BK(Ca)}$ at 50 mV under control conditions was 0.163 nA (individual values: 0.16 and 0.17 nA; n = 2), increased to 0.30 after PT1 (individual values: 0.30 and 0.31 nA; n = 2) and after dorsomorphin and PT1 to 0.35 (individual values 0.28 and 0.41 nA; n = 2).

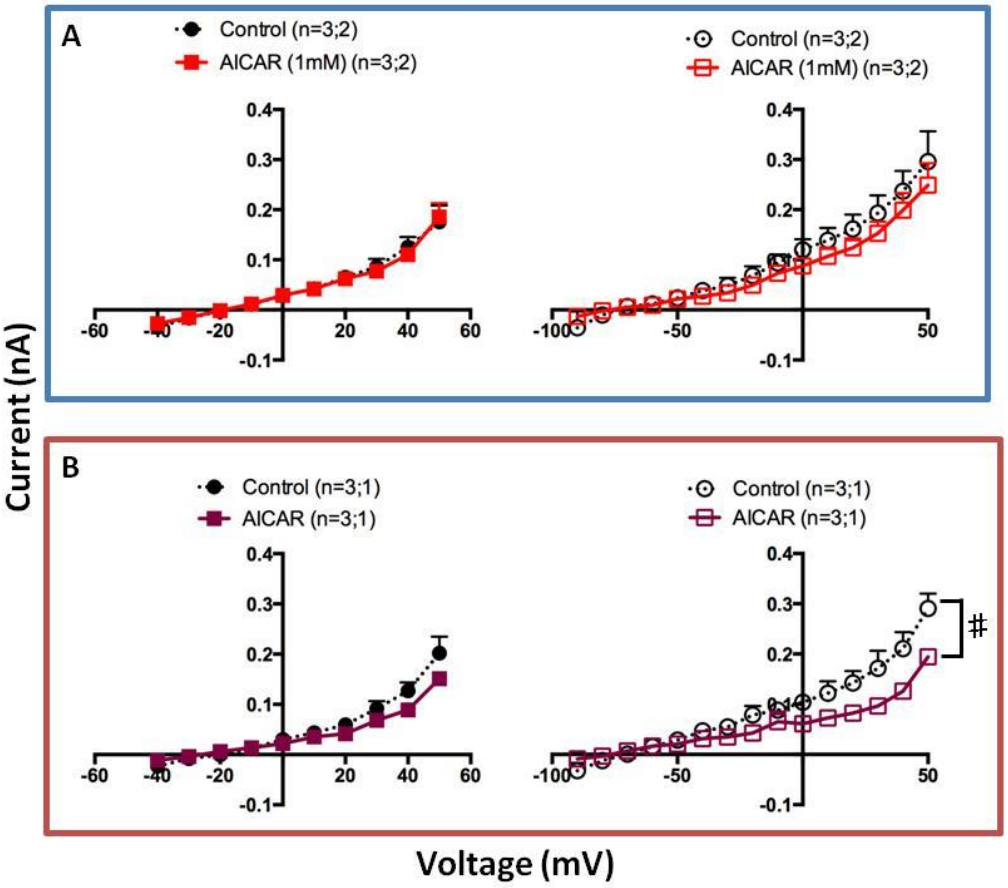

Figure 4.13. Effect of 1 mM AICAR on BK_{Ca} (left) and whole cell K^+ (right) current in mesenteric artery (A) and aortic smooth myocytes (B). AICAR did not produce any significant changes to the BKCa channel current in either mesenteric artery or aortic myocytes. Whole cell K^+ was significantly reduced by AICAR in aortic myocytes (♯ Significant difference from the control using non-parametric paired t-test; $p < 0.05$). n = number of myocytes; number of rats. Error bars represent SEM.

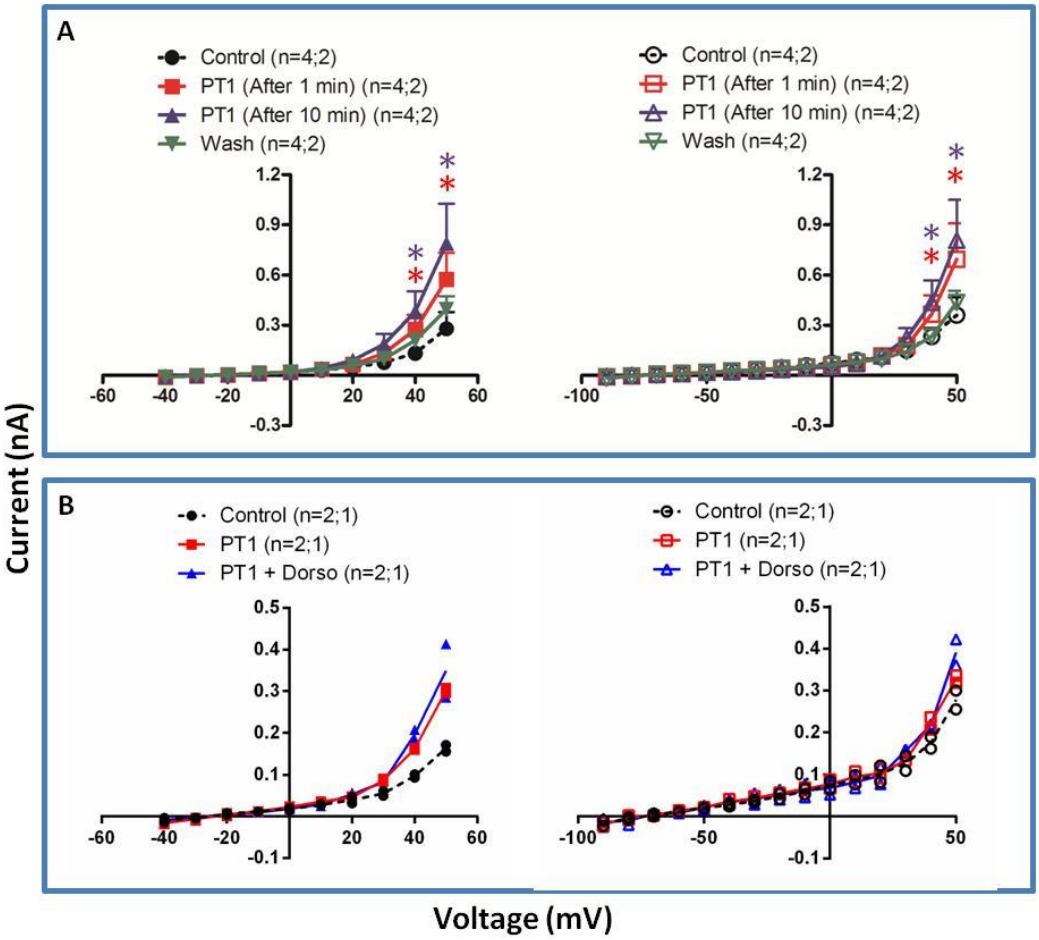

Figure 4.14. Effect of 20 µM PT1 on BK_{Ca} (left) and whole cell K^+ (right) current in mesenteric artery myocytes. A. Voltage-current curves of myocytes before and after applying PT1 (current recorded after 1 and 10 min exposure to PT1). PSS was re-applied to wash away the drug. **B.** Dorsomorphin (Dorso) at 2 µM was added to assess whether the PT1 response could be reversed. The individual data points are illustrated with the means connected. * Significantly different from the control data ($P < 0.05$) by using two-way ANOVA tests followed by Bonferroni post-hoc tests. n = number of myocyte; number of rat.

4.3 Discussion

4.3.1 5-HT as a spasmogen

In Chapter 3, the anticontractile effect of white PVAT was demonstrated using mesenteric arteries. Like white PVAT, brown PVAT can also release factors and has anticontractile effects on the vasculature as demonstrated on both rat (Löhn et al. 2002; Gao et al. 2007) and human thoracic aortas (Gao et al. 2005). Löhn et al. (2002) showed brown PVAT to reduce maximal contractile responses by 95, 80 and 30 % against the three different spasmogens, angiotensin II, 5-HT and phenylephrine, respectively. It seems that with 5-HT, the PVAT anticontractile effect is sub-maximal. Thus, 5-HT was chosen as the spasmogen in this project to allow detect of the effects of other drugs which might enhance or reduce contractions. However, 5-HT has dual effects on vessel contractility and the net outcome is the balance between its relaxant effect via endothelial cells (Schoeffter & Hoyer 1990) and contractile effects on the myocytes (see review by Vanhoutte et al. 1984). To simplify the system, endothelial cells were removed from the aorta rings used. In the present study, brown PVAT reduced 5-HT-induced vessel contractility by approximately 70 % (in agreement with the findings of Löhn et al. 2002).

4.3.2 Lack of iberiotoxin effects in PVAT-intact aorta

Since recent papers (Lynch et al. 2013; Weston et al. 2013) suggested BK_{Ca} channels are important for the PVAT anticontractile effects, iberiotoxin was used to see whether it would inhibit the PVAT effect in tension experiments. BK_{Ca} channels are the dominant channels in the regulation of myogenic tone, and their inhibition leads to cell membrane depolarisation and myocyte contraction (Brayden & Nelson 1992). As expected, iberiotoxin increased vascular contractility, but only in PVAT-free segments of aorta. Surprisingly, this iberiotoxin effect was lost in PVAT-intact vessels. This is possibly due to a mechanical barrier effect of PVAT. Iberiotoxin is a relatively large molecule (a 37 amino acid peptide; Galvez et al. 1990) and intact PVAT layers may prevent effective diffusion of iberiotoxin to the smooth muscle cell layers. Or alternatively, this would also be consistent with a relaxant factor being released from the PVAT which exert anticontractile effect independently of BK_{Ca} channels. Thus, in order to focus the effect of ADRF on the vascular myocytes it is desirable to isolate myocytes from the other cell types.

4.3.3 BK_{Ca} channel current versus whole cell K^+ channel currents

Two voltage protocols were used here in the present study to stimulate cell current. The voltage protocol with a holding potential of -10 mV intended to separate the BK_{Ca} channel current from currents conducted by other voltage-sensitive K^+ channels expressed by the vascular myocytes. This is because at -10 mV, most of the voltage-sensitive channels (but not BK_{Ca} channels) are inactivated. By comparing the voltage-current relationship curves, the differences in the current triggered by the two different voltage protocols can be observed. The most obvious difference occurs between -50 mV and around 0 mV where there is limited number of BK_{Ca} channel being activated (as observed by the voltage-current relationship curve for BK_{Ca} channel voltage protocol; also see review Magleby 2003). Thus, current observed within this region is mainly conducted by other voltage-sensitive K^+ channels, such as the delayed rectifiers (i.e. K_V7 channels). Selective BK_{Ca} channel activator NS1619 did not increase current within this region and confirms the lack of BK_{Ca} channel activity. At the most positive potentials, current triggered by both voltage protocols was increased by NS1619, indicating the activation of BK_{Ca} channels at such potentials masking other currents (due to BK_{Ca} channel high conductance).

4.3.4 The A-769,662 effect

To address the first question of whether AMPK activation would lead to BK_{Ca} channel activation, the effect of A-769,662 on BK_{Ca} channels was determined in vascular myocytes. A-769,662 was discovered in 2006 (Cool et al. 2006) and has since been recognized as one of the most effective AMPK activators currently available – it is 50 times more potent than AMP (Göransson et al. 2007). In the present study, the experimental results demonstrated reversible activation of BK_{Ca} channels by A-769,662 – an effect that was more profound in aortic myocytes than mesenteric artery myocytes. The whole cell K^+ current was not affected by A-769,662 at potentials between -50 and 0 mV, which indicate that other voltage-sensitive K^+ channels were not activated, whereas the involvement of BK_{Ca} channels was confirmed using iberiotoxin. Similar results were obtained by Weston et al. (2013) using sharp electrode recordings in mesenteric arteries. Weston and co-workers showed that superfusion with A-769,662 hyperpolarized the cell resting membrane potential, an effect which was reversed by dorsomorphin and iberiotoxin. Thus, it seemed likely that AMPK would lead to activation of BK_{Ca} channels. However,

the data from the present study are not totally consistent with the involvement of AMPK as dorsomorphin did not reverse the A-769,662 effect.

The reason why dorsomorphin failed to block the effect of A769,662 in the isolated myocytes is unknown. Perhaps the most obvious reason is that AMPK simply was not activated in any of these responses, i.e. A-769,662 activated BK_{Ca} channels either directly or via AMPK-independent mechanisms. A-769,662 has previously been shown to have off-target effects (Scott et al. 2008; Benziane et al. 2009). Thus, Scott et al. (2008) observed A-769,662 (100 μM) to regulate hepatic glucose output independently of AMPK activation and Benziane et al. (2009) reported A-769,662 to reduce Na^+/K^+ ATPase activity as well as reduce its surface expression in cultured L6 myotubes. Similar to the observations made in the present project, Benziane et al. (2009) failed to reverse the A-769,662 effects by the usage of dorsomorphin. However, the A-769,662 concentration used by Benziane et al (2009) was much higher than the concentration used in this study (100 μM versus 5 μM). Also, Benziane et al (2009) incubated A-769,662 with their L6 myogenic cells for 40 min at 37 °C, whereas the data obtained in the present study showed that BK_{Ca} channel current was increased after a short exposure to the drug (less than 3 min). It is much more common to see the off-target effect of a drug when the cells are incubated in higher concentrations and for extended periods of time. At 5 μM used here, it is unlikely that the drug would exert an unspecific effect. Additionally, out of the three A-769,662 concentrations used (1, 3 and 5 μM), 1 μM, A-769,662 seemed to have caused approximately half of the maximal effect, which agrees with the EC_{50} (the half maximal effective concentration) of 0.8 μM given by the drug manufacturer (Tocris Bioscience, 2013). All of these suggest that the A-769,662 effects on BK_{Ca} channels are indeed by activating the AMPK. However, further experiments, for example western blots, should be carried out to confirm the phosphorylation of AMPK by 5 μM A-769,662.

The exact mechanism by which most AMPK modulators alter AMPK activity is still unclear. A-769,662 has been suggested to bind to the N-terminus of the β1 subunit (Scott et al. 2008), distinct from the nucleotide binding modules located on the γ subunit (Sanders et al. 2007; Göransson et al. 2007). Dorsomorphin was suggested to act as a competitive inhibitor of AICAR (which interacts with the γ subunit of AMPK). Thus, another possibility to explain why dorsomorphin did not inhibit the effect of A769,662 could be that the two AMPK modulators have different binding sites. Thus, dorsomorphin may not be effective at blocking the A-769,662 effects. However, both Ikematsu et al. (2011) and

Weston et al. (2013) have reported dorsomorphin to inhibit the A-769,662 effects; although these two studies carried out their experiments at higher temperatures (30 and 37 °C, respectively). Therefore, the lack of dorsomorphin observed in the present study may be due to experimental conditions.

In tension studies, 5 μM A-769,662 did not change vessel contractility in de-endothelialised and PVAT-free aorta. This was somewhat unexpected as A-769,662 increases $I_{BK(Ca)}$ in the whole-cell configuration and thus should have reduced vessel contractility. Others who performed similar experiments with AICAR on isolated mouse aortic rings have found AICAR to have vasorelaxant effects against spasmogens (Davis et al. 2012). Ford & Rush (2011) also found the AICAR effect to be more profound in hypertensive than normotensive rats, possibly due to lower expression or expression of a less active form of AMPK in hypertensive rat tissues. Furthermore, in primary cultures of rat aortic myocytes, several vasoconstrictors as well as acetylcholine were shown to activate AMPK (Horman et al. 2008; Lee & Choi 2013). In the present study, the aorta segments were exposed both to a vasoconstrictor (KCl) and to acetylcholine at the start of the experiments and, in addition, the subject vessels were from normotensive rat. Therefore, the aorta segments may already contained high levels of activated form of AMPK, such that further activation is no longer possible.

The observation that A-769,662 increased both the frequency and averaged amplitude to STOCs suggests that the A-769,662-induced increase in the BK_{Ca} channel current is via activation of ryanodine receptors, since STOCs are triggered by the opening of ryanodine receptors on the sarcoplasmic reticulum. However, regulation of ryanodine receptor activity by AMPK is currently unclear. In primary rat aortic myocytes, AMPK activation was suggested to positively regulate the cAMP-dependent protein kinase (PKA) pathway (Stone et al. 2012) and Wellman et al. (2001) showed that activated PKA increased STOCs in isolated rat cerebral artery myocytes. Thus, it is likely that AMPK activation by A-769,662 can regulate BK_{Ca} channels via the PKA/ryanodine receptor pathway, although this hypothesis requires confirmation.

4.3.5 The reversal of A-769,662 effect by long incubation with glibenclamide

Glibenclamide is a sulphonylurea which is used clinically to control diabetes by inhibiting K_{ATP} channels (see review by Ashcroft 2005). These K_{ATP} channels have been suggested by some to be activated by the presence of PVAT such that opening of K_{ATP} leads to the PVAT anticontractile effect (Löhn et al. 2002; Fang et al. 2009). Additionally,

the AMPK activator AICAR and AMP activate K_{ATP} channels by increasing channel open probability in cardiac cells (Yoshida et al. 2012). Therefore, glibenclamide was used in this study to investigate whether AMPK activator-induced increase in K^+ channel current was in fact due to activation of K_{ATP} channels. Brief exposure (less than 5 min) of aortic myocytes with glibenclamide did not reverse the A-769,662 effect. The lack of effect when glibenclamide was applied for a short time suggests that the AMPK activation by A-769,662 does not lead to activation of K_{ATP} channels. In addition, since K_{ATP} is a voltage-independent channel, any a-769,662-induced K_{ATP} channel opening could be observed as an increased outward current in between potentials -60 and 0 mV which was not observed. Together, these results suggest that, in aortic myocytes, at least, AMPK activation is not linked to K_{ATP} channel opening.

4.3.6 AICAR and PT1

Apart from A-769,662, AICAR and PT1 were also used to determine whether AMPK activators would consistently enhance BK_{Ca} channel activity. The results showed that PT1 did increase BK_{Ca} current, whereas AICAR did not. PT1 and AICAR have very different mechanisms of AMPK activation. AICAR is cell-permeable and has to be converted to ZMP intracellular in order to activate AMPK (Corton et al. 1995). Accumulation of ZMP within the myocytes is essential for activation of AMPK and with 1 mM AICAR, 15 min incubation was required for it to reach its maximum effect (Corton et al. 1995). The lack of AICAR effect observed in my experiments could therefore be due to the inability of the isolated myocytes to convert AICAR to ZMP. Alternatively, myocytes could have metabolized ZMP too rapidly and thus prevented ZMP accumulation. On the other hand, PT1 did increase BK_{Ca} currents. PT1 was discovered in 2008 to be the first small molecule to act directly on the α subunit of AMPK complex to relieve the autoinhibition confirmation of the structure (Pang et al. 2008). The fact that PT1 also increases BK_{Ca} current suggests a link between AMPK activation and BK_{Ca} channels opening.

4.3.7 Conclusion

In this chapter, I have demonstrated an A-769,662-induced increase in BK_{Ca} channel current in both aortic myocytes and mesenteric myocytes; this was sensitive to iberiotoxin (as demonstrated in aortic myocytes), but not to dorsomorphin. Despite the lack of dorsomorphin inhibition, the evidence altogether suggests that this A-769,662 effect is due

to the activation of AMPK. An alternative AMPK activator PT1 also activated BK_{Ca} channels which further support that AMPK activation can indeed lead to BK_{Ca} channel opening.

Chapter 5

Effect of adipocyte-derived factor and adiponectin on vascular myocyte BK_{Ca} channel current

5.1 Introduction

Adiponectin, an endogenous AMPK activator (via adiponectin receptors; Yamauchi et al. 2002), is one of many adipokines released by adipocytes and was originally found to be dysregulated in obesity-linked disorders (Arita et al. 1999). *In vitro*, adiponectin was shown to increase NO production in endothelial cells via activation of AMPK (Chen et al. 2003) and was proposed to be the reason for the vaso-protective effect of adiponectin (Antoniades et al. 2009). In the previous chapter, the effect of AMPK activators on BK_{Ca} channels was investigated – both A-769,662 and PT1 increased $I_{BK(Ca)}$. These data suggest that AMPK activation by adiponectin could also prevent myocyte contraction, at least in part, by activating BK_{Ca} channels. In humans, lower adiponectin levels were observed in patients with diabetes (Yu et al. 2002) and coronary artery disease (Ouchi et al. 1999).

The study described in this chapter aimed to determine whether factors released by PVAT could open myocyte BK_{Ca} channels and whether the effect could be mimicked by adiponectin. The adipocyte-derived hyperpolarising factor (ADHF) appeared to open BK_{Ca} channels in sharp electrode studies (Weston et al. 2013) and so was expected to increase the whole-cell BK_{Ca} channel current in the present study; it was anticipated that this would be mimicked by adiponectin, a putative AMPK activator.

5.2 Results

5.2.1 PVAT released factors that activated $BK_{(Ca)}$ channels

To investigate the anticontractile mechanisms of PVAT-derived factors, PVAT was isolated from rat mesenteric bed and incubated in PSS for 1 h at 37 °C. The bath solution (referred as 'PVAT solution') was then collected and superfused over both mesenteric artery myocytes and aortic myocytes. The small increases in $I_{BK(Ca)}$ and I_K currents induced by the PVAT solution are presented in Figure 5.01.

The PVAT solution significantly enhanced $I_{BK(Ca)}$ in both aortic and mesenteric artery myocytes. At +50 mV, $I_{BK(Ca)}$ was increased from 0.18 ± 0.02 to 0.33 ± 0.07 nA in mesenteric artery myocytes ($n = 5$; $p < 0.001$) and from 0.27 ± 0.03 to 0.49 ± 0.08 nA in aortic myocytes ($n = 9$; $p < 0.001$). The region between -50 and 0 mV of the I_K voltage-current relationship curve was not affected by this PVAT solution.

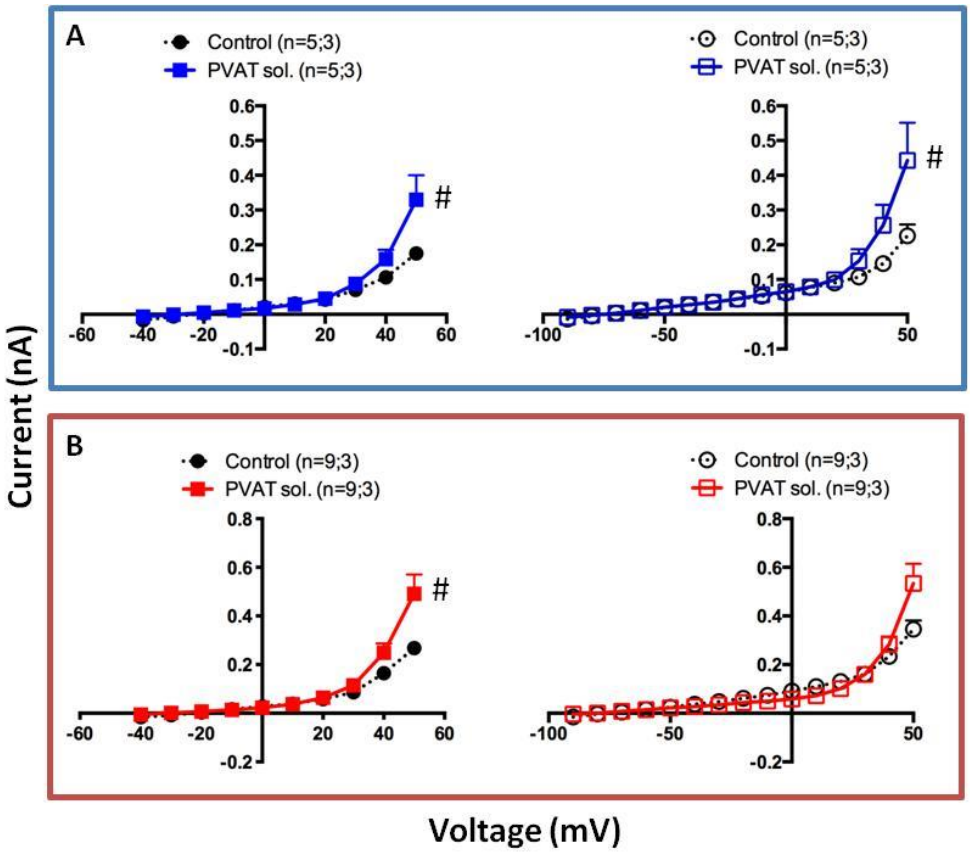

Figure 5.01. Effect of mesenteric perivascular adipose tissue (PVAT) released factor(s) on BK_{Ca} (left) and whole cell K^+ (right) currents in mesenteric artery myocytes (A) and aortic myocytes (B). PVAT was isolated from rat mesentery and incubated in PSS for 1 h at 37 °C. The PVAT was then removed and the remaining bath solution (PVAT sol.) was superfused to freshly isolated myocytes. The bath solution increased BK_{Ca} channel current in both mesenteric artery myocytes (**A**) and aortic myocytes (**B**). The whole cell K^+ current was increased by the bath solution only in mesenteric artery myocytes. # Statistically different from the control data using the non-parametric paired t-tests; $p < 0.05$. n = number of myocytes; number of rats.

5.2.2 Iberiotoxin or low intracellular [Ca^{2+}], but not dorsomorphin, inhibited the ADHF effects

To confirm the activation of $I_{BK(Ca)}$ by the PVAT solution and to investigate the mechanism behind, 100 nM iberiotoxin or 2 μM dorsomorphin was added to the PVAT bath solution after incubation and the solution was superfused over mesenteric artery myocytes. Figures 5.02A and B show how iberiotoxin and dorsomorphin altered the PVAT solution-related effects.

The presence of iberiotoxin completely inhibited the PVAT solution-induced increase in $I_{BK(Ca)}$ (Figure 5.02A). The control peak $I_{BK(Ca)}$ (at 50 mV) was 0.16 ± 0.04 nA (n = 4) and was reduced slightly to 0.09 ± 0.02 nA (n = 4) after PVAT solution with the addition of iberiotoxin (although the reduction was not statistically significant). On the other hand, 2 μM dorsomorphin did not inhibit the PVAT solution effect; superfusion of the PVAT solution with dorsomorphin increased peak $I_{BK(Ca)}$ from 0.23 ± 0.04 to 0.59 ± 0.16 nA (n = 4; $p < 0.01$).

The importance of intracellular Ca^{2+} was determined by lowering the intracellular pipette free Ca^{2+} concentration from 200 nM to 8 nM. The PVAT solution was prepared and superfused to mesenteric artery myocytes as before.

Figure 5.02C shows $I_{BK(Ca)}$ and I_K before and after perfusion of the PVAT solution when intracellular free Ca^{2+} concentration was reduced to 8 nM. The results show that low free Ca^{2+} level completely abolished the PVAT solution effects. The peak $I_{BK(Ca)}$ at control conditions remained similar after superfusion of PVAT solution (0.11 ± 0.01 nA to 0.12 ± 0.02 nA after PVAT solution; n = 6). I_K was significantly reduced after the PVAT solution (n = 6; $p < 0.01$); the maximum effect occurred at 30 mV, where the current increased from 0.13 ± 0.01 nA to 0.09 ± 0.01 nA (n = 6).

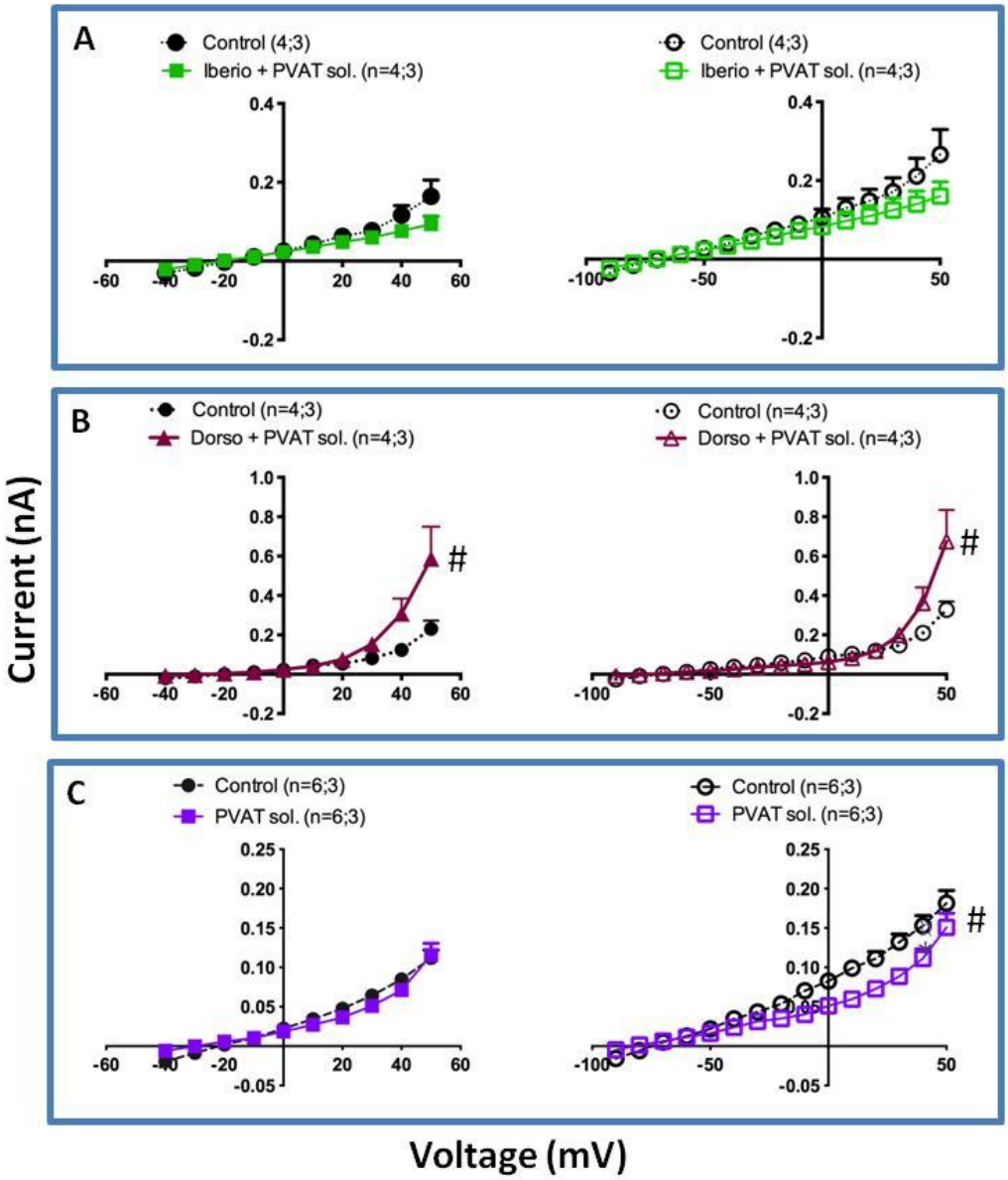

Figure 5.02. Voltage-current relationship curves for BK_{Ca} channels (left) and whole cell K^+ channels in rat mesenteric artery myocytes. A. PVAT isolated from mesentery was incubated with PSS for 1 h at 37 °C. At the end of incubation, 100 nM iberiotoxin (Iberio) was added to the bath solution (PVAT sol.) and superfused over freshly isolated myocytes. In the presence of iberiotoxin, the bath solution did not alter BK_{Ca} or whole cell K^+ channel currents. **B.** In a separate experiment, dorsomorphin (2 μM; Dorso) was added to the bath solution (after incubation) and superfused over the myocytes. In the presence of dorsomorphin, the bath solution significantly increased both BK_{Ca} and whole-cell K^+ channel currents (♯ Significantly different in comparison with control by paired non-parametric t-tests; $p < 0.05$). **C.** Effect of lowering intracellular pipette solution free Ca^{2+} from 200 nM to 8 nM on the K^+ channel currents before (Control) and after PVAT bath solution. When this pipette solution was used, superfusion of the PVAT bath solution did not alter the BK_{Ca} channel current. However, the whole cell K^+ channel current was significantly reduced (♯ As above). n = number of myocytes; number of rats.

5.2.3 PVAT-released factor did not activated K_V7 channels

KCNQ channels on myocytes are suggested to be activated by ADRF which results in myocyte membrane hyperpolarisation (Schleifenbaum et al. 2010). To investigate whether myocyte K_V7 channels are opened by the PVAT solution which resulted in increased I_K, 30 μM XE-991 was added to the PVAT solution and applied to mesenteric artery myocytes. XE-991 is a potent and specific K_V7 channel blocker (Zaczek et al. 1998).

Figure 5.03 shows that XE-991 had no effect on the PVAT solution-induced increase in $I_{BK(Ca)}$ and I_K. In the presence of XE-991, superfusion of the PVAT solution continued to have a significant positive effect on $I_{BK(Ca)}$ as the peak current was increased 67 % from 0.18 ± 0.05 to 0.30 ± 0.07 nA (n = 5; P < 0.01) after the PVAT solution. This was similarly observed for I_K where peak current was significantly increased from 0.22 ± 0.04 to 0.35 ± 0.10 nA (n = 5; p < 0.01). XE-991 on its own did not affect $I_{BK(Ca)}$ – peak $I_{BK(Ca)}$ was left unaltered (0.18 ± 0.05 nA; n = 5 before XE-991 to 0.19 ± 0.05 nA after; n = 5).

5.2.4 H_2O_2 was not responsible for increasing BK_{Ca} currents

Catalase catalyzes the breakdown of H_2O_2 and can therefore inhibit any effects related to H_2O_2. PVAT was isolated from rat mesenteric as before and was incubated in PSS either with or without catalase (1000 U/ml) for 1 h at 37 °C. Figure 5.05A shows the effect of PVAT solutions with or without catalase on mesenteric artery myocytes. Figure 5.05B shows the effects of 1000 U/ml catalase alone on the BK_{Ca} channel voltage-current relationship. Catalase was incubated in PSS for 1 h at 37 °C.

The presence of catalase did not prevent the increase in $I_{BK(Ca)}$ by the PVAT solution. The peak $I_{BK(Ca)}$ was increased by 118 % to 0.28 ± 0.13 nA (n = 4; p < 0.05). Catalase on its own did not alter $I_{BK(Ca)}$ channels, as peak $I_{BK(Ca)}$ remained at similar levels (0.20 ± 0.06 nA before versus 0.25 ± 0.10 nA after catalase; n = 3).

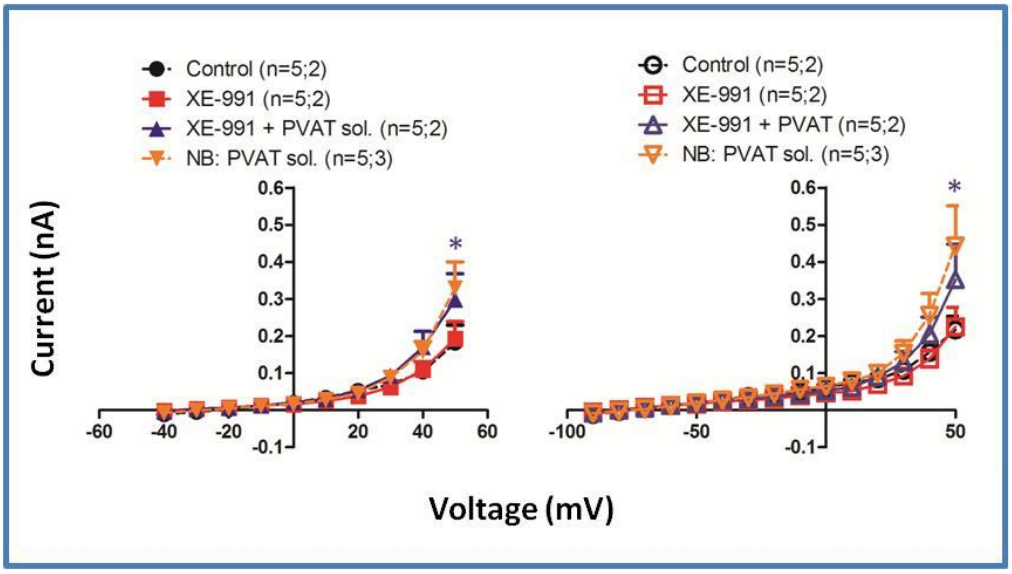

Figure 5.03. Effects of 30 μM XE-991 on perivascular adipose tissue (PVAT)-induced current changes in mesenteric arteries myocytes. Myocytes BK_{Ca} current (left graph) and whole cell K^+ current (right) was measured with the superfusion of physiological saline solution (PSS) (Control), in the presence of XE-991 or the PVAT bath solution with the addition of 30 μM XE-991. XE-991 did not significantly alter BK_{Ca} or whole cell K^+ channel activity. In the presence of XE-991, PVAT bath solution significantly increased both BkCa and whole cell K+ channel currents (* Statistically different at the indicated point in comparison with control by two-way repeated measures ANOVA followed by post-hoc Bonferroni test; $p < 0.05$). **NB.** PVAT sol. curves were taken from Figure 5.01A and displayed here for comparison and were not statistically compared with rest of the data. n = number of myocytes; number of rats.

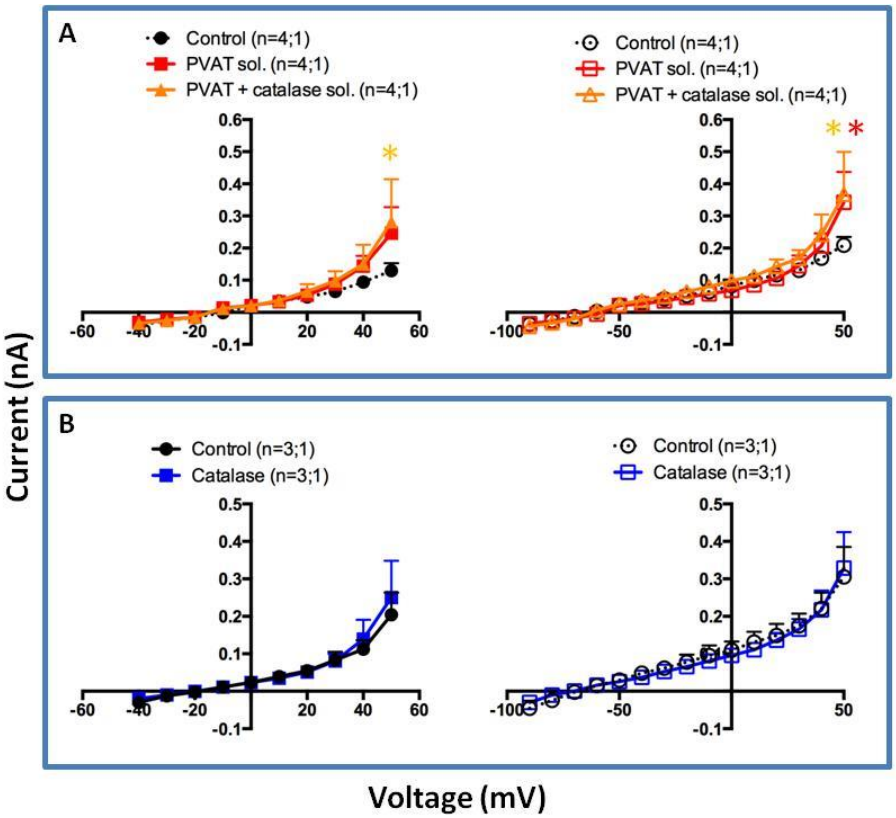

Figure 5.04. Effect of 1000 U/ml catalase on perivascular adipose tissue (PVAT) bath solution (PVAT sol.)-induced current changes in mesenteric artery myocytes. A. Isolated mesenteric PVAT was incubated for 1 h at 37 °C with or without catalase. The PVAT bath solution significantly increased whole cell K^+ currents (* Statistically different at the indicated points from control by two-way repeated measures ANOVA followed by post-hoc Bonferroni test; $p < 0.05$). In the presence of catalase, PVAT bath solution continued to enhance BK_{Ca} channel and whole cell K^+ current (* As above). **B.** Catalase (incubated in PSS for 1 h at 37 °C) did not affect basal BK_{Ca} channel or whole cell K^+ currents. n = number of myocytes; number of rats.

5.2.5 Activation of β3 adrenoceptors by CL-316,243 did not enhance the PVAT effect

Adipocytes express high levels of β3 adrenoceptors (Langin et al. 1991). To determine if stimulating these adrenoceptors would increase the release of hyperpolarising factors from adipocytes, CL-316,243 (a selective β3 adrenoceptor activator) was used. PVAT was isolated from rat mesentery as before and half was incubated (1 h at 37 °C) in PSS, while the other half was similarly incubated in PSS containing 10 μM CL-316,243 (referred as 'PVAT & CL-316,243 solution'). After incubation, the bath solutions were superfused to mesenteric artery myocytes.

Figure 5.05A shows the BK_{Ca} and whole cell K^+ channel voltage-current curves under control conditions and after exposure to the two different PVAT solutions. As before, PVAT solution significantly increased $I_{BK(Ca)}$ by 160 % from 0.19 ± 0.03 to 0.50 ± 0.17 nA ($n = 3$; $p < 0.01$). With the addition of CL-316,243, the PVAT solution-related effect was slightly enhanced ($I_{BK(Ca)}$ at 50 mV was increased to 0.7 ± 0.2 nA; $n = 3$), but this change was not significant (by repeated measures two-way ANOVA tests).

To assess whether CL-316,243 affects BK_{Ca} channels by itself, 10 μM CL-316,243 was incubated in PSS for 1 h at 37 °C and the bath solution was then superfused over mesenteric myocytes. Figure 5.03B shows that applying this solution to the mesenteric myocytes produced no changes in current amplitudes were observed (peak current from 0.19 ± 0.05 to 0.22 ± 0.08 nA after CL-316,243; $n = 4$).

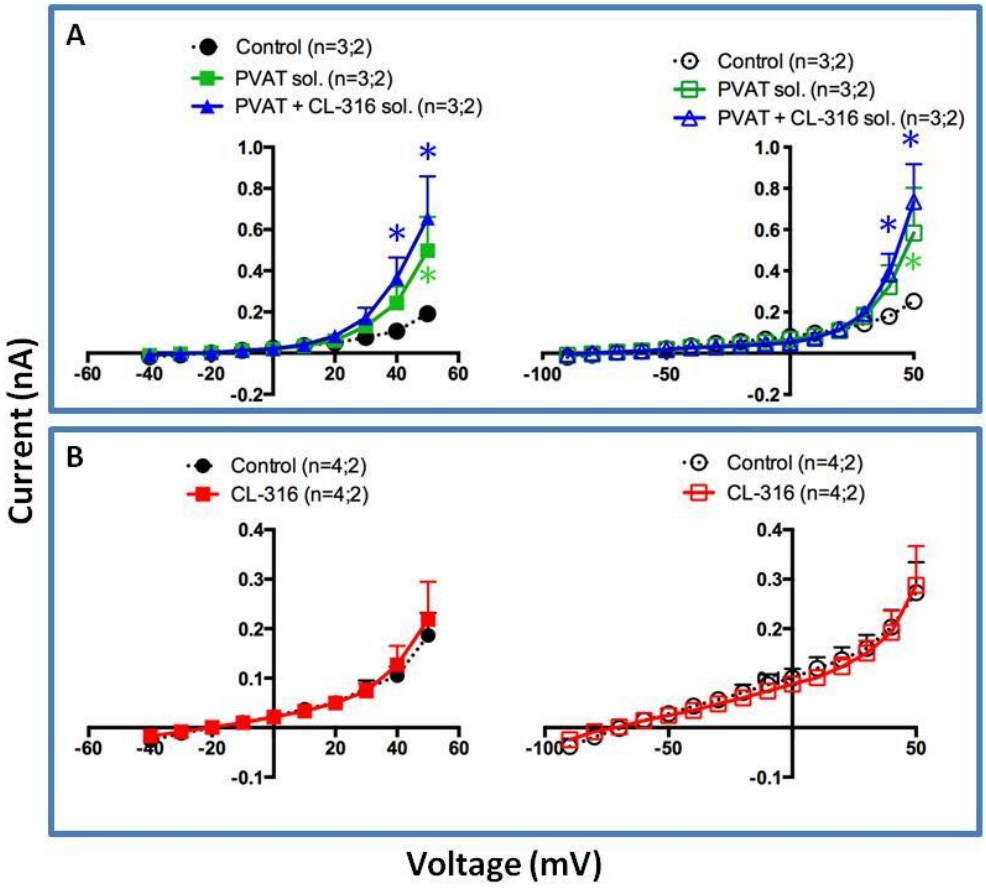

Figure 5.05. Effect of β3 adrenoceptor stimulation by CL-316,243 (CL-316) on perivascular adipose tissue (PVAT)-derived factor(s) with rat mesenteric artery myocytes. A. Myocyte BK_{Ca} channel (left) and whole cell K^+ (right) current before and after superfusing cells with two different solutions: PVAT (from rat mesenteric bed) incubated in PSS (PVAT sol.) or PVAT incubated in PSS containing 10 μM CL-316,243 (PVAT + CL-316). Both solutions increased K^+ currents (* Statistically different at the relevant points from the control by repeated measures two-way ANOVA tests followed by Bonferroni post-hoc tests; $p < 0.05$). **B.** CL-316,243 alone (incubated in PSS for 1 h at 37 °C) did not affect BK_{Ca} channel or whole cell K^+ currents. n = number of myocytes; number of rats.

5.2.6 The PVAT anticontractile effect is lost in adiponectin-deficient mouse mesenteric arteries

The importance of adiponectin in vascular tone control was investigated using mesenteric tissue collected from adiponectin deficient mice. Figure 5.06 shows cirazoline concentrations response curves for PVAT-free and PVAT-intact vessels in control (A) and adiponectin gene knockout mouse (B) mesenteric arteries.

In control mouse vessels, PVAT-intact vessels demonstrated lower contractility responses to cirazoline when compared with PVAT-free vessels – cirazoline pEC50 values of 6.15 ± 0.17 and 5.90 ± 0.26 for PVAT-denuded and PVAT-intact vessels, respectively (Figure 5.06A). The maximum percentage of contraction was also reduced by PVAT from 112 ± 3 % (n = 4) to 66 ± 10 % (n = 5). The PVAT anticontractile effect was statistically significant by repeated t-tests ($P < 0.001$). Adiponectin deficient mouse PVAT no longer displayed any anticontractile properties on isolated mesenteric arteries (Figure 5.06B). Cirazoline pEC_{50} values were identical (7.0 ± 0.18 for PVAT-denuded and 7.0 ± 0.13 for PVAT-intact vessels). The maximum percentage vessel contractility was unaffected by the presence of PVAT (PVAT-free vessels 128 ± 12 %, PVAT-intact vessels 112 ± 4 % of 60 mM KCl constriction, each n = 4).

For adiponectin deficient vessels, addition of 10 μM CL-316,243 significantly reduced vessel contraction only in PVAT-intact vessels: cirazoline pEC_{50} value reduced from 7.0 ± 0.13 before CL-316,243 to 6.5 ± 0.16 after (n = 3-4); maximum percentage of contraction was also reduced from 112 ± 4 % to 79 ± 8 % (n = 3-4); this CL-316,243 effect was significant by repeated measures two-way ANOVA tests ($p < 0.01$).

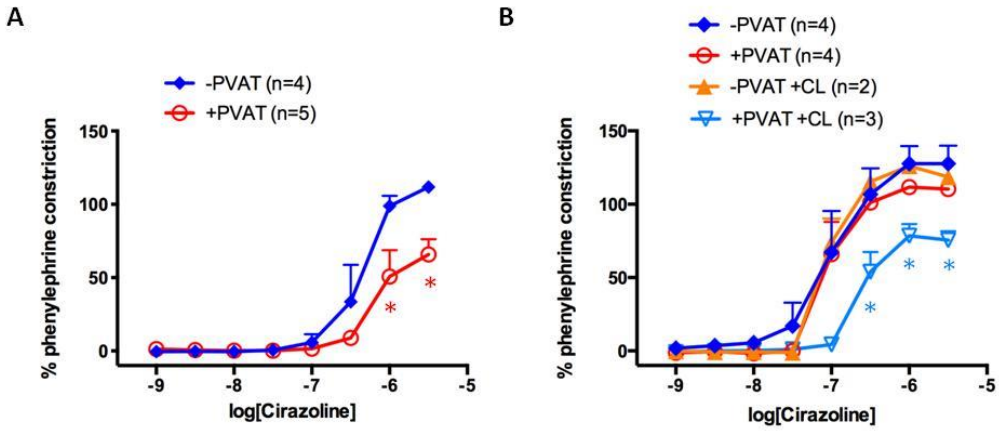

Figure 5.06. Cirazoline concentration-response curves of mesenteric arteries without (-) or with (+) perivascular adipose tissue (PVAT) from control mice (A) or adiponectin-deficient mice (B). A. The PVAT anticontractile effects can be observed in mesenteric arteries isolated from control mice (* Significantly different at the relevant points from PVAT-denuded vessels using repeated non-parametric paired t-tests; $P < 0.05$). **B.** The anticontractile effect of the PVAT was lost in adiponectin-deficient mouse tissue. CL-316,243 caused rightward shift in the concentration-response curves only when PVAT was present (* Significantly different from perivascular adipose tissue-intact vessels using repeated measures two-way ANOVA tests; $p < 0.05$). All vessels were a mixture of endothelium-free and endothelium-intact vessels.

5.2.7 Adiponectin also caused an increase in $I_{BK(Ca)}$

The effects of adiponectin (5 μg/ml) on currents in mesenteric artery myocytes and aortic myocytes are illustrated in Figure 5.07A and B, respectively. Adiponectin caused a leftward shift in the current-voltage relationship curve for $I_{BK(Ca)}$ for both cell types. In mesenteric artery myocytes, peak $I_{BK(Ca)}$ at 50 mV was 0.19 ± 0.02 nA (n = 7); after adiponectin, this peak current was significantly increased to 0.46 ± 0.12 nA (n = 6). The presence of dorsomorphin did not affect the adiponectin effect (peak current 0.42 ± 0.08 nA, n = 5). Similar responses were observed in aortic myocytes. The initial $I_{BK(Ca)}$ at +50 mV (0.33 ± 0.08 nA) was significantly increased (to 0.59 ± 0.12 nA) after adiponectin and at 0.71 ± 0.27 nA, was significantly greater than the control current in the additional presence of dorsomorphin (n = 3 for all).

5.2.8 Adiponectin did not increase the spontaneous transient outward currents

STOCs before and after adiponectin were recorded from one single myocyte and the data presented in Figure 5.08. At the holding potential of -20 mV, 5 μg/ml of adiponectin did not produce any changes to the amplitude or frequency of STOCs.

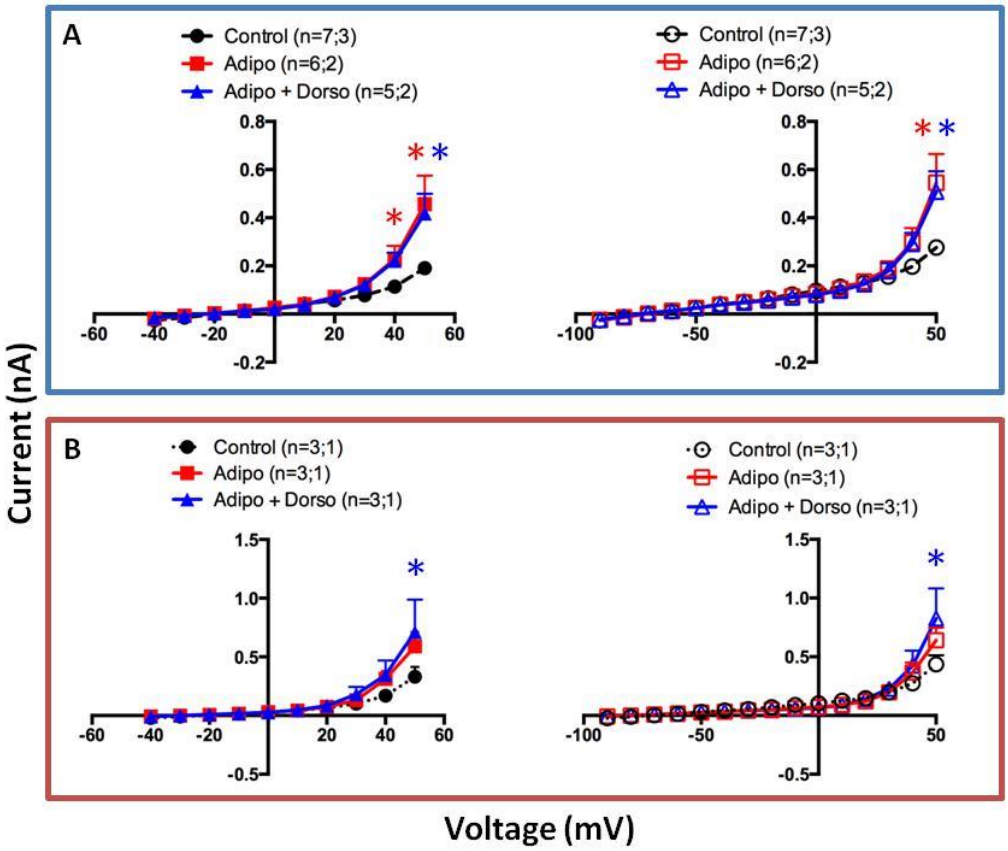

Figure 5.07. Effects of adiponectin (Adipo; 5 µg/ml) and dorsomorphin (Dorso; 2 µM) on BK_{Ca} channel current (left) and whole cell K^+ current (right) using freshly isolated mesenteric artery myocytes (A) and aortic myocytes (B). A. Adiponectin increased both BK_{Ca} channel and whole-cell K^+ channel current and this was not affected by the presence of dorsomorphin (* Significantly different at the relevant data point in comparison with control by repeated measures two-way ANOVA tests; $p < 0.05$). **B.** In aortic myocytes, adiponectin with dorsomorphin increased BK_{Ca} and whole cell K^+ currents (* Same as above).

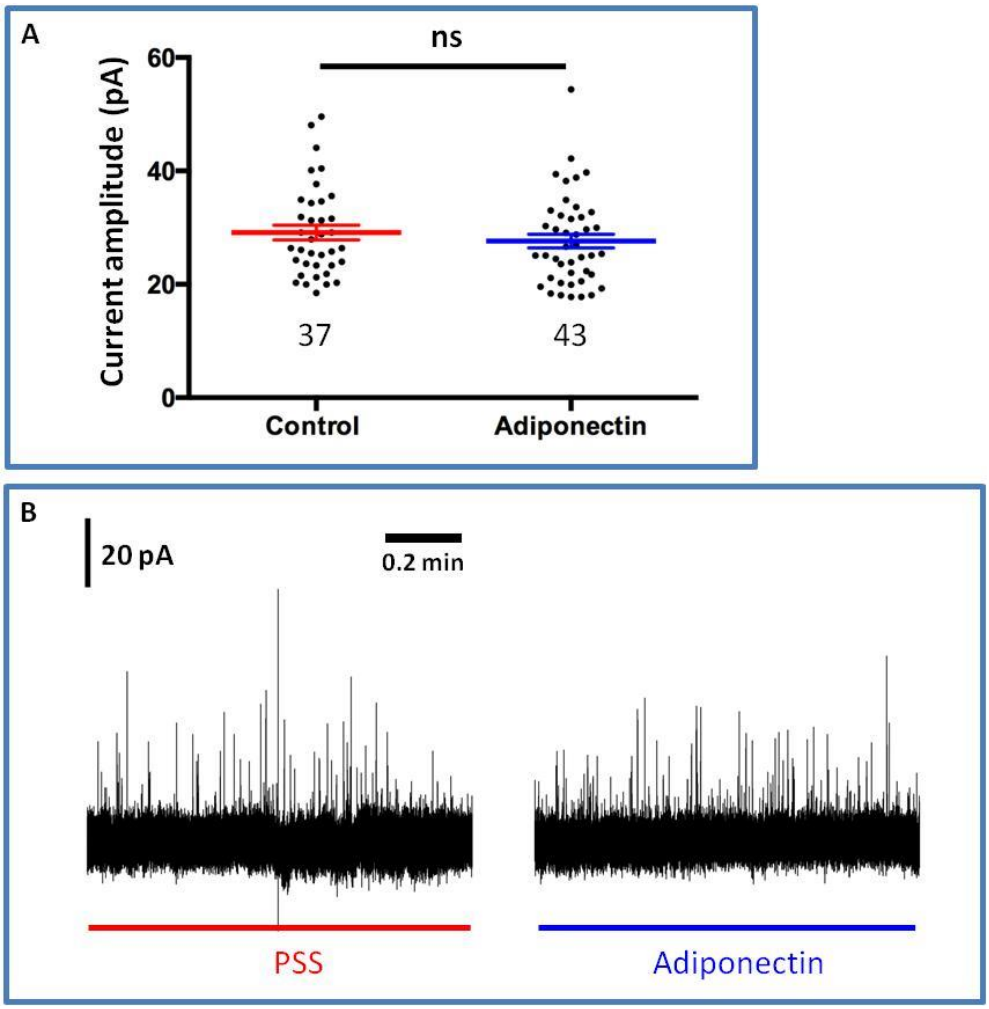

Figure 5.08. Spontaneous transient outward currents (STOCs) in a mesenteric artery myocyte before and after 5 µg/ml adiponectin. STOCs were recorded at the holding potential of -20 mV. **A.** The STOC amplitude from one single myocyte. The dots on the scatter diagrams represent the amplitudes of individual STOCs recorded within 1 min duration. The coloured lines represent mean ± SEM. The numbers below the dots represent the total number of STOCs within the 1 min duration. **B.** Current traces recorded in the myocyte when perfused with physiological saline solution (PSS) or adiponectin. ns: non-significantly different using non-parametric t-test.

5.3 Discussion

5.3.1 PVAT-derived adipocyte-derived hyperpolarisation factor

The results presented in this section so far suggest that mesenteric artery PVAT is able to release a factor or factors, which can activate channels that were sensitive to iberiotoxin. Furthermore, removal of intracellular Ca^{2+} also abolished the effect of ADRF. Together, these data suggest that this factor activates BK_{Ca} channels in vascular myocytes. By activating BK_{Ca} channels, this factor causes membrane hyperpolarisation and is therefore termed adipocyte-derived hyperpolarisation factor (ADHF), as suggested by Weston et al 2013. The release of ADHF does not require any external stimulation and these factors are relatively stable (they remained active for up to five hours, the duration of the experiments). It is likely that these ADHFs detected in this project are the same as the ADRFs described in other studies (Löhn et al. 2002; Verlohren et al. 2004; Gao et al. 2007; Schleifenbaum et al. 2010). The identity of this or these ADRF factors is currently unknown and is very much in debate, although it is commonly agreed that they can activate K^+ channels expressed on the vascular myocytes. The putative K^+ channel activated by ADRFs include: K_V7 channels (Schleifenbaum et al. 2010); K_V channels (Verlohren et al. 2004); K_{ATP} channels (Löhn et al. 2002); SK_{Ca} and IK_{Ca} channels (Gao et al. 2007). In the present study, ADRF activates BK_{Ca} channels which agree with the conclusions drawn by several previous studies (Lynch et al. 2013; Weston et al. 2013). The superfusion of myocytes with the PVAT bath solution did not affect the current in between voltages of -50 to 0 mV of the whole cell K^+ current. As introduced in Chapter 4, BK_{Ca} channels are not activated within those voltages and any current recorded within this region is due to opening of other K^+ channels. Thus, this result suggests that none of the other K^+ channels are activated by ADHF.

Although the original aim of this project was not to elucidate the identity of ADHF, a few attempts were made to narrow down the possibilities. H_2O_2 was originally identified to be released from endothelium cells, and had been proposed to be an endothelium-derived hyperpolarisation factor (Yada et al. 2003). Gao et al. (2007) suggested that adipocytes also released H_2O_2 and caused endothelium-independent vessel relaxation. There are several possible ways H_2O_2 may cause vessel relaxation (see review by Shimokawa 2010), one of them is via activation of BK_{Ca} channels, as observed in both porcine (Barlow & White 1998) and human (Liu et al. 2011) coronary arteries. Thus, the increase in BK_{Ca} current by PVAT-release factor observed in this study may be the result of H_2O_2 release

from adipocytes. However, catalase failed to prevent ADHF effects on BK_{Ca} channels, suggesting that ADHF is not H_2O_2.

H_2S has received attention from two groups as the putative ADRF (Fang et al. 2009; Schleifenbaum et al. 2010; Köhn et al. 2012). Gollasch and co-workers (Schleifenbaum et al. 2010; Köhn et al. 2012) proposed that H_2S is produced by adipocytes and that it acts via opening K_V7 channels on the smooth myocytes. This group based its conclusion primarily on the observations that XE-991 (30 μM) reversed the anticontractile effects of PVAT in rat aorta. XE-991 is a potent K_V7 channel blocker (with IC_{50} values of less than 1 μM; Wang 1998). It is only selective at lower concentrations (it can block K_V4 channels with an IC_{50} value of 43 μM; Wang 1998) and therefore is generally used at less than 10 μM (Jepps et al. 2009; Ng et al. 2011). At a concentration of 30 μM (used by Schleifenbaum et al. 2010 and Köhn et al. 2012), other K^+ channels may be effected; thus, any depolarisation or contraction effects caused by 30 μM XE-991 should be treated with caution. Nevertheless, in this project, 30 μM XE-991 did not inhibit ADHF-related increase in BK_{Ca} channel currents. Therefore, under the conditions employed in the present study, ADHF does not activated K_V7 channels. Additionally, Köhn et al. (2012) drew their conclusion that H_2S is important for the PVAT anticontractile effect because pharmacological inhibition of CSE (cystathionine γ-lyase; a H_2S-producing enzyme) reversed the PVAT effect. However, using rat mesenteric arteries, preliminary data with CSE inhibitor DL-propargylglycine in the present study showed that it did not reverse the white PVAT anticontractile effects in rat mesenteric arteries (data not shown). Most of the experiments carried out by Schleifenbaum et al (2010) and Köhn et al (2012) were done with aortic PVAT which is surrounded by brown fat. Therefore, although the data presented here provide no evidence to support a role for H_2S in the control of vascular tone by white PVAT, it does not exclude the possibility that H_2S may be released by brown adipocytes to reduce vessel contractility.

5.3.2 Adiponectin

Growing numbers of studies have now shown adiponectin to contribute to the hyperpolarising and/or relaxant effects of PVAT (Greenstein et al. 2009; Lynch et al. 2013; Weston et al. 2013). *In vivo* administration of adiponectin to mice reduces plasma free fatty acid, glucose levels and promotes weight loss without affecting food intake (Fruebis et al. 2001). The importance of adiponectin in vascular tone has been demonstrated in this project with mesenteric arteries isolated from adiponectin-deficient mice. Tension studies

with these vessels showed that PVAT had lost its anticontractile effects. Additionally, PVAT from adiponectin-deficient mice had no effect on wild type mesenteric arteries, the anticontractile effect remained absent (Lynch et al. 2013). Together, these data highlight the importance of adiponectin in PVAT basal vascular tone control.

The biological effects of adiponectin have been proposed to be mediated, at least partly, by activation of AMPK (Tomas et al. 2002; Yamauchi et al. 2002; Wu et al. 2003). Similar to the majority of the AMPK activators, adiponectin also activated BK_{Ca} channels in the present study. Again, dorsomorphin failed to reverse this adiponectin-induced increase in BK_{Ca} channel activity; the reasons are unknown, but were speculated in Chapter 4. Hence, the absolute involvement of AMPK in the adiponectin-induced effects remains to be confirmed. To elucidate the anticontractile mechanism of adiponectin further, mesenteric artery myocyte STOCs were recorded before and after adiponectin on one myocyte (due to time restrictions). The lack of effect of adiponectin on STOCs suggests that different from A-769,662, adiponectin-induced increase in BK_{Ca} channel current is not by activation of the ryanodine receptors. The difference between A-769,662- and adiponectin-induced opening of BK_{Ca} channels may be due to differences in the intracellular pathways involved. While A-769,662 can directly activate AMPK, adiponectin-induced AMPK activation is via recruitment of adapter proteins (see review Buechler et al. 2010).

The fact that superfusing adiponectin over isolated vascular myocytes generated similar effects on the BK_{Ca} channels as ADHF, it is very likely that adiponectin is in fact the ADHF. However, the direct evidence to show the link between the two is still lacking. This is limited by the lack of knowledge on the mechanism of adiponectin released from adipocytes. Thus, the only method to inhibit the release of adiponectin is via genetically modified mice, which may not readily available.

5.3.3 β3 adrenoceptor stimulation and PVAT anticontractile functions

The results discussed so far have suggested that PVAT can release ADHF under basal conditions (i.e. constitutive release of ADHF). In Chapter 3, NO assay results showed that CL-316,243 did not increase NO release from PVAT. Additionally, L-NMMA did not completely the reverse CL-316,243-induced reduction in vessel contractility. Thus, CL-316,243 further stimulates the release of a factor which is different from NO. Several previous studies have administered CL-316,243 chronically to rodents and found β_3-adrenergic stimulation increases resting metabolic rates and insulin sensitivity, and

therefore has beneficial anti-diabetic and anti-obesity effects (Yoshida et al 1994; Ghorbani et al. 1997; Grujic et al. 1997). β3 adrenoceptor activation also lowers blood pressure in vivo (Shen et al. 1996). While this may be due to an endothelium-dependent release of NO as observed in human coronary arteries (Dessy et al. 2004) and rat thoracic aorta (Trochu et al. 1999), data from our lab also indicate an endothelium-independent effect. Weston et al. (2013) have demonstrated that CL-316,243 caused endothelium-independent vascular myocyte hyperpolarisation. In tension studies with endothelium-denuded rat mesenteric arteries, Egner showed that CL-316,243 incubation with PVAT-intact vessels increased the anticontractile effects of PVAT (Egner 2012). Therefore, it was predicted that CL-316,243 incubation with PVAT would enhance the release of ADHF, leading to a further activation of BK_{Ca} channels. It is therefore somewhat surprising that, in the present study, CL-316,243 incubated with PVAT did not further increase BK_{Ca} current. It is possible that CL-316,243 increased ADHF release from PVAT, but the experimental system was not sensitive enough to pick up the change. PVAT was incubated in an excess amount of PSS and thus, may have dampened down the increased release of ADHF via dilution. In intact vessels, the ADHF release is more localised and ADHF may reach a higher concentration in the restricted space between the PVAT and myocytes, thus, the CL-316,243 may produce a greater effect.

Fu et al. (2008) found blood serum adiponectin levels to be increased by chronic *in vivo* administration of CL-316,243 to obese and diabetic mice. The importance of adiponectin to the CL-316,243 responses was observed when Weston et al. (2013) showed that CL-316,243 failed to cause hyperpolarisation in tissues collected from adiponectin-deficient mice. However, in the present study, β3 adrenoceptor stimulation with CL-316,243 on adiponectin-deficient mouse PVAT was able to elicit an anticontractile effect in mesenteric arteries, which could be due to CL-316,243 triggering endothelium-dependent relaxation (as observed by Dessy et al. 2004; Trochu et al. 1999).

5.3.4 Conclusion

Rat mesenteric PVAT has been demonstrated to release a factor that can activate BK_{Ca} channels. The identity of this factor is still unknown, although H_2O_2 and H_2S are unlikely to be responsible for the effects observed. Adiponectin-deficient mouse PVAT did not produce anticontractile effects and superfusion of adiponectin increased BK_{Ca} channels activity. Thus, adiponectin may be the ADHF which activates BK_{Ca} channels on the myocytes leading to cell membrane hyperpolarisation. β3 adrenoceptor activation by CL-

316,243 with rat mesenteric PVAT did not enhance the BK_{Ca} channel-opening effects of PVAT. Furthermore, CL-316,243 exerted an anticontractile effect in adiponectin-deficient PVAT, suggesting the release of an additional relaxing factor from the PVAT.

5.4 Future experiments

Dorsomorphin failed to reverse the effects of A-769,662, PT1, adiponectin and ADHF on BK_{Ca} channels; which may doubt the involvement of AMPK. However, the coherent effects of A-769,662, PT1 (both well established AMPK activators) and adiponectin (a putative AMPK activator) strongly suggest that the increase in BK_{Ca} channel current is indeed via AMPK activation. The reason why dorsomorphin did not show an effect in these experiments is currently unknown, and could be because of the experimental conditions (i.e. temperature) or a less selective nature of dorsomorphin. The lack of alternative AMPK inhibitors is a major limitation within the field of AMPK research. This limitation could be overcome by using an AMPK knockout mouse (use of these mice has been demonstrated in numerous studies, such as Goirand et al. 2007; Wang et al. 2011). Electrophysiology experiments could therefore be repeated to assess whether adiponectin or ADHF are able to open BK_{Ca} channels with tissue from these AMPK-deficient mice.

Chapter 6

Attempts to generate an inducible knockout mouse

6.1 Introduction

cGMP-dependent protein kinase G (PKG), activated by an increase in cGMP levels, is important for regulation of many aspects of biological processes. There are two isoforms of PKG: PKGI (Sandberg et al. 1989) and PKGII (Uhler 1993). PKGI is present at high concentrations in smooth muscle cells, cerebellum, hippocampus and kidney (Feil et al. 2005; Lohmann et al. 1981). In vascular endothelium, cardiac cells and brain nuclei, low levels of PKGI can also be found (Feil et al. 2005). PKGII is present in intestinal mucosa and has wide distribution in the central nervous system, but is absent in vascular myocytes (de Vente et al. 2001; Lohmann et al. 1981). The importance of PKG is displayed in PKG knockout mice, which display a wide range of defects including multiple cardiovascular, gastrointestinal and neuronal disorders, leading to early mortality (Pfeifer et al. 2006; Pfeifer et al. 2008).

PKGI exists as two different isoforms (PKGIα and PKGIβ) due to the alternative splicing at the N-terminus (see review Hofmann et al. 2006). Endothelium releases NO, which activates soluble guanylyl cyclase in vascular myocytes to produce cGMP. Elevated levels of cGMP then activate PKGI, resulting in vasorelaxation. Thus, PKGI is essential for vasodilation – the absence of which is associated with an elevated blood pressure in rodents (Pfeifer et al. 1998). More recently, preliminary data showed PKG1 knockout mouse mesenteric PVAT demonstrated a loss of anticontractile activity and as a result, mesenteric arteries from these mice displayed an increased vasoconstrictor response to norepinephrine (Withers et al. 2011). Thus, it seems that PKGI also plays a role in PVAT-dependent vasorelaxation. However, the ubiquitous expression of PKGI in both vascular myocytes and adipocytes makes the function of PKGI in the normal anticontractile activity of PVAT difficult to determine. Additionally, the PKGI knockout mice have intestinal dysfunction and demonstrate caecal dilatation as well as pyloric stenosis; these mice, therefore, are unsuitable for long-term studies.

The disadvantage of the classical gene knockout system can be overcome by deleting the target gene in a spatio-temporal manner – i.e. inducible PKGI gene deletion restricted to smooth muscle cells. Such a tissue-specific and inducible gene knockout mouse model can be generated by adopting the Cre/loxP recombination system, in which the targeted PKGI gene is flanked (or ‘floxed’) by two recombinase recognition sites (loxP sites). The Cre enzyme, a member of the recombinase family, can excise the DNA segment flanked by the two loxP sites; thus, deleting the gene segment in between. Cre expression can be

controlled and tight regulation of Cre expression is therefore critical to the success of this inducible mouse model. The spatial control of Cre expression can be achieved by directing Cre activity to the cells of interest. In this case, Cre can be added to the endogenous SM22 gene, the expression only occurs in smooth muscle cells in adult mice (Kühbandner et al. 2000). To control Cre expression in a temporal manner, Cre is fused to the ligand-binding domain of a steroid receptor. Expression of Cre is initiated when an appropriate synthetic ligand (e.g. tamoxifen) is present.

This chapter describes the process of genotyping mice and selecting those that meet the criteria for tamoxifen injection. The genotype of the injected mice will be presented in the results section to confirm whether or not PKGI is successfully deleted.

6.2 Methods

6.2.1 Mouse models

To generate inducible PKGI mice, two mouse models were initially used: a transgenic mouse line with homozygous L2/L2 (loxP sites flanking exon 10 is known as the L2 allele; Wegener et al. 2002) and a second knockin mouse that expresses an inducible Cre recombinase under the SM22 promoter (SM22-Cre-ERT2) (Kühbandner et al. 2000). These two different mice were then bred with a heterozygous +/L1 mouse, carrying one wild-type allele (+) and one L1 allele where the two loxP sites were already recombined to delete exon 10 in order to generate a knockout allele. All of these mouse models were developed by Dr M Werner, University of Manchester. The offspring mice were with a mixture of genotypes and reverse transcription polymerase chain reaction (RT-PCR) was used to determine their genetic composition.

6.2.2 DNA extraction from ear punch samples

The offspring DNA was obtained from ear punch samples by digesting the tissue in 500 µl of lysis buffer (see later section 6.2.5) for 2 hours at 56 ºC. After this digestion period, 280 µl of saturated NaCl solution was added and centrifuged for 1 min at 13000rpm (revolution per minute). Then, 300µl of the supernatant was transferred to a fresh eppendorf tube with 300 µl of isopropanol and was centrifuged further for 10 min at 13000 rpm, after which the supernatant was discarded and the remaining pellet was air dried before addition of 250 µl of RNase-free H_2O. The resuspended samples were stored at -20 ºC until required.

6.2.3 Reverse transcription polymerase chain reaction

6.2.3.1 PKGI L2 and L1 alleles

The extracted DNA samples were first amplified for PKGI L2 and L1 alleles. The DNA amplification solution contains (in mM, unless otherwise stated; all from Bioline, UK): BIOTAQ DNA polymerase (Bioline) 0.06 U/µl; dNTPs 1; $MgCl_2$ 1.5. Two pairs of primers (one forward primer plus two different reverse primers; see Table 6.01) were added to the mixture to a final concentration of 0.25 µM each. DNA samples (3 µl), extracted from ear punch samples, were added to the mixture to give a final volume of 25 µl. To visualize the bands, 5 µl of loading dye was added to the final PCR mixture. PCR conditions were: 94 °C for 5 min; 35 cycles of 94 °C 10 s, 55 °C 45 s, 72 °C 30 s followed by a final elongation stage at 72 °C for 5 min. PCR products were electrophoresed on 1% agarose gels (weight/volume) containing 0.5 µg/ethidium bromide (Sigma-Aldrich, UK) with the presence of TBE electrophoresis buffer.

Gene	Primer sequence	Size (bp)
Wild-type/L2	Forward CCT GGC TGT GAT TTC ACT CCA Reverse GTCAAGTGACCACTATG	284/338
KO	Forward CCT GGC TGT GAT TTC ACT CCA Reverse AAA TTA TAA CTT GTC AAA TTC TTG	250

Table 6.01. The primers table. All supplied by Eurofin, UK.

Wild-type offspring mice DNA produced two PCR bands as observed for mouse number 2, 10,11, 12 and 14 in Figure 6.01. The appearance of two bands was due to the alternative splicing of the PKG1 gene which resulted in mRNA with two different lengths. Some mice (such as mouse number 4, 5 and 6) were L1/L1 (PKGI knockout); while others were L2/L1 (mouse number 1, 3, 7, 8, 9, 13 and 15). Samples from offspring mice with L2/L1 genotype were further tested by RT-PCR for Cre expression.

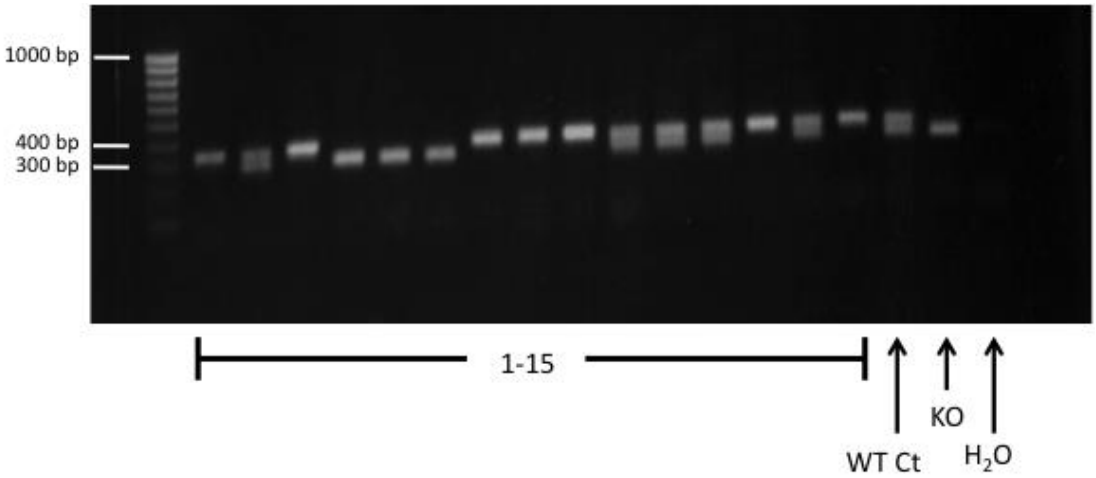

Figure 6.01. Reverse transcription polymerase chain reaction analysis of the expression of L2 and L1 alleles of fifteen mice (labeled 1 to 15). The first lane is the DNA molecular weight standard control at 100 bp intervals. The final three lanes are wild-type genotype control (WT Ct), complete knockout control (KO) and H_2O negative control (H_2O).

6.2.3.2 Cre

The DNA amplification solution for Cre contained (in mM, unless otherwise stated; all from Bioline, UK): BIOTAQ DNA polymerase 0.04 U/µl; dNTPs 1; $MgCl_2$ 1.8. A pair of primers (see Table 6.02) were added to the mixture at a final concentration of 0.5 µM each. A volume of 3 µl of the same DNA sample (extracted from ear punch tissues) was added to the amplification solution to give a final volume of 25 µl. PCR conditions were: 94 °C for 2 min; 35 cycles of 94 °C 20 s, 57 °C 30 s, 72 °C 1 min followed by a final elongation stage at 72 °C for 10 min. The amplified DNA samples were ran on 1 % agarose gels as before. The appearance of a Cre band (as for mice 7, 8, 13 and 15) confirmed the expression of Cre.

Gene	Primer sequence	Size (bp)
Cre	Forward CCA ATT TAC TGA CCG TAC ACC Reverse GTT TCA CTA AGG TTA CGG	1000

Table 6.02. The primers for Cre. Supplied by Eurofin, UK.

6.2.4 Inducing PKGI knockout

Offspring mice which were L2/L1 and Cre positive (such as mouse number 7, 8, 13 and 15) as well as L2/L1 and Cre negative were injected with 3 mg tamoxifen per day on 5 consecutive days to activate the Cre recombinase. L2/L1- and Cre-negative mice (such as mouse number 1,3 and 9) were similarly injected with tamoxifen and served as negative controls. The injection solution was prepared by dissolving 40 mg of tamoxifen (Sigma-Aldrich, UK) in 200 µl of ethanol and 800 µl of sunflower oil. After the injections, the mice were kept under normal conditions and carefully monitored for 3 weeks, before they were killed by a Schedule 1 method and their bladders were taken out.

The urothelium layer of the bladder (consisting mainly of epithelial cells) was carefully cut free from the rest of the bladder under a dissection microscope. This urothelium was used as a positive control. The rest of the bladder (bladder detrusor), consisted of smooth muscle cells, was used to test for the success of the conditional gene knockout. The bladder samples (both the urothelium and detrusor) were digested and genotyped for PKGI L2/L1 as before. Homozygous L2/L2 and Cre positive female mice were bred with +/L1 Cre negative male mice to maintain the mouse line.

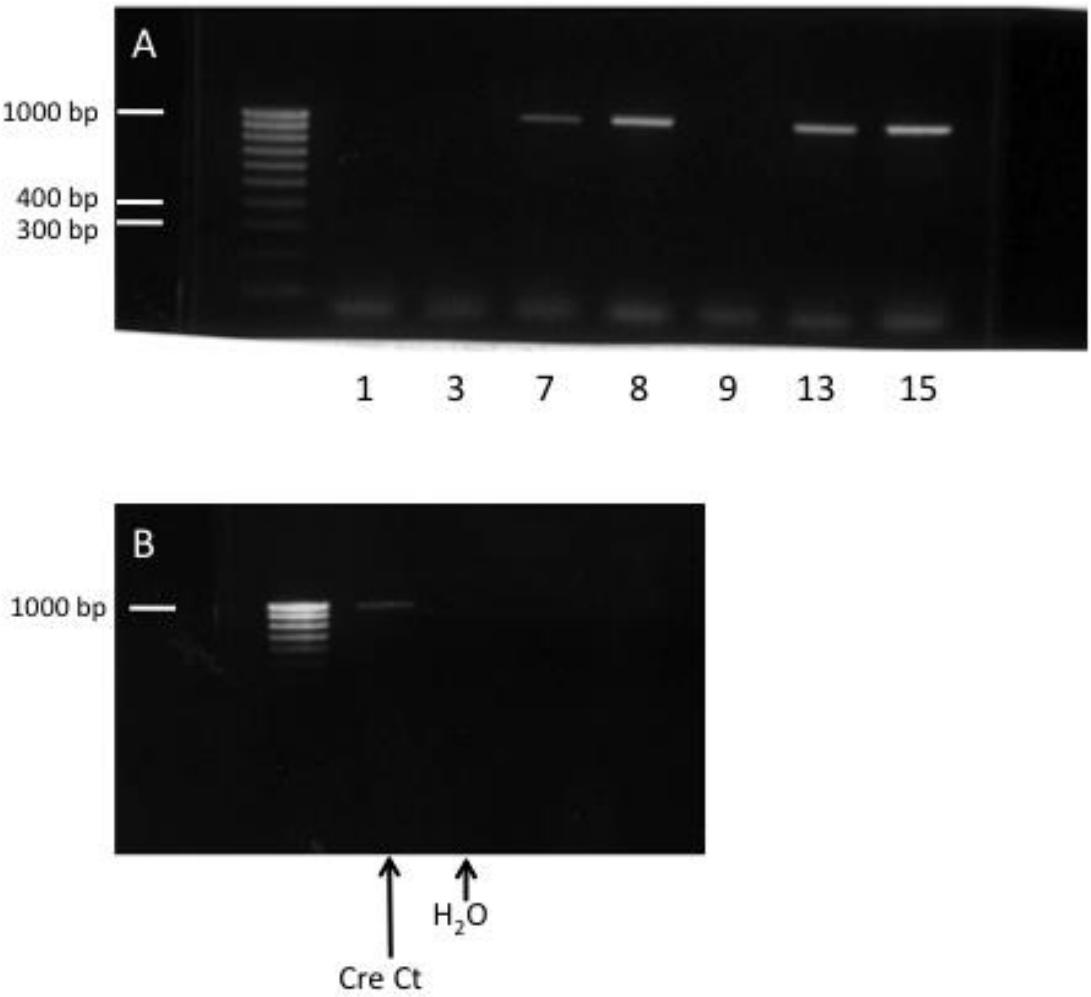

Figure 6.02. Reverse transcription polymerase chain reaction analysis of the expression of Cre in mice that had the genotype of L2/L1 (A). B. The second and third lanes contain positive control (Cre Ct) and negative control (H_2O), respectively. The first lane for both A and B is the DNA molecular weight standard control at 100 bp intervals.

6.2.5 Solutions

All solutions were prepared at room temperature. All components were purchased from Sigma-Aldrich, UK.

- **Lysis buffer** (in mM, unless otherwise stated): Tris-HCl (1 M stock with a pH of 7.6) 50; EDTA (0.5 M stock with a pH of 8.0) 100; NaCl 100; 1 % sodium dodecyl sulphate (SDS); proteinase K 0.1 mg/ml.
- **TBE electrophoresis buffer** (in mM): Tris-HCl (with a pH of 8.0) 50; H_3BO_3 50; EDTA (with a pH of 8.0) 1.
- **Loading dye** (all weight by volume in TBE electrophoresis buffer): 5 % glycerol; 0.1 % bromophenol blue; 0.1 % xylencyanol.

6.3 Results

The aim of the inducible PKGI conditional knockout was to selectively delete both alleles of the PKGI gene only within smooth muscle cells. Before tamoxifen injection, all cells within the selected mice contained one functional PKG1 gene (L2) and one knockout gene (L1). By injecting tamoxifen, expression Cre is induced to excise the L2 allele. However, since expression of Cre is restricted to smooth muscle cells, excision can only occur in smooth muscle cells. Successfully generating this mouse means that the epithelial cells in the urothelium of the bladder should still contain one allele of the gene (L2, whilst the bladder detrusor contains two alleles of L1). Figure 6.03 shows RT-PCR analysis of the urothelium and detrusor tissue from one inducible and one negative control mouse.

Figure 6.03 shows that even after administration of tamoxifen, the L2 allele was still present in both mice. Furthermore, to confirm the expression of PKGI in smooth muscle cells, corpus cavernosum was tested in organ bath experiments for any relaxation response to NO. When corpus cavernosum from a L2/L1 and Cre positive mouse was challenged with 60 mM KCl, application of NO was able to produce tissue relaxation in the same way as control mouse tissue (data not shown). These data suggest that PKGI L2 was not deleted and the reason for failing to induce the L2 gene deletion by Cre recombinase is unclear.

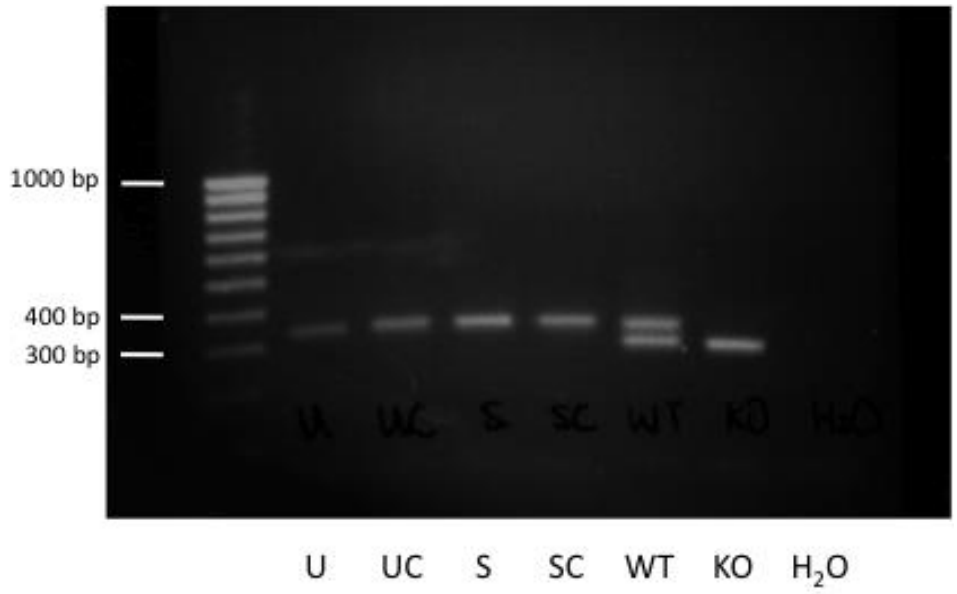

Figure 6.03. Reverse transcription polymerase chain reaction analysis to confirm that deletion of the L2 allele was successfully induced by tamoxifen injection. Two mice (L2/L1 and Cre positive; L2/L1 and Cre negative as negative control) were treated with the Cre inducer tamoxifen. Bladder urothelium and detrusor were taken from each mouse and used to extract DNA. U: bladder urothelium; UC: bladder urothelium from negative control mouse; S: bladder detrusor; SC: bladder detrusor from negative control mouse; WT: wild-type control; KO: gene knockout control; H_2O: H_2O was added instead of DNA extraction sample to test for non-specific DNA contamination. The first lane is the DNA molecular weight standard control with markers at 100 bp intervals.

Chapter 7

General discussion

7.1 The anticontractile effect of PVAT under basal conditions

The overall aim of this project was to determine the mechanism behind the anticontractile effect of PVAT. Depending on the studied vasculature, the vessels are primarily surrounded by one of two types of PVAT, brown or white. While the anticontractile effects of both types on rat vessels are described in this thesis, only the anticontractile mechanism of the white PVAT was investigated in detail. The overall data suggested that this white PVAT can release NO and an ADHF under basal (unstimulated) conditions and that these may act as PVAT-derived anticontractile factors via different mechanisms.

7.1.1 Adipocyte-derived nitric oxide

Vascular tension studies with sildenafil provided indirect evidence that adipose tissue can release NO independent of the endothelium. Thus, in the absence of the endothelium, the shift in the concentration response curve to cirazoline by sildenafil is greater in the presence than in the absence of PVAT. This constitutive production of NO was observed in both tension studies and assays for NO release (measured as a detectable NO_2^- level in the PVAT bathing solution under basal conditions). The amount of NO released from the adipocytes can be further enhanced by A-769,662, possibly via activation of eNOS within the adipocytes. Chen et al (1999) have described AMPK phosphorylation and activation of rat heart eNOS. This is highly relevant as adiponectin is a putative AMPK activator (Yamauchi et al. 2007), and can therefore be released by adipocytes to act in an autocrine manner to increase NO production. Indeed, adiponectin was previously demonstrated to increase NO production from cultured endothelial cells via activation of AMPK (Chen et al. 2003; Cheng et al. 2007). However, it is not known whether there is constitutive release of NO or whether basal release of adiponectin responsible for the basal release of NO from adipocytes.

In vivo, released NO can react with superoxide anions and binds avidly with haemoglobin within the blood; hence, NO has a half-life of just a few seconds (Hakim et al. 1996). However, the proximity of the PVAT to the arteries ensures effective diffusion of NO to the vascular myocytes and which then causes relaxation of the underlying myocytes by activating the soluble guanylyl cyclase/cGMP/PKG pathway. NO is known to exert multiple protective effects on the cardiovascular system such as anti-inflammatory (see review Liu & Huang 2008). Studies have found that a high fat diet can reduce epididymal

white adipocyte-derived NO by reducing eNOS expression (Sansbury et al. 2012) and phosphorylation (Handa et al. 2011) in mice. Hence, under obesogenic conditions, this basal release of NO from adipocytes is likely to be reduced leading to increased vessel contractility.

7.1.2 Adipocyte-derived hyperpolarising factor

Egner (2012), who carried out tension studies with rat mesenteric arteries, showed that the NOS inhibitor L-NMMA did not completely reverse the anticontractile effect of PVAT, and concluded that additional factors were involved. The results obtained in the present project are consistent with the basal release of ADHF (adipocyte-derived hyperpolarising factor), a transferable factor that remained stable for an extended period which could activate K^+ channels on the myocytes. In contrast to previous studies (Gao et al. 2007; Schleifenbaum et al. 2010), the present study found no evidence to suggest that the factor was either H_2O_2 or H_2S. In addition, since K_{ATP} and K_V7 channels blockers glibenclamide and XE-991, respectively, did not reverse the ADHF effect, whereas iberiotoxin did, it can be concluded that ADHF opens BK_{Ca} channels to cause its hyperpolarising effect and thus reduce myocyte contractility. Adipocytes can release NO which had been proposed to activated BK_{Ca} channels either directly (Bolotina et al. 1994) or via the sGC/cGMP/PKG pathway (as reviewed by Waldron & Cole 1999), it is possible that the effects observed may be due to NO. However, this explanation seems unlikely as NO is broken down rapidly even in an *in vitro* condition (Hakim et al. 1996); its activity would have been lost during the long (1 hour) incubation.

7.1.2.1 Importance of adiponectin

In an attempt to find out more about the ADHF, the effects of adiponectin on whole vessels and isolated vascular myocyte were determined. Greenstein et al. (2009) proposed that adiponectin was the PVAT-derived anticontractile factor in human vessels, since an adiponectin blocking peptide inhibited the PVAT vascular effects. Several studies followed on from this and further anticipated the involvement of both AMPK and BK_{Ca} channels to the proper functioning of adiponectin (Lynch et al. 2013; Weston et al. 2013). In the current study, the importance of adiponectin to the anticontractile effect of PVAT was illustrated as PVAT from adiponectin-deficient mice had lost its anticontractile effects in vessel tension experiments. Furthermore, by recording BK_{Ca} channels in the whole-cell patch configuration, application of adiponectin also increased BK_{Ca} channel current. These findings support the observations made by Weston et al. (2013), that adiponectin causes

myocyte hyperpolarisation (detected using sharp electrodes to measure myocyte resting membrane potential), an effect that was sensitive to the BK_{Ca} channel blocker iberiotoxin. Together, these data showed that non-stimulated PVAT released ADHF and adiponectin and that both of these factors could activate BK_{Ca} channels on the myocytes. It is likely that adiponectin is the ADHF. Hence, the anticontractile effect of adiponectin apparently via two different mechanisms: firstly, by activating the BK_{Ca} channels on the myocytes to cause hyperpolarisation; secondly, it may also trigger the production of NO from both adipocytes and endothelial cells.

7.1.2.2 The involvement of AMPK

Whole-cell patch recording also demonstrated that the AMPK activators A-769,662 and PT1 both increased the BK_{Ca} channel current. In addition, it is well established that adiponectin activates AMPK by binding to the AdipoR1 receptor (Yamauchi et al. 2007). Together, it seems likely that AMPK activation can result in opening of BK_{Ca} channels. Several protein kinases such as protein kinase A, protein kinase C and protein kinase G have been demonstrated to regulate BK_{Ca} channel activity by phosphorylation, mainly at a site on the C-terminus of the channel α subunit by protein kinases (reviewed by Schubert & Nelson 2001). The effects of phosphorylation depend on the kinase involved and sites of phosphorylation which alter Ca^{2+} and voltage sensitivity of the channel, leading to a change of channel activity (Schubert & Nelson 2001). Whether AMPK can phosphorylation BK_{Ca} channels to increase channel activity is yet to be elucidated.

7.2 β3 adrenoceptor activation and PVAT anticontractile effects

β3 adrenoceptor stimulation of mesenteric artery PVAT by CL-316,243 enhanced its anticontractile effects (Porter 2011; Egner 2012); an effect which was independent of adipocyte-derived NO (as demonstrated by the NO assay data presented in this study). In adiponectin-deficient mouse mesenteric arteries, the basal anticontractile effect of PVAT was lost, whereas CL-316,243-induced reduction in vessel contractility remained. However, using the same tissues, Weston et al. (2013) found the CL-316,243-induced myocyte hyperpolarisation was lost. These observations suggest that, in mouse mesenteric arteries at least, β3 adrenoceptor stimulation by CL-316,243 enhanced the anticontractile effect of PVAT via two independent pathways. One pathway involves the stimulated release of adiponectin which acts on myocytes via the AMPK/BK_{Ca} pathway whereas the other involves an alternative factor which reduces contractility without activation of BK_{Ca}

channels. This CL-316,243-induced factor which acts independently of K^+ channel opening is thus distinct from ADRF described in other studies (Löhn et al. 2002; Verlohren et al 2004; Gao et al. 2007; Schleifenbaum et al. 2010). The identity of this ADRF may be H_2O_2, possibly via activating the cGMP/PKG pathway.

See Figure 7.01 for the schematic presentation of the proposed anticontractile mechanisms of PVAT.

7.3 Similarities between aortic myocytes and mesenteric artery myocytes

Both aorta and mesenteric arteries are frequently used in the research of anticontractile effects of PVAT. In rodents, aorta and mesenteric arteries are surrounded by brown and white PVAT, respectively. While both vessel types have reduced contractility in the presence of PVAT, it is unknown whether the two different vessel myocytes would respond differently to the PVAT-derived anticontractile factors. The experimental data clearly showed that the two cell types respond very similarly. A-769,662, PT1 and ADHF and adiponectin all significantly increased BK_{Ca} currents in both aortic and mesenteric artery myocytes; AICAR, dorsomorphin did not have much of an effect on either cell type. ADHF remains stable for hours and adiponectin can be found at high concentration in the circulating blood. Thus, rather than a localized effect, ADHF or adiponectin may exert vasoprotective effects on the whole circulation via similar mechanisms.

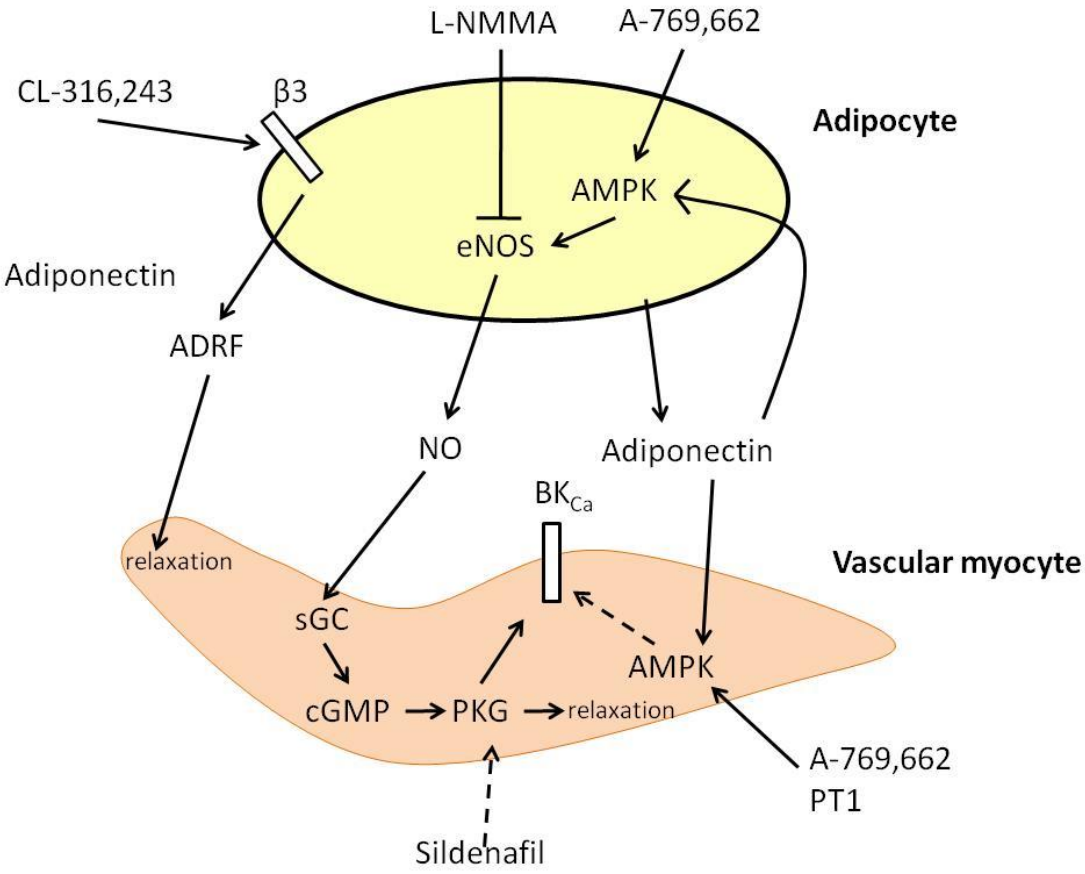

Figure 7.01. The proposed anticontractile mechanism of perivascular adipocyte on vascular myocyte. ADRF: adipocyte-derived relaxing factor; AMPK: AMP-activated protein kinas; β3: β3 adrenoceptor; BK_{Ca}: large conductance Ca^{2+}-activated K^+ channels; cGMP: cyclic guanosine monophosphate; eNOS: endothelial nitric oxide synthase; L-NMMA: L-NG-monomethyl-L-arginine; NO: nitric oxide; PKG: cGMP-dependent protein kinase; sGC: soluble guanylyl cyclase.

References

Abu-Elheiga L, Almerza-Ortega DB, Baldini A & Wakil SJ (1997). Human acetyl-CoA carboxylase 2. Molecular cloning, characterization, chromosomal mapping, and evidence for two isoforms. *J Biol Chem*, 272, pp.10669–10677.

Adams DJ, Barakeh J, Laskey R & Van Breemen C (1989). Ion channels and regulation of intracellular calcium in vascular endothelial cells. *FASEB J*, 3, pp.2389-2400.

Amberg GC, Koh SD, Imaizumi Y, Ohya S & Sanders KM (2003).A-type potassium currents in smooth muscle. *Am J Physiol Cell Physiol*, 284, pp.C683-C595.

Ammälä C, Moorhouse A, Gribble F, Ashfield R, Proks P, Smith PA, Sakura H, Coles B, Ashcroft SJ & Ashcroft FM (1996). Promiscuous coupling btween the sulphoylurea receptor and inwardly rectifying potassium channels. *Nature*, 379, pp.545-548.

Antoniades C, Antonopoulos AS, Tousoulis D & Stefanadis C (2009). Adiponectin: from obesity to cardiovascular disease. *Obes Rev*, 10, pp.269-279.

Arita Y, Kihara S, Ouchi N, Takahashi M, Maeda K, Miyagawa J, Hotta K, Shimomura I, Nakamura T, Miyaoka K, Kuriyama H, Nishida M, Yamashita S, Okubo K, Matsubara K, Muraguchi M, Ohmoto Y, Funahashi T & Matsuzawa Y(1999). Paradoxical decrease of an adipose-specific protein, adiponectin, in obesity. *Biochem Biophys Res Commun*, 257, pp.79–83.

Armani A, Marzolla V, Rosano GM, Fabbri A & Caprio M (2011). Phosphodiesterase type 5 (PDE5) in the adipocyte: a novel player in fat metabolism? *Trends Endocrinol Metab*, 22, pp.404-11.

Ashcroft FM (2005). ATP-sensitive potassium channelopathies: focus on insulin secretion. *J Clin Invest*, 115, pp.2047–2058.

Bain J, Plater L, Elliott M, Shpiro N, Hastie CJ, McLauchlan H, Klevernic I, Arthur JS, Alessi DR, Cohen P(2007). The selectivity of protein kinase inhibitors: a further update. *Biochem J*, 408, pp.297–315.

Banks WA, Kastin AJ, Huang W, Jaspan JB & Maness LM (1996). Leptin enters the brain by a saturable system independent of insulin. *Peptides*, 17, pp.305–311.

Bao L, Vlcek C, Paces V & Kraus JP (1998). Identification and tissue distribution of human cystathionine beta-synthase mRNA isoforms. *Arch Biochem Biophys*, 350, pp.95–103.

Barlow RS & White RE (1998). Hydrogen peroxide relaxes porcine coronary arteries by stimulating BKCa channel activity. *Am J Physiol*, 275, pp.H1283–9.

Beech DJ, Zhang H, Nakao K & Bolton TB (1993). K channel activation by nucleotide diphosphates and its inhibition by glibenclamide in vascular smooth muscle cells. *Br J Pharmacol*, 110, pp.573-582.

Bender & Beavo (2006). Cyclic nucleotide phosphodiesterases: molecular regulation to clinical use. *Pharmacol Rev*, 58, pp.488-520.

Benham CD & Bolton TB (1986). Spontaneous transient outward currents in single visceral and vascular smooth muscle cells of the rabbit. *J Physiol*, 381, pp.385–406.

Benkhoff S, Loot AE, Pierson I, Sturza A, Kohlstedt K, Fleming I, Shimokawa H, Grisk O, Brandes RP & Schröder K (2012). Leptin potentiates endothelium-dependent relaxation by inducing

endothelial expression of neuronal NO synthase. Arteriosclerosis, *Thrombosis, and Vascular Biol*, 32, pp.1605–1612.

Benziane B, Björnholm M, Lantier L, Viollet B, Zierath JR & Chibalin AV (2009). AMP-activated protein kinase activator A-769662 is an inhibitor of the Na(+)-K(+)-ATPase. *Am J Physiol Cell Physiol*, 297, pp.C1554–66.

Berkowitz DE, Nardone NA, Smiley RM, Price DT, Kreutter DK, Fremeau RT & Schwinn DA (1995). Distribution of beta 3-adrenoceptor mRNA in human tissues. *Eur J Pharmacol*, 289, pp.223–228.

Bloom JD, Dutia MD, Johnson BD, Wissner A, Burns MG, Largis EE, Dolan JA & Claus TH (1992). Disodium(R,R)-5-[2-[[2-(3-chlorophenyl)-2-hydroxyethyl]-amino]propyl]-1,3-benzodioxole-2,2-dicarboxylate (CL 316,243). A potent β-adrenergic agonist virtually specific for β3 receptors. A promising antidiabetic and antiobesity agent. *J Med Chem*, 35, pp.3081-4.

Böhm F & Pernow J (2007). The importance of endothelin-1 for vascular dysfunction in cardiovascular disease. *Cardiovasc Res*, 76, pp.8-18.

Bojanic D, Jansen JD, Nahorski SR & Zaagsma J (1985). Atypical characteristics of the beta-adrenoceptor mediating cyclic AMP generation and lipolysis in the rat adipocyte. *Br J Pharmacol,* 84, pp.131-137.

Bolotina VM, Najibi S, Palacino JJ, Pagano PJ & Cohen RA (1994). Nitric oxide directly activates calcium-dependent potassium channels in vascular smooth muscle. *Nature*, 368, pp.850–853.

Bolton TB & Imaizumi Y (1996). Spontaneous transient outward currents in smooth muscle cells. *Cell Calcium*, 20, pp.141–152.

Bosnyak S, Jones ES, Christopoulos A, Aguilar MI, Thomas WG & Widdop RE (2011). Relative affinity of angiotensin peptides and novel ligands at AT1 and At2 receptors. *Clin Sci (Lond),* 121, pp.297-303.

Brayden JE & Nelson MT (1992). Regulation of arterial tone by activation of calcium-dependent potassium channels. *Science*, 256, pp.532-535.

Brede M & Hein L (2001). Transgenic mouse models of angiotensin receptor subtype function in the cardiovascular system. *Regul Pept*, 96, pp.125-132.

Bredt DS & Snyder SH (1990). Isolation of nitric oxide synthetase, a calmodulin-requiring enzyme. *Proc Natl Acad Sci U S A,* 87, pp.682-685.

Brown DA, Constanti A & Adams PR (1983). Ca-activated potassium current in vertebrate sympathetic neutons. *Cell Calcium*, 4, pp.407-420.

Brueggemann LI, Moran CJ, Barakat JA, Yeh JZ, Cribbs LL & Byron KL (2007). Vasopressin stimulated action potential firing by protein kinase C-dependent inhibition of KCNQ5 in A7r5 rat aortic smooth muscle cells. *Am J Physiol Heart Circ Physiol*, 292, pp.H1352-1363.

Buechler C, Wanninger J &Neumeier M (2010). Adiponectin receptor binding proteins - recent advances in elucidating adiponectin signalling pathways. *FEBS Lett,* 584, pp. 4280-4286.

Busse R,Fichtner H, Lückhoff A & Kohlhardt M (1988). Hyperpolarization and increased free calcium

in acetylcholine-stimulated endothelial cells. *Am J Physiol*, 255, pp.H965-H969.

Canová NK, Lincová D, Kmonícková E, Kameníková L & Farghali H (2006). Nitric oxide production from rat adipocytes is modulated by beta3-adrenergic receptor agonists and is involved in a cyclic AMP-dependent lipolysis in adipocytes. *Nitric oxide,* 14, pp.200-211.

Catterall WA (1991). Functional subunit structure of voltage-gated calcium channels. *Science*, 253, pp.1499-1500.

Chang L, Villacorta L, Li R, Hamblin M, Xu W, Dou C, Zhang J, Wu J, Zeng R & Chen YE (2012). Loss of perivascular adipose tissue on peroxisome proliferator-activated receptor-γ deletion in smooth muscle cells impairs intravascular thermoregulation and enhances atherosclerosis. *Circulation*, 126, pp.1067-1078.

Chang TH & Polakis SE (1978). Differentiation of 3T3-L1 fibroblasts to adipocytes. Effect of insulin and indomethacin on the levels of insulin receptors. *J Biol Chem*, 253, pp.4693-4696.

Chauhan S, Hobbs A & Ahluwalia A (2004). C-type natriuretic peptide: new candidate for endothelium-derived hyperpolarising factor. *Int J Biochem Cell Biol*, 36, pp.1878–1881.

Chaves VE, Frasson D & Kawashita NH (2011). Several agents and pathways regulate lipolysis in adipocytes. *Biochimie*, 93, pp.1631-1640.

Chen H, Montagnani M, Funahashi T, Chimomura I & Quon MJ (2003). Adiponectin stimulates production of nitric oxide in vascular endothelial cells. *J Biol Chem*, 278, pp.45021-45026.

Chen P, Poddar R, Tipa EV, Dibello PM, Moravec CS, Robinson K, Green R, Kruger WD, Garrow TA & Jacobsen (1999). Homocysteine metabolism in cardiovascular cells and tissues: implications for hyperhomocysteinemia and cardiovascular disease. *Adv Enzyme Regul*, 39, pp.93-109.

Chen YJ, Tanverse JH, Hou M, Li Y, Du R & Bache RJ (2003). Effect of PDE5 inhibition on coronary hemodynamics in pacing-induced heart failure. *Am J Physiol Heart Circ Physiol*, 284, pp.H1513-H1520.

Chen Z, Peng IC, Sun W, Su MI, Hsu PH, Fu Y, Zhu Y, DeFea K, Pan S, Tsai MD & Shyy JY (2009). AMP-activated protein kinase functionally phosphorylates endothelial nitric oxide synthase Ser633. *Circ Res*, 104, pp. 496-505.

Cheng KK, Lam KS, Wang Y, Huang Y, Carling D, Wu D, Wong C & Xu A (2007). Adiponectin-induced endothelial nitric oxide synthase activation and nitric oxide production are mediated by APPL1 in endothelial cells. *Diabetes*, 56, pp.1387-1394.

Chin D & Means AR (2000). Calmodulin: a prototypical calcium sensor. *Trends Cell Biol, 10*, pp.322–328.

Chow WS, Cheung BM, Tso AW, Xu A, Wat NM, Fong CH, Ong LH, Tam S, Tan KC, Janus ED, Lam TH & Lam KS (2007). Hypoadiponectinemia as a predictor for the development of hypertension: a 5-year prospective study. *Hypertension*, 49, pp.1455–1461.

Christodoulides N, Durante W, Kroll MH & Scafer AI (1995). Vascular smooth muscle cell hemeoxygenases generate guaylyl cyclase-stimulatory carbon monoxide. *Circulation*, 91,

pp.2306-2309.

Cinti S (2011). Between brown and white: novel aspects of adipocyte differentiation. *Ann Med*, 43, pp.104–115.

Cole WC & Clément-Chomienne O (2003). ATP-sensitive K+ channels of vascular smooth muscle cells. *J Cardiovasc Electrophsiol*, 14, pp.94-103.

Cole WC, Malcolm T, Walsh MP & Light PE (2000). Inhibition by protein kinase C of the K(CDP) subtype of vascular smooth muscle ATP-sensitive potassium channel. *Circ Res*, 87, pp.112-117.

Coleman HA, Tare M &Parkington HC (2004). Endothelialpotassiumchannels, endothelium-dependenthyperpolarization and the regulation of vasculartone in health and disease. *Clin Exp Pharmacol Physiol*, 31, pp.641-649.

Collins S, Cao W & Robidoux J (2004). Learning new tricks from old dogs: beta-adrenergic receptors teach new lessons on firing up adipose tissue metabolism. *Mol Endocrinol*, 18, pp.2123-2131.

Combs TP, Berg AH, Rajala MW, Klebanov S, Iyengar P, Jimenez-Chillaron JC, Patti ME, Klein SL, Weinstein RS & Scherer PE (2003). Sexual differentiation, pregnancy, calorie restriction, and aging affect the adipocyte-specific secretory protein adiponectin. *Diabete*s, 52, pp268-276.

Cool B, Zinker B, Chiou W, Kifle L, Cao N, Perham M, Dickinson R, Adler A, Gagne G, Iyengar R, Zhao G, Marsh K, Kym P, Jung P, Camp HS & Frevert E (2006). Identification and characterization of a small molecule AMPK activator that treats key components of type 2 diabetes and the metabolic syndrome. *Cell Metab,* 3, pp.403-416.

Coppack SW, Evans RD, Fisher RM, Frayn KN, Gibbons GF, Humphreys SM, Kirk ML, Potts JL & Hockaday TD (1992). Adipose tissue metabolism in obesity: lipase action in vivo before and after a mixed meal. *Metabolism*, 41, pp.264-272.

Corton JM, Gillespie JG, Hawley SA & Hardie DG (1995). 5-aminoimidazole-4-carboxamide ribonucleoside.A specific method for activating AMP-activated protein kinase in intact cells? *Eur J Biochem*, 229, pp.558-565.

Cosentino F, Patton S, d'Uscio LV, Werner ER, Werner-Felmayer G, Moreau P, Malinski T & Lüscher TF (1998). Tetrahydrobiopterin alters superoxide and nitric oxide release in prehypertensive rats. *J Clin Invest*, 101, pp.1530-1537.

Dallas ML, Scragg JL, Wyatt CN, Ross F, Hardie DG, Evans AM & Peers C (2009). Modulation of O(2) sensitive K (+) channels by AMP-activated protein kinase. *Adv Exp Med Biol*, 648, pp.57-63.

Dart C & Standen NB (1993). Adenosine-activated potassium currents in smooth muscle cells isolated from the pig coronary artery. *J Physiol*, 471, pp.767-786.

Davies SP, Helps NR, Cohen PT & Hardie DG (1995). 5'-AMP inhibits dephosphorylation, as well as promoting phosphorylation, of the AMP-activated protein kinase. Studies using bacterially expressed human protein phosphatase-2C alpha and native bovine protein phosphatase-2AC. *FEBS Lett*, 377, pp.421-425.

Davis B, Rahman A & Arner A (2012). AMP-activated kinase relaxes agonist induced contractions in

the mouse aorta via effects on PKC signaling and inhibits NO-induced relaxation. *Eur J Pharmacol*, 695, pp.88-95.

Davis BJ, Xie Z, Viollet B & Zou MH (2006). Activation of the AMP-activated kinase by antidiabetes drug metformin stimulates nitric oxide synthesis in vivo by promoting the association of heat shock protein 90 and endothelial nitric oxide synthase. *Diabetes*, 55, pp.496-505.

de Vente J, Asan E, Gambaryan S, Markerink-van Ittersum M, Axer H, Gallatz K, Lohmann SM & Palkovits M (2001). Localization of cGMP-dependent protein kinase type II in rat brain. *Neuroscience*, 108, pp.27-49.

Denafield JE, Halcox JP & Rabelink TJ (2007). Endothelial function and dusfunction:testing and clinical relevance. *Circulation*, 115, pp.128-1295.

Deng Y & Scherer PE (2010). Adipokines as novel biomarkers and regulators of the metabolic syndrome. *Ann N Y AcadSci*, 1212, pp.E1-E19.

Dessy C, Moniotte S, Ghisdal P, Havaux X, Noirhomme P & Balligand JL (2004). Endothelial beta3-adrenoceptors mediate vasorelaxation of human coronary microarteries through nitric oxide and endothelium-dependent hyperpolarization. *Circulation*, 24, pp.948-954.

Dubrovska G, Verlohren S, Luft FC & Gollasch M (2004). Mechanisms of ADRF release from rat aortic adventitial adipose tissue. *Am J Physiol Heart Circ Physiol*, 286, pp.H1107-H1113.

Earley S, Heppner TJ, Nelson MT & Brayden JE (2005). TRPV4 forms a novel Ca2+ signaling complex with ryanodine receptors and BKCa channels. *Circ Res*, 97, pp.1270-1279.

Edwards G & Weston A (1998). Endothelium-derived hyperpolarizing factor--a critical appraisal. *Prog Drug Res*, 50, pp.107-133.

Edwards G, Niederste-Hollenberg A, Schneider J, Noack T & Weston AH (1994). Ion channel modulation by NS 1619, the putative BKCa channel opener, in vascular smooth muscle. *Br J Pharmacol*, 113, pp.1538-1547.

Egner I (2012). Novel roles of endothelial cells and adipocytes in the vasculature: modification in disease. Ph.D. Thesis. University of Manchester, UK.

Egner I, Weston A, Porter E & Edwards G (2010). Hyperpolarising effect of perivascular adipose tissue in rat mesenteric artery myocyte: stimulation by beta-3 adrenoceptor activation [abstract]. Proceedings of the British Pharmacological Society, http://www.pA2online.org/abstracts/vol8Issue1abst141P.pdf. [Accessed Aug 2013].

Elizalde M, Rydén M, van Harmelen V, Eneroth P, Gyllenhammar H, Holm C, Ramel S, Olund A, Arner P &Andersson K (2000). Expression of nitric oxide synthases in subcutaneous adipose tissue of nonobese and obese humans. *J Lipid Res*, 41, pp.1244-1251.

Elmedyb P, Calloe K, Schmitt N, Hansen RS, Gunnet M & Olesen SP (2007). Modulation of ERG channels by XE991. *Basic Clin Pharmacol Toxicol*, 100, pp.316-322.

Erickson PF, Maxwell IH, Su LJ, Baumann M &Glode LM (1990). Sequence of cDNA for rat cystathionine gamma-lyase and comparison of deduced amino acid sequence with related Escherichia coli enzymes. *Biochem J*, 269, pp.335-340.

Fang L, Zhao J, Chen Y, Ma T, Xu G, Tang C, Liu X & Geng B (2009). Hydrogen sulfide derived

from periadventitial adipose tissue is a vasodilator. *J Hypertens*, 27, pp.2174-2185.

Faulkner MA & Burke RA (2013). Safety profile of two novel antiepileptic agents approved for the treatment of refractory partial seizures: ezogabine (retigabine) and perampanel. *Expert Opin Drug Saf*, [epub ahead of print].

Feil S, Zimmermann P, Knorn A, Brummer S, Schlossmann J, Hofmann, F & Feil R (2005). Distribution of cGMP-dependent protein kinase type I and its isoforms in the mouse brain and retina. *Neuroscience*, 135, pp.863–868.

Flagg TP, Enkvetchakul D, Koster JC & Nichols CG (2010). Muscle KATP channels: recent insights to energy sensing and myoprotection. *Physiol Rev*, 90, pp.799-829.

Ford RJ & Rush JW (2011). Endothelium-dependent vasorelaxation to the AMPK activator AICAR is enhanced in aorta from hypertensive rats and is NO and EDCF dependent. *Am J Physiol Hear Circ Physiol*, 300, pp. H64-H75.

Förstermann U (2010). Nitric oxide and oxidative stress in vascular disease. *Pflugers Arch*, 459, pp.923-939.

Francis SH, Busch JL & Corbin JD (2010). cGMP-dependent protein kinases and cGMP phosphodiesterases in nitric oxide and cGMP action. *Pharmacol Rev*, 62, pp.525-563.

Fruebis J, Tsao TS, Javorschi S, Ebbets-Reed D, Erickson MR, Yen FT, Bihain BE & Lodish HF (2001). Proteolytic cleavage product of 30-kDa adipocyte complement-related protein increases fatty acid oxidation in muscle and causes weight loss in mice. *Proc Natl Acad Sci U S A*, 98, pp.2005-2010.

Fu L, Isobe K, Zeng Q, Suzukawa K, Takekoshi K & Kawakami Y (2008). The effects of beta(3)-adrenoceptor agonist CL-316,243 on adiponectin, adiponectin receptors and tumor necrosis factor-alpha expressions in adipose tissues of obese diabetic KKAy mice. *Eur J Pharmacol*, 584, pp.202-206.

Fukata, Y, Amano M&Kaibuchi K (2001). Rho-Rho-kinase pathway in smooth muscle contraction and cytoskeletal reorganization of non-muscle cells. *Trends Pharmacol Sci*, 22, pp.32–39.

Funahashi T, Nakamura T, Shimomura I, Maeda K, Kuriyama H, Takahashi M, Arita Y, Kihara S & Matsuzawa Y (1999). Role of adipocytokines on the pathogenesis of atherosclerosis in visceral obesity. *Intern Med*, 38, pp.202-206.

Furchgott RF & Zawadzki JV (1980).The obligatory role of endothelial cells in the relaxation of arterial smooth muscle by acetylcholine. *Nature*. 288,373-376.

Furchgott RF, Carvalho MH, Khan MT & Matsunaga K (1987). Evidence for endothelium-dependent vasodilation of resistance vessels by acetylcholine. *Blood Vessels*, 24, pp145-149.

Galvez A, Gimenez-Gallego G, Reuben JP, Roy-Contancin L, Feigenbaum P, Kaczorowski GJ & Garcia ML (1990). Purification and characterization of a unique, potent, peptidyl probe for the high conductance calcium-activated potassium channel from venom of the scorpion Buthus tamulus. *J Biol Chem*, 265, pp.11083-11090.

Gao YJ, Lu C, Su LY, Sharma AM & Lee RM (2007). Modulation of vascular function by perivascular adipose tissue: the role of endothelium and hydrogen peroxide. *Br J Pharmacol*, 151, pp.323–

331.

Gao YJ, Takemori K, Su LY, An WS, Lu C, Sharma AM & Lee RM (2006). Perivascular adipose tissue promotes vasoconstriction: the role of superoxide anion. *Cardiovasc Res*, 71, pp.363-373.

Gao YJ, Zeng ZH, Teoh K, Sharma AM, Abouzahr L, Cybulsky I, Lamy A, Semelhago L & Lee RM (2005). Perivascular adipose tissue modulates vascular function in the human internal thoracic artery. *J Thorac Cardiovasc Surg*, 130, pp.1130-1136.

Garrido AM & Griendling KK (2009). NADPH oxidases and angiotensin II receptor signaling. *Mol Cell Endocrinol*, 302, pp.148-158.

Gellai M & Ruffolo RR (1987). Renal effects of selective alpha-1 and alpha-2 adrenoceptor agonists in conscious, normotensive rats. *J Pharmacol Exp Ther*, 240, pp.723-728.

Ghorbani M, Claus TH & Himms-Hagen Jc (1997). Hypertrophy of brown adipocytes in brown and white adipose tissues and reversal of diet-induced obesity in rats treated with a beta3-adrenoceptor agonist. *Biochem Pharmacol*, 54, pp.121-131.

Giangiacomo KM, Garcia ML & McManus OB (1992). Mechanism of iberiotoxin block of the large-conductance calcium-activated potassium channel from bovine aortic smooth muscle. *Biochemistry,* 31, pp.6719-6727.

Giordano A, Tonello C, Bulbarelli A, Cozzi V, Cinti S, Curruba MO & Nisoli E (2002). Evidence for a functional nitric oxide synthase system in brown adipocyte nucleus. *FEBS Lett*, 514, pp.135-140.

Godfraind T & Govoni S (1995). Recent advances in the pharmacology of Ca2+ and K+ channels. *Trends Pharmacol Sci*,16, pp.1-4.

Goirand F, Solar M, Athea Y, Viollet B, Mateo P, Fortin D, Leclerc J, Hoerter J, Ventura-clapier R & Garnier A (2007). Activation of AMP kinase alpha1 subunit induces aortic vasorelaxation in mice. *J Physiol*, 581, pp.1163-1171.

Göransson O, McBride A, Hawley SA, Ross FA, Shpiro N, Foretz M, Viollet B, Hardie DG & Sakamoto K (2007). Mechanism of action of A-769662, a valuable tool for activation of AMP-activated protein kinase. *J Biol Chem*, 282, pp.32549-32560.

Greenstein AS, Khavandi K, Withers SB, Sonoyama K, Clancy O, Jeziorska M, Laing Y, Yates AP, Pemberton PW, Malik RA & Heagerty AM (2009). Local inflammation and hypoxia abolish the protective anticontractile properties of perivascular fat in obese patients. *Circulation*, 119, pp.1661-1670.

Gribkoff VK (2008). The therapeutic potential of neuronal KV7(KCNQ) channel modulators: an update. *Expert Opin Ther Targets*, 12, pp.565-581.

Grimm PR & Sansom SC (2010). BKCa channels and a new form of hypertension. *Kidney Int*, 78, pp.956-962.

Grujic D, Susulic VS, Harper ME, Himms-Hagen J, Cunningham BA, Corkey BE & Lowell BB (1997). Beta3-adrenergic receptors on white and brown adipocytes mediate beta3-selective agonist-induced effects on energy expenditure, insulin secretion, and food intake. A study using

transgenic and gene knockout mice. *J Biol Chem*, 272, pp.17686-17693.

Guimarães S & Moura D (2001). Vascular adrenoceptors: an update. *Pharmacol Rev,* 53, pp.319-356.

Gupte M, Boustany-Kari CM, Bharadwaj K, Police S, Thatcher S, Gong MC, English VL & Cassis LA (2008). ACE2 is expressed in mouse adipocytes and regulated by a high-fat diet. *Am J Physiol Regul Integr Comp Physiol*, 295, pp.R781-R788.

Gutman GA, Chandy KG, Grissmer S, Lazdunski M, McKinnon D, Pardo LA,Robertson GA, Rudy B, Sanguinetti MC, Stühmer W & Wang X (2005).International Union of Phamacology. LIII. Nomenclature and molecular relationships of voltage-gated potassium channels. *Pharmacol Rev*, 57, pp.473-508.

Ha J, Lee JK, Kim KS, Witters LA & Kim KH (1996). Cloning of human acetyl-CoA carboxylase-beta and its unique features. *Proc Natl Acad Sci U S A*, 93, pp.11466-11470.

Hakim TS, Sugimori K, Camporesi EM & Anderson G (1996). Half-life of nitric oxide in aqueous solutions with and without haemoglobin. *Physiol Meas*, 17, pp.267-277.

Halaas JL, Gajiwala KS, Maffei M, Cohen SL, Chait BT, Rabinowitz D, Lallone RL, Burley SK & Friedman JM (1995). Weight-reducing effects of the plasma protein encoded by the obese gene. *Science*, 269, pp.543–546.

Handa P, Tateya S, Rizzo NO, Cheng AM, Morgan-Stevenson V, Han CY, Clowes AW, Daum G, O'Brien KD, Schwartz MW, Chait A & Kim F (2011). Reduced vascular nitric oxide-cGMP signaling contributes to adipose tissue inflammation during high fat feeding. *Arterioscler Thromb Vasc Biol*, 31, pp.2827-2835.

Hanner M, Schmalhofer WA, Munujos P, Knaus HG, Kaczorowski GJ & Garcia ML (1997). The beta subunit of the high-conductance calcium-activated potassium channel contributes to the high-affinity receptor for charybdotoxin. *Proc Natl Acad Sci U S A,* 94, pp.2853-2858.

Hardie DG, Ross FA & Hawley SA (2012). AMP-activated protein kinase: a target for drugs both ancient and modern. *Chem Biol*, 19, pp.1222-1236.

Hausman GJ (1985a). Anatomical and enzyme histochemical differentiation of adipose tissue. *Int J Obes,* 9 Suppl 1, pp.1-6.

Hausman GJ (1985b). The comparative anatomy of adipose tissue, In new perspectives in adipose tissue: structure, function and development. London: Butterworths. Pp.1-21.

Hawley SA, Boudeau J, Reid JL, Mustard KJ, Udd L, Mäkelä TP, Alessi DR & Hardie DG (2003). Complexed between the LKB1 tumor suppressor, STRAD alpha/beta and MO25 alpha/beta are upstream kinases in the AMP-activated protein kinase cascade. *J Biol*, 2, 28.

Hawley SA, Pan DA, Mustard KJ, Ross L, Bain J, Edelman AM, Frenguelli BG & Hardie DG (2005). Calmodulin-dependent protein kinase kinase-beta is an alternative upstream kinase for AMP-activated protein kinase. *Cell Metab*, 2, pp.9-19.

Hayabuchi Y, Nakaya Y, Matsuoka S & Kuroda Y (1998). Endothelium-derived hyperpolarizing factor activates Ca2+-activated K+ channels in porcine coronary artery smooth muscle cells. *J Cardiovasc Pharmacol*, 32, pp.642–649.

Helliwell RM & Large WA (1997). Alpha 1-adrenoceptor activation of a non-selective cation currents in rabbit portal vein by 1,2-diacyl-sn-glycerol. *J Physiol*, 499, pp.417-428.

Henin N, Vincent MF, Gruber HE & Van den Berghe G (1995). Inhibition of fatty acid and cholesterol synthesis by stimulation of AMP-activated protein kinase. *FASEB J*, 9, pp.541-546.

Hofmann F (2005). The biology of cyclic GMP-dependent protein kinases. *J Biol Chem*, 280, pp.1-4.

Hofmann F, Feil R, Kleppisch T & Schlossmann J (2006). Function of cGMP-dependent protein kinases as revealed by gene deletion. *Physiol Rev*, 86, 1-23.

Horman S, Morel N, Vertommen D, Hussain N, Neumann D, Beauloye C, El Najjar N, Forcet C, Viollet B, Walsh MP, Hue L & Rider MH (2008). AMP-activated protein kinase phosphorylates and desensitizes smooth muscle myosin light chain kinase. *J Biol Chem*, 283, pp.18505-18512.

Hosoki R, Matsuki N & Kimura H (1997).The possible role of hydrogen sulfide as an endogenous smooth muscle relaxant in synergy with nitric oxide. *Biochem Biophys Res Commun*, 237, pp.527-531.

Hurley RL, Anderson KA, Franzone JM, Kemp BE, Means AR & Witters LA (2005). The Ca2+/calmodulin-dependent protein kinase kinases are AMP-activated protein kinase kinases. *J Biol Chem*, 280, pp.29060-29066.

Iesaki T, Gupte SA, Kaminski PM & Wolin MS (1999). Inhibition of guanylate cyclase stimulation by NO and bovine arterial relaxation to peroxynitrite and H2O2. *Am J Physiol*, 277, pp.H978-85.

Ikematsu N, Dallas ML, Ross FA, Lewis RW, Rafferty JN, David JA, Suman R, Peers C, Hardie DG & Evans AM (2011). Phosphorylation of the voltage-gated potassium channel Kv2.1 by AMP-activated protein kinase regulates membrane excitability. *Proc Natl Acad Sci USA*, 108, pp.18132-18137.

Ivey ME, Osman N & Little PJ (2008). Endothelin-1 signalling in vascular smooth muscle: pathways controlling cellular functions associated with atherosclerosis. *Atherosclerosis*, 199, 237-247.

Iwai M & Horiuchi M (2009). Devil and angel in the renin-angiotensin system: CAE-angiotensin II-AT1 receptor axis vs. ACE2-angiotensin-(1-7)-Mas receptor axis. *Hypertens Res*, 32, pp.533-536.

Jaiswal N, Lambrecht G, Mutschler E, Tacke R & Malik KU (1991). Pharmacological characterization of the vascular muscarinic receptors mediating relaxation and contraction in rabbit aorta. *J Pharmacol Exp Ther,* 258, pp.842-850.

Janigro D, West GA, Gordon EL & Winn HR (1993). ATP-sensitive K+ channels in rat aorta and brain microvascular endothelial cells*. Am J Physiol*, 265, pp.C812-C821.

Jensen BS, Strobaek D, Christophersen P, Jorgensen TD, Hansen C, Silahtaroglu A, Olesen SP & Ahring PK (1998). Characterization of the cloned human intermediate-conductance Ca2+-activated K+ channel. *Am J Physiol*, 275, pp.C848-C856.

Jepps TA, Greenwood IA, Moffatt JD, Sanders KM & Ohya S (2009). Molecular and functional characterization of Kv7 K+ channel in murine gastrointestinal smooth muscles. *Am J Physiol Gastrointest Liver Physiol*, 297, pp.G107-G115.

Kadowaki T & Yamauchi T (2005). Adiponectin and adiponectinreceptors. *Endocr Rev*, 26, pp.439-

451.

Kochegarov AA (2003). Pharmacological modulators of voltage-gated calcium channels and their therapeutical application. *Cell Calcium*, 33, pp.145-162.

Köhler M, Hirschberg B, Bond CT, Kinzie JM, Marrion NV, Maylie J & Adelman JP (1996). Small-conductance, calcium-activated potassium channels from mammalian brain. *Science*, 273, pp.1709-1714.

Köhn C, Schleifenbaum J, Szijártó IA, Markó L, Dubrovska G, Huang Y & Gollasch M (2012). Differential effects of cystathionine-γ-lyase-dependent vasodilatory H2S in periadventitial vasoregulation of rat and mouse aortas. *PLoS ONE*, 7, pp.e41951.

Kubota N, Terauchi Y, Yamauchi T, Kubota T, Moroi M, Matsui J, Eto K, Yamashita T, Kamon J, Satoh H, Yano W, Froguel P, Nagai R, Kimura S, Kadowaki T & Noda T (2002). Disruption of adiponectin causes insulin resistance and neointimal formation. *J Biol Chem*, 277, pp. 25863-25866.

Kühbandner S, Brummer S, Metzger D, Chambon P, Hofmann, F & Feil R (2000). Temporally controlled somatic mutagenesis in smooth muscle. *Genesis*, 28, pp.15–22.

Kurth-Kraczek EJ, Hirshman MF, Goodyear LJ & Winder WW (1999). 5' AMP-activated protein kinase activation causes GLUT4 translocation in skeletal muscle. *Diabetes*, 48, 1667-1671.

Langin D, Portillo MP, Saulnier-Blache JS & Lafontan M (1991). Coexistence of three beta-adrenoceptor subtyes in white fat cells of various mammlian species. *Eur J Pharmacol*, 199, pp.291-301.

Langin D, Ekholm D, Ridderstrale M, Lafontan M & Belfrage P (1992). cAMP-dependent protein kinase activation mediated by beta 3-adrenergic receptors parallels lipolysis in rat adipocytes. *Biochim Biophys Acta*, 1135, pp.349-352.

Latorre R & Brauchi S (2006). Large conductance Ca2+-activated K+ (BK) channel: activation by Ca2+ and voltage. *Biol Res*, 39, pp.385-401.

Lee KY & Choi HC (2013). Acetylcholine-induced AMP-activated protein kinase activation attenuates vasoconstriction through ab LKB1-dependent mechanism in rat aorta. *Vascul Pharmacol*, Epub ahead of print. Doi:10.1016/j.vph.2013.07.007.

Lee RM, Lu C, Su LY & Gao YJ (2009). Endothelium-dependent relaxation factor released by perivascular adipose tissue. *J Hypertens*, 27, pp.782-790.

Leitman DC, Andresen JW, Catalano RM, Waldman SA, Tuan JJ &Murad F (1988). Atrial natriuretic peptide binding, cross-linking, and stimulation of cyclic GMP accumulation and particulate guanylatecyclase activity in cultured cells. *J Biol Chem*, 263, pp.3720-3728.

Lincoln TM, Dey N & Sellak H (2001). Invited review: cGMP-dependent protein kinase signaling mechanisms in smooth muscle: from the regulation of tone to gene expression. *J Appl Physiol*, 91, pp.1421-1430.

Liu VW & Huang PL (2008). Cardiovascular roles of nitric oxide: a review of insights from nitric oxide synthase gene disrupted mice. *Cardiovasc Res*, 77, pp.19-29.

Liu Y, Bubolz AH, Mendoza S, Zhang DX & Gutterman DD (2011). H2O2 Is the Transferrable Factor

Mediating Flow-Induced Dilation in Human Coronary Arterioles. *Circ Res*, 108, pp.566-573.

Lohmann SM, Walter U, Miller PE, Greengard P & De Camilli P (1981). Immunohistochemical localization of cyclic GMP-dependent protein kinase in mammalian brain. *Proc Natl Acad Sci U S A*, 78, pp.653–657.

Löhn M, Dubrovska G, Lauterbach B, Luft FC, Gollasch M & Sharma AM (2002). Periadventitial fat releases a vascular relaxing factor. *FASEB J*, 16, pp.1057-1063.

Lu C, Su LY, Lee RM & Gao YJ (2010). Mechanism for perivascular adipose tissue-mediated potentiation of vascular contraction to perivascular neuronal stimulation: the role of adipocyte-derived angiotensin II. *Eur J Pharmacol*, 634, pp.107-112.

Luoma JS, Srålin P, Marklund SL, Hiltunen TP & Ylä-Herttuala S (1998). Expression of extracellular SOD and iNOS in macrophages and smooth muscle cells in human and rabbit atherosclerotic lesions: colocalization with epitopes characteristic of oxidized LDL and peroxynitrite-modified proteins. *Arterioscler Thromb Vasc Biol*, 18, pp.157-167.

Lynch FM, Withers SB, Yao Z, Werner ME, Edwards G, Weston AH & Heagerty AM (2013). Perivascular adipose tissue-derived adiponectin activates BKCa channels to induce anticontractile responses. *Am J Physiol Heart Circ Physiol,* 304, pp.H786-H795.

Ma L, Ma S, He H, Yang D, Chen X, Luo Z, Liu D& Zhu Z (2010). Perivasculr fat-mediated vascular dysfunction and remodelling through the AMPK/mTOR pathway in high-fat diet induced obese rats. *Hypertens Res*, 33, pp.446-453.

Mackie AR, Brueggemann LI, Henderson KK, Shiels AJ, Cribbs LL, Scrogin KE & Byron KL (2008). Vascular KCNQ potassium channels as novel targets for the control of mesenteric artery constriction by vasopressin, based on studies in single cells, pressurized arteries, and in vivo measurements of mesenteric vascular resistance. *J Pharmacol Exp Ther*, 325, pp.475-483.

Maeda N, Shimomura I, Kishida K, Nishizawa H, Matsuda M, Nagaretani H, Furuyama N, Kondo H, Takahashi M, Arita Y, Komuro R, Ouchi N, Kihara S, Tochino Y, Okutomi K, Horie M, Takeda S, Aoyama T, Funahashi T & Matsuzawa Y (2002). Diet-induced insulin resistance in mice lacking adiponectin/ACRP30. *Nat Med*, 8, pp.731-737.

Magleby KL (2003). Gating mechanism of BK (Slo1) channels: so near, yet so far. *J Gen Physio*l, 121, pp.81-96.

Marchesi C, Ebrahimian T, Angulo O, Paradis P & Schiffrin EL (2009). Endothelial nitric oxide synthase uncoupling and perivascular adipose oxidative stress and inflammation contribute to vascular dysfunction in a rodent model of metabolic syndrome. *Hypertension*, 54, pp.1384-1392.

Marty A (1981). Ca-dependent K channels with large unitary conductance in chromaffin cell membranes. *Nature*, 291, pp.497-500.

McBride A, Ghilagaber S, Nikolaev A & Hardie DG (2009). The glycogen-binding domain on the AMPK beta subunit allows the kinase to act as a glycogen sensor. *Cell Metab,* 9, pp.23–34.

McCrossan ZA & Abbott GW (2004). The MinK-related peptides. *Neuropharmacology*, 47, pp.787-821.

McKeown L, Swanton L, Robinson P& Jones OT (2008).Surface expression and distribution of voltage-gated potassium channels in neurons. *Mol Membr Biol*, 25, pp.332-343.

McManus OB, Helms LM, Pallanck L, Ganetzky B, Swanson R & Leonard RJ (1995). Functional role of the beta subunit of high conductance calcium-activated potassium channels. *Neuron*, 14, pp.645-650.

Meera P, Wallner M, Jiang Z & Toro L (1996). A calcium switch for the functional coupling between alpha (hslo) and beta subunits (KV,Ca beta) of maxi K channels. *FEBS Lett,* 382, pp.84-88.

Melo LG, Veress AT, Ackermann U & Sonnenberg H (1998). Chronic regulation of arterial blood pressure by ANP: role of endogenous vasoactive endothelial factors. *Am J Physiol*, 275, pp.H1826-33.

Meredith AL, Thorneloe KS, Werner ME, Nelson MT & Aldrich RW (2004). Overactive bladder and incontinence in the absence of the BK large conductance Ca2+-activated K+ channel. *J Biol Chem*, 279, pp.36746-36752.

Miki T, Taira M, Hockman S, Shimada F, Lieman J, Napolitano M, Ward D, Taira M, Makino H & Manganiello VC (1996). Characterization of the cDNA and gene encoding human PDE3B, the cGIP1 isoform of the human cyclic GMP-inhibited cyclic nucleotide phosphodiesterase family. *Genomics*, 36, pp.476-485.

MillerFJJr, Gutterman DD, Rios CD, Heistad DD & Davidson BL (1998). Superoxide production in vascular smooth muscle contributes to oxidative stress and impaired relaxation in atherosclerosis. *Circ Res*, 82, pp.1298 -1305.

Mitschke MM, Hoffmann LS, Gnad T, Scholz D & Kruithoff K (2013). Increased cGMP promotes healthy expansion and browning of white adipose tissue. *FASEB J,* 27, pp.1621-1630.

Momcilovic M, Hong SP & Carlson M (2006). Mammalian TAK1 activates Snf1 protein kinase in yeast and phosphorylates AMP-activated protein kinase in vitro. *J Biol Chem*, 281, pp.25336-25343.

Morrow VA, oufelle F, Connell JMC, Petrie JR, Gould GW & Salt IP (2003). Direct activation of AMP-activated protein kinase stimulates nitric-oxide synthesis in human aortic endothelial cells. *J BiolChem,* 278, pp.31629-31639.

Mulvany MJ & Halpern W (1976). Mechanical properties of vascular smooth muscle cells in situ. *Nature*, 260, pp.617-619.

Mulvany MJ & Halpern W (1977). Contractile properties of small arterial resistance vessels in spontaneously hypertensive and normotensive rats. *Circ Res*, 41, pp.19-26.

N'Gouemo P (2011). Targeting BK (big potassium) channels in epilepsy. *Expert Opin Ther Targets*. 15, pp.1283-1295.

Naik JS, O'Donaughy TL & Walker BR (2003). Endogenous carbon monoxide is an endothelial-derived vasodilator factor in the mesenteric circulation. *Am J Physiol Heart Circ Physiol*, 284, pp.H838-H845.

Neher E & Sakmann B (1976). Single-channel currents recorded from membrane of denervated frog muscle fibres. *Nature*, 5554, pp.799-802.

Nelson MT, Cheng H, Rubart M, Santana LF, Boney AD, Knot HJ & Lederer WJ (1995). Relaxation of arterial smooth muscle by calcium sparks. *Science,* 270, pp.633-637.

Nelson MT & Quayle JM (1995). Physiological roles and properties of potassium channels in arterial smooth muscle. *Am J Physiol*, 268, pp.C799-C822.

Ng FL, Davis AJ, Jepps TA, Harhun MI, Yeung SY, Wan A, Reddy M, Melville D, Nardi A, Khong TK & Greenwood IA (2011). Expression and function of the K+ channel KCNQ genes in human arteries. *Br J Pharmacol*, 162, pp.42-53.

Nichols CG & Lederer WJ (1990). The regulation of ATP-sensitive K+ channel activity in intact and permeabilized rat ventricular myocytes. *J Physiol*, 423, pp.91-110.

Nichols CG & Lopatin AN (1997). Inward rectifier potassium channels. *Annu Rev Physiol*, 59, pp.171-191.

Nichols CG (2006). KATP channels as molecular sensors of cellular metabolism. *Nature*, 440, pp.470-476.

Nishikimi T, Lemura-Inaba C, Akimoto K, Ishikawa K, Koshikawa S & Matsuoka H (2009). Stimulatory and Inhibitory regulation of lipolysis by the NPR-A/cGMP/PKG and NPR-C/Gi pathways in rat cultured adipocytes. *Regul Pept*, 153, pp.56-63.

Nishimura M, Izumiya Y, Higuchi A, Shibata R, Qiu J, Kudo C, Shin HK, Moskowitz MA & Ouchi N (2008). Adiponectin prevents cerebral ischemic injury through endothelial nitric oxide synthase dependent mechanisms. *Circulation*, 117, pp.216-223.

Oh W, Abu-Elheiga L, Kordari P, Gu Z, Shaikenov T, Chirala SS & Wakil SJ (2005). Glucose and fat metabolism in adipose tissue of acetyl-CoA carboxylase 2 knockout mice. *Proc Natl Acad Sci U S A*, 102, pp.1384-1389.

Okamoto Y, Kihara S, Ouchi N, Nishida M, Arita Y, Kumada M, Ohashi K, Sakai N, Shimomura I, Kobayashi H, Terasaka N, Inaba T, Funahashi T& Matsuzawa Y (2002). Adiponectin reduces atherosclerosis in apolipoprotein E-deficient mice. *Circulation*, 106, pp.2767-2770.

Olesen SP, Munch E, Moldt P& Drejer J (1994). Selective activation of Ca(2+)-dependent K+ channels by novel benzimidazolone. *Eur J Pharmacol*, 251, pp.53–59.

Oliver G & Schäfer EA (1894). The physiological action of the suprarenal capsule. *J Physiol,* 16, pp.1-4.

Omae T, Nagaoka T, Tanano I &Yoshida A (2013). Adiponectin-induced dilation of isolated procine retinal arterioles via production of nitric oxide from endothelial cells. *Invest Ophthalmol Vis Sci*, 54, pp.4586-4594.

Omori K & Kotera J (2007). Overview of PDEs and Their Regulation. *Circ Res*, 100, pp.309-327.

Orallo F (1996). Regulation of cytosolic calcium levels in vascular smooth muscle. *Pharmacol Ther*, 69, pp.153-171.

Ouchi N, Kihara S, Arita Y, Maeda K, Kuriyama H, Okamoto Y, Hotta K, Nishida M, Takahashi M, Nakamura T, Yamashita S, Funahashi T & Matsuzawa Y (1999). Novel modulator for endothelial adhesion molecules: adipocyte-derived plasma protein adiponectin. *Circulation*, 100,

pp.2473-2476.

Ouchi N, Shibata R & Walsh K (2006). Cardioprotection b adiponectin. *Trends Cardiovasc Med*, 16, pp.141-146.

Ouchi N, Ohishi M, Kihara S, Funahashi T, Nakamura T, Nagaretani H, Kumada M, Ohashi K, Okamoto Y, Nishizawa H, Kishida K, Maeda N, Nagasawa A, Kobayashi H, Hiraoka H, Komai N, Kaibe M, Rakugi H, Ogihara T& Matsuzawa Y (2003).Association of hypoadiponectinemia with impaired vasoreactivity. *Hypertension*, 42, pp.231-234.

Pajvani UB, Hawkins M, Combs TP, Rajala MW, Doebber T, Berger JP, Wagner JA, Wu M, Knopps A, Xiang AH, Utzschneider KM, Kahn SE, Olefsky JM, Buchanan TA & Scherer PE (2004). Complex distribution, not absolute amount of adiponectin, correlates with thiazolidinedione-mediated improvement in insulin sensitivity. *J Biol Chem*, 279, pp.12152-12162.

Palmer RM, Ferrige AG & Moncada (1987). Nitric oxide release accounts for the biological activity of endothelium-derived relaxing factor. *Nature*, 327, pp.524-526.

Pang T, Zhang ZS, Gu M, Qiu BY, Yu LF, Cao PR, Shao W, Su MB, Li JY, Nan FJ & Li J (2008). Small molecule antagonizes autoinhibition and activates AMP-activated protein kinase in cells. *J Biol Chem*, 283, pp.16051-16060.

Papazian DM, Timpe LC, Jan YN & Jan LY (1991). Alteration of voltage-dependence of Shaker potassium channel by mutation in the S4 sequence. *Nature*, 349, pp.305-310.

Pfeifer A, Aszodi A, Seidler U, Ruth P, Hofmann F & Fassler R (1996). Intestinal secretory defects and dwarfism in miace lacking cGMP-dependent protein kinase II. *Science*, 274, pp.2082-2086.

Pfeifer A, Klatt P, Massberg S, Ny L, Sausbier M, Hirneiss C, Wang GX, Korth M, Aszódi A, Andersson KE, Krombach F, Mayerhofer A, Ruth P, Fässler R & Hofmann F (1998). Defective smooth muscle regulation in cGMP kinase I-deficient mice. *EMBO J*, 17, pp.3045-3051.

Porter EL (2011). Intercellular signalling in the rat mesenteric artery. Ph.D. Thesis. University of Manchester, UK.

Procopio C, Andreozzi F, Laratta E, Cassese A, Bequinot F, Arturi F, Hribal ML, Perticone F & Sesti G (2009). Leptin-stimulated endothelial nitric-oxide synthase via an adenosine 5'-monophosphate-activated protein kinase/Akt signaling pathway is attenuated by interaction with C-reactive protein. *Endocrinology*, 150, pp.3584–3593.

Rees DD, Palmer RM, Schulz R, Hodson HF & Moncada S (1990).Characterization of three inhibitors of endothelial nitric oxide synthase in vitro and in vivo. *Br J Pharmacol,* 101, pp.746-752.

Reusch JE, Colton LA & Klemm DJ (2000). CREB activation induces adipogenesis in 3T3-L1 cells. *Mol Cell Biol*, 20, pp.1008-1020.

Ribiere C, Jaubert AM, Gaudiot N, Sabourault D, Marcus ML, Boucher JL, Denis-Henriot D & Giudicelli Y (1996). White adipose tissue nitric oxide synthase: a potential source for NO production. *Biochem Biophys Res Commun*, 222, pp.706-712.

Rodríguez A, Fortuño A, Gómez-Ambrosi J, Zalba G, Díez J & Frühbeck G (2007). The inhibitory effect of leptin on angiotensin II-induced vasoconstriction in vascular smooth muscle cells is

mediated via a nitric oxide-dependent mechanism. *Endocrinology*, 148, pp.324-331.

Rosen GM & Freeman BA (1984).Detection of superoxide generated by endothelial cells. *Proc Natl Acad Sci U S A*, 81, pp.7269-7273.

Rubin LJ, Magliola L, Feng X, Jones AW & Hale CC (2005). Metabolic activation of AMP kinase in vascular smooth muscle. *J Appl Physiol*, 98, pp.296-306.

Russell FD & Davenport AP (1999). Secretory pathways in endothelin synthesis. *Br J Pharmacol*, 126, 391-398.

Sandberg M, Natarajan V, Ronander I, Kalderon D, Walter U, Lohmann SM &Jahnsen T (1989). Molecular cloning and predicted full-length amino acid sequence of the type I beta isozyme of cGMP-dependent protein kinase from human placenta. Tissue distribution and developmental changes in rat. *FEBS Lett*, 255, pp.321-329.

Sanders MJ, Ali ZS, Hegarty BD, Heath R, Snowden MA & Carline D (2007). Defining the mechanism of activation of AMP-activated protein kinase by the small molecule A-769662, a member of the thienopyridone family. *J Biol Chem*, 282, pp.32539-32548.

Sansbury BE, Cummins TD, Tang Y, Hellmann J, Holden CR, Harbeson MA, Chen Y, Patel RP, Spite M, Bhatnagar A & Hill BG (2012). Overexpression of endothelial nitric oxide synthase prevents diet-induced obesity and regulated adipocyte phenotype. *Circ Res*, 111, pp.1176-1189.

Santos RA, Ferreira AJ, Verano-Braga T & Bader M (2013). Angiotensin-converting enzyme 2, angiotensin-(1-7) and Mas: new players of the renin-angiotensin system. *J Endocrinol*, 216, pp.R1-R17.

Santos RA, Simoes e Silva AC, Maric C, Silva DM, Machado RP, de Buhr I, Heringer-Walther S, Pinheiro SV, Lopes MT, Bader M, Mendes EP, Lemos VS, Campagnole-Santos MJ, Schultheiss HP, Speth R & Walther T (2003). Angiotensin-(1-7) is an endogenous ligand for the G protein-coupled receptor Mas. *Proc Natl Acad Sci U S A*, 100, pp.8258-8263.

Santos SH, Fernandes LR, Mario EG, Ferreira AV, Pôrto LC, Alvarez-Leite JI, Botion LM, Bader M, Alenina N & Santos RA (2008). Mas deficiency in FVB/N mice produces marked changes in lipid and glycemic metabolism. *Diabetes*, 57, pp.340-347.

Sarzani R, Dessl-Fulgheri P, Paci VM, Espinosa E & Rappelli A (1996). Expression of natriuretic peptide receptors in human adipose and other tissues. *J Endocrinol Invest*, 19, pp.581-585.

Sastry B, Narasimhan C, Reddy NK & Raju BS (2004). Clinical efficacy of sildenafil in primary pulmonary hypertension: a randomized, placebo-controlled, double-blind crossover study. *J Am Coll Cardiol*, 43, pp.1149-1153.

Scherer (2006). Adipose tissue: from lipid storage compartment to endocrine organ. *Diabetes*, 55, pp.1537-1545.

Scherer PE, Williams S, Fogliano M, Baldini G & Lodish HF (1995). A novel serum protein similar to C1q, produced exclusively in adipocytes. *J Biol Chem*, 270, pp.26746-26749.

Schleifenbaum J, Köhn C, Voblova N, Dubrovska G, Zavariskava O, Gloe T, Crean CS, Luft FC, Huang Y, Schubert R & Gollasch M (2010). Systemic peripheral artery relaxation by KCNQ

channel openers and hydrogen sulfide. *J Hypertens*, 28, pp.1875-1882.

Schling P, Mallow H, Trindl A & Löffler G (1999). Evidence for a local rennin angiotensin system in primary cultured human preadipocytes. *Int J Obes Relat Metab Disord*, 23, pp.336-341.

Schoeffter P & Hoyer D (1990). 5-Hydroxytryptamine (5-HT)-induced endothelium-dependent relaxation of pig coronary arteries is mediated by 5-HT receptors similar to the 5-HT1D receptor subtype. *J Pharmacol Exp Ther*, 252, pp.387-395.

Schubert R & Mulvany MJ (1999). The myogenic response: established facts and attractive hypotheses. *Clin Sci (Lond),* 96, pp.313-326.

Schubert R & Nelson MT (2001). Protein kinases: tuners of the BKCa channel in smooth muscle. *Trends Pharmacol Sci*, 22, pp.505-512.

Scott JW, van Denderen BJ, Jorgensen SB, Honeyman JE, Steinberg GR, Oakhill JS, Iseli TJ, Koay A, Gooley PR, Stapleton D & Kemp BE (2008). Thienopyridone drugs are selective activators of AMP-activated protein kinase beta1-containing complexes. *Chem Biol*, 15, pp.1220-1230.

Seale P, Conroe HM, Estall J, Kajimura S, Frontini A, Ishibashi J, Cohen P, Cinti S & Spiegelman BM (2011). Prdm16 determines the thermogenic program of subcutaneous white adipose tissue in mice. *J Clin Invest*, 121, pp.96-105.

Sengenès C, Berlan M, De Glisenzinski I, Lafontan M & Galitzky J (2000). Natriuretic peptides: a new lipolytic pathway in human adipocytes. *FASEB J*, 14, pp.1345-1351.

Shabb JB, Ng L & Corbin JD (1990). One amino acid change produces a high affinity cGMP-binding site in cAMP-dependent protein kinase. *J Biol Chem*, 265, pp.16031-16034.

Shakur Y, Holst LS, Landstrom TR, Movsesian M, Degerman E & Manganiello V (2001). Regulation and function of the cyclic nucleotide phophodiesterase (PDE3) gene family. *Prog Nucleic Acid Res Mol Biol*, 66, pp.241-277.

Shen YT, Cervoni P, Claus T & Vatner SF (1996). Differences in beta 3-adrenergic receptor cardiovascular regulation in conscious primates, rats and dogs. *J Pharmacol Exp Ther*, 278, pp.1435-1443.

Shibata R, Ouchi N & Murohara T (2009). Adiponectin and cardiovascular disease. *Circ J*, 73, pp.608-614.

Shimokawa H (2010). Hydrogen peroxide as an endothelium-derived hyperpolarizing factor. *Pflugers Arch*, 459, pp.1-8.

Smorlesi A, Frontini A, Giordano A & Cinti S (2012). The adipose organ: white-brown adipocyte plasticity and metabolic inflammation. *Obes Rev*, 13 Suppl 2, pp.83-96.

Soltis EE & Cassis LA (1991). Influence of perivascular adipose tissue on rat aortic smooth muscle responsiveness. *Clin Exp Hypertens A*, 13, pp. 227-296.

Starke K (1972). Alpha sympathemimetic inhibition of adrenergic and cholinergic transmission in the rabbit heart. *Naunyn Schmiedebergs Arch Pharmacol*, 274, pp.18-45.

Stingo AJ, Clavell AL, Heublein DM, Wei CM, Pittelkow MR & Burnett JC Jr (1992). Presence of C-

type natriuretic peptide in cultured human endothelial cells and plasma. *Am J Physiol*, 263, pp.H1318–21.

Stipanuk MH & Beck PW (1982). Characterization of the enzymic capacity for cysteine desulphhydration in liver and kidney of the rat. *Biochem J*, 206, pp.267-277.

Stone JD, Narine A & Tullis DA (2012). Inhibition of vascular smooth muscle growth via signaling crosstalk between AMP-activated protein kinase and cAMP-dependent protein kinase. *Front Physiol*, 3, pp.1-12.

Szabó C (2007). Hydrogen sulphide and its therapeutic potential. *Nat Rev Drug Discov*, 6, pp.917-935.

Taira M, Hockman SC, Calvo JC, Taira M, Belfrage P & Manganiello VC (1993). Molecular cloning of the rat adipocyte hormone-sensitive cyclic GMP-inhibited cyclic nucleotide phosphodiesterase. *J Biol Chem*, 268, pp.18573-18579.

Teramoto N, Tomoda T, Yunoki T & Ito Y (2006). Different glibenclamide-sensitive of ATP-sensitive K+ currents using different patch-clamp recording methods. *Eur J Pharmacol*, 531, pp.34-40.

Tocris Bioscience (2013). A 769662. Available at: http://www.tocris.com/dispprod.php?ItemId=219396#.UaiyBOvWSRQ [Accessed June 2013].

Tomas E, Tsao TS, Saha AK, Murrey HE, Zhang CC, Itani SI, Lodish HF & Ruderman NB (2002). Enhanced muscle fat oxidation and glucose transport by ACRP30 globular domain: acetyl-CoA carboxylase inhibition and AMP-activated protein kinase activation. *Proc Natl Acad Sci U S A*, 99, pp.16309-16313.

Trochu JN, Leblais V, Raurueau Y, Bévére llj F, Le Marec H, Berdeaux A & Gauthier C (1999). Beta 3-adrenoceptor stimulation induces vasorelaxation mediated essentially by endothelium-derived nitric oxdie in rat thoracic aorta. *Br J Pharmacol*, 128, pp.69076.

Tsao TS, Murrey HE, Hug C, Lee DH & Lodish HF (2002). Oligomerization state-dependent activation of NF-kappa B signaling pathway by adipocyte complement-related protein of 30 kDa (Acrp30*). J Biol Chem*, 277, pp.29359-29362.

Tsukamoto O, Fujita M, Kato M, Yamazaki S, Asano Y, Ogai A, Okazaki H, Asai M, Nagamachi Y, Maeda N, Shintani Y, Minamino T, Asakura M, Kishimoto I, Funahashi T, Tomoike H & Kitakaze M (2009). Natriuretic peptides enhance the production of adiponectin in human adipocytes and in patients with chronic heart failure. *J Am Coll Cardiol*, 53, pp.2070-2077.

Uhler MD (1993). Cloning and expression of a novel cyclic GMP-dependent protein kinase from mouse brain. *J Biol Chem*, 268, pp.13586-13591.

Umekawa T, Yoshida T, Sakane N & Kondo M (1997). Effect of CL316,243, a highly specific beta(3)-adrenoceptor agonist, on lipolysis of epididymal, mesenteric and subcutaneous adipocytes in rats. *Endocr J*, 44, pp.181-185.

Vanhoutte PM, Cohen RA & Van Nueten JM (1984). Serotonin and arterial vessels. *J Cardiovasc Pharmacol*, 6 Suppl 2: S421-S428.

Verdon CP, Burton BA & Prior RL (1995). Sample pretreatment with nitate reductase and glucose-6-phosphate dehydrogenase quantitatively reduces nitrate while avoiding interference b NADP+

when the Griess reaction is used to assay for nitrite. *Anal Biochem*, 224, pp.502-508.

Verlohren S, Dubrovska G, Tsang SY, Essin K, Luft FC, Huang Y & Gollasch M (2004). Visceral periadventitial adipose tissue regulates arterial tone of mesenteric arteries. *Hypertension*, 44, pp.271–276.

Waldron GJ & Cole WC (1999). Activation of vascular smooth muscle K^+ channels by endothelium-derived relaxing factors. *Clin Exp Pharmacol Physiol,* 26, pp.180-184.

Walker DK, Ackland MJ, James GC, Muirhead GJ, Rance DJ, Wastabll P & Wright PA (1999). Pharmacokinetics and metabolism of sildenafil in mouse, rat, rabbit, dog and man. *Xenobiotica*, 29, pp.297-310.

Wang H (1998). KCNQ2 and KCNQ3 Potassium Channel Subunits: Molecular Correlates of the M-Channel. *Science*, 282, pp.1890-1893.

Wang HD, Pagano PJ, Du Y, Cayatte AJ, Quinn MT, Brecher P & Cohen RA (1998). Superoxide anion from the adventitia of the rat thoracic aorta inactivates nitric oxide. *Circ Res*, 82, pp.810-818.

Wang R, Wang Z & Wu L (1997). Carbon monoxide-induced vasorelaxation and the underlying mechanisms. *Br J Pharmacol*, 121, pp.927-934.

Wang S, Liang B, Viollet B & Zou MH (2011). Inhibition of the AMP-activated protein kinase-α2 accentuates agonist-induced vascular smooth muscle contraction and high blood pressure in mice. *Hypertension*, 57, pp.1010-1017.

Wang S, Song P & Zou MH (2012). AMP-activated protein kinase, stress responses and cardiovascular diseases. *Clin Sci (Lond)*, 122, pp.555-573.

Watts SW, Morrison SF, Davies RP & Barman SM (2012). Serotonin and blood pressure regulation. *Pharmacol Rev*, 64, pp.359-388.

Webb DJ, Freestone S, Allen MJ & Muirhead GJ (1999). Sildenafil citrate and blood-pressure-lowering drugs: results of drug interaction studies with an organic nitrate and a calcium antagonist. *Am J Cardiol*, 83, pp.21-28.

Webb RC (2003). Smooth muscle contraction and relaxation. *Adv Physiol Educ*, 27, pp.201-206.

Wegener JW, Nawrath H, Wolfsgruber W, Kühbandner S, Werner C, Hofmann F & Feil R (2002). cGMP-dependent protein kinase I mediates the negative inotropic effect of cGMP in the murine myocardium. *Circ Res*, 90, pp.18-20.

Wei A, Solaro C, Lingle C & Salkoff L (1994). Calcium sensitivity of BK-type KCa channels determined by a separable domain. *Neuron*, 13, pp.671-681.

Wellman GC & Nelson MT (2003). Signaling between SR and plasmalemma in smooth muscle: sparks and the activation of Ca2+-sensitive ion channels. *Cell Calcium*, 34, pp.211-229.

Wellman GC, Santana LF, Bonev AD & Nelson MT (2001). Role of phospholamban in the modulation of arterial CA(2+) sparks and Ca(2+)-activated K(+) channels by cAMP. *Am J Physiol Cell Physiol*, 281, pp.C1029-C1037.

Weston AH, Egner I, Dong Y, Porter EL, Heagerty AM & Edwards G (2013). Stimulated release of a

hyperpolarizing factor (ADHF) from mesenteric artery perivascular adipose tissue; involvement of myocyte BKCa channels and adiponectin. *Br J Pharmacol*, 169, pp.1500-1509.

Wilcox JN, Augustine A, Goeddel DV & Lowe DG (1991).Differential regional expression of three natriuretic peptide receptor genes within primate tissues. *Mol Cell Biol,* 11, pp.3454-3462.

Withers SB, Simpson L, Werner ME & Heagerty AM (2011). The role of cGMP dependent protein kinase (PKG) in mediating the anticontractile function of perivascular fat [abstract]. Proceedings of The Physiological Society, http://www.physoc.org/proceedings/abstract/Proc%20Physiol%20Soc%2025C11%20and%20PC11 [Accessed Aug 2013].

Wong MS & Vanhoutte PM (2010). COX-mediated endothelium-dependent contractions: from the past to recent discoveries. *Acta Pharmacol Sin*, 31, pp.1095-1102.

Wong WT & Huang Y (2009). Angiotensin AT2 receptor as a potential therapeutic target in hypertension. *Clin Exp Pharmacol Physiol*, 36, pp.3-4.

Woods A, Johnstone SR, Dickerson K, Leiper FC, Fryer LG, Neumann D, Schlattner U, Wallimann T, Carlson M & Carling D (2003). LKB1 is the upstream kinase in the AMP-activated protein kinase cascade. *Curr Biol*, 13, pp.2004-2008.

World Health Organisation (2013). Obesity and overweight. Fact sheet number 311. Available at http://www.who.int/mediacentre/factsheets/fs311/en/index.html [Accessed August 2013].

Wu SN, Li HF, Jan CR & Shen AY (1999). Inhibition of Ca2+-activated K+ current by clotrimazole in rat anterior pituitary GH3 cells. *Neuropharmacology*, 38, pp.979-989.

Wu X, Motoshima H, Mahadev K, Stalker TJ, Scalia R & Goldstein BJ (2003). Involvement of AMP-activated protein kinase in glucose uptake stimulated by the globular domain of adiponectin in primary rat adipocytes. *Diabetes*, 52, pp.1355-1363.

Wulff H, Kolski-Andreaco A, Sankaranarayanan A, Sabatier JM & Shakkottai V (2007). Modulators of small- and intermediate-conductance calcium-activated potassium channels and their therapeutic indications. *Curr Med Chem*, 14, pp.1437-1457.

Wulff H, Miller MJ, Hansel W, Grissmer S, Cahalan MD & Chandy KG (2000). Design of a potent and selective inhibitor of the intermediate-conductance Ca2+-activated K+ channel, IKCa1: a potential immunosuppressant. *Proc Natl Acad Sci U S A*, 97, pp.8151-8156.

Xia XM, Fakler B, Rivard A, Wayman G, Johnson-Pais T, Keen JE, Ishii T, Hirschberg B, Bond CT, Lutsenko S, Maylie J & Adelman JP (1998). Mechanism of calcium gating in small-conductance calcium-activated potassium channels. *Nature*, 395, pp.503-507.

Xie M, Zhang D, Dyck JR, Li Y, Zhang H, Morishima M, Mann DL, Taffet GE, Baldini A, Khoury DS & Schneider MD (2006). A pivotal role for endogenous TGF-beta-activated kinase-1 in the LKB1/AMP-activated protein kinase energy-sensor pathway. *Proc Natl Acad Sci U S A*, 103, pp.17378-17383.

Xiong Q, Sun H, Zhang Y, Nan F & Li M (2008). Combinatorial augmentation of voltage-gated KCNQ potassium channels by chemical openers. *Proc Natl Acad Sci U S A*, 105, pp.3128-3133.

Yada T, Shimokawa H, Hiramatsu O, Kajita T, Shigeto F, Goto M, Ogasawara Y & Kajiya F (2003).

Hydrogen peroxide, an endogenous endothelium-derived hyperpolarizing factor, plays an important role in coronary autoregulation in vivo. *Circulation*, 107, pp.1040-1045.

Yamauchi T, Kamon J, Minokoshi Y, Ito Y, Waki H, Uchida S, Yamashita S, Noda M, Kita S, Ueki K, Eto K, Akanuma Y, Froguel P, Foufelle F, Ferre P, Carling D, Kimura S, Nagai R, Kahn BB & Kadowaki T (2002). Adiponectin stimulates glucose utilization and fatty-acid oxidation by activating AMP-activated protein kinase. *Nat Med*, 8, pp.1288-1295.

Yamauchi T, Nio Y, Maki T, Kobayashi M, Takazawa T, Iwabu M, Okada-Iwabu M, Kawamoto S, Kubota N, Kubota T, Ito Y, Kamon J, Tsuchida A, Kumagai K, Kozono H, Hada Y, Ogata H, Tokuyama K, Tsunoda M, Ide T, Murakami K, Awazawa M, Takamoto I, Froguel P, Hara K, Tobe K, Nagai R, Ueki K & Kadowaki T (2007). Targeted disruption of AdipoR1 and AdipoR2 causes abrogation of adiponectin binding and metabolic actions. *Nat Med*, 13, pp.332-339.

Yamauchi T, Kamon J, Ito Y, Tsuchida A, Yokomizo T, Kita S, Sugiyama T, Miyagishi M, Hara K, Tsunoda M, Murakami K, Ohteki T, Uchida S, Takekawa S, Waki H, Tsuno NH, Shibata Y, Terauchi Y, Froguel P, Tobe K, Koyasu S, Taira K, Kitamura T, Shimizu T, Nagai R & Kadowaki T (2003). Cloning of adiponectin receptor that mediate antiabetic metabolic effects. *Nature*, 423, pp.762-768.

Yamauchi T, Kamon J, Waki H, Terauchi Y, Kubota N, Hara K, Mori Y, Ide T, Murakami K, Tsuboyama-Kasaoka N, Ezaki O, Akanuma Y, Gavrilova O, Vinson C, Reitman ML, Kagechika H, Shudo K, Yoda M, Nakano Y, Tobe K, Nagai R, Kimura S, Tomita M, Froguel P & Kadowaki T (2001). The fat-derived hormone adiponectin reverses insulin resistance associated with both lipoatrophy and obesity. *Nat Med,* 7, pp.941-946.

Yanagisawa M, Kurihara H, Kimura S, Tomobe Y, Kobayashi M, Mitsui Y, Yazaki Y, Goto K & Masaki T (1988). A novel potent vasoconstrictor peptide produced by vascular endothelial cells. *Nature*, 332, pp.411-415.

Yang G, Wu L, Jiang B, Yang W, Qi J, Cao K, Meng Q, Mustafa AK, Mu W, Zhang S, Snyder SH & Wang R (2008). H2S as a physiologic vasorelaxant: hypertension in mice with deletion of cystathionine gamma-lyase. *Science*, 322, pp.587-590.

Yeung SY, Pucovsky V, Moffatt JD, Saldanha L, Schwake M, Ohya S & Greenwood IA (2007). Molecular expression and pharmacological identification of a role for K(v)7 channels in murine vascular reactivity. *Br J Pharmacol*, 151, pp.758-770.

Yoshida H, Bao L, Kefaloyianni E, Taskin E, Okorie U, Hong M, Dhar-Chowdhury P, Kaneko M & Coetzee WA (2012). AMP-activated protein kinase connects cellular energy metabolism to KATP channel function. *J Mol Cell Cardiol,* 52, pp.410–418.

Yoshida T, Sakane N, Wakabayashi Y, Umekawa T & Kondo M (1994). Anti-obesity and anti-diabetic effect of CL 316,243, a highly specific beta 3-adrenoceptor agonist, in yellow KK mice. *Life Sci,* 54, pp.491-498.

Yu JG, Javorschi S, Hevener AL, Kruszynska YT, Norman RA, Sinha M & Olefsky JM (2002). The effect of thiazolidines on plasma adiponectin levels in normal obese, and type 2 diabetic subjects. *Diabetes*, 51, pp.2968-2974.

Zaczek R, Chorvat RJ, Saye JA, Pierdomenico ME, Maciag CM, Logue AR, Fisher BN, Rominger DH & Earl R (1998). Two new potent neurotransmitter release enhancers, 10,10-bis(4-pyridinylmethyl)-9(10H)-anthracenone and 10,10-bis(2-fluoro-4-pyridinylmethyl)-9(10H)-

anthracenone: comparison to linopirdine. *J Pharmacol Exp Ther*, 285, pp.724-730.

Zhang X, Ji J, Yan G, Wu J, Sun X, Shen J, Jiang H & Wang H (2010). Sildenafil promotes adipogenesis through a PKG pathway. *Biochem Biophys Res Commun*, 396, pp.1054-1059.

Zhang HL & Bolton TB (1996). Two types of ATP-sensitive potassium channels in rat portal vein smooth muscle cells. *Br J Pharmacol*, 118, pp.105-114.

Zhang Y, Proenca R, Maffei M, Barone M, Leopold L & Friedman JM (1994). Positional cloning of the mouse obese gene and its human homologue. *Nature*, 372, pp.425–432.

Zhao W, Zhang J, Lu Y & Wang R (2001). The vasorelaxant effect of H(2)S as a novel endogenous gaseous K(ATP) channel opener. *EMBO J*, 20, pp.6008-6016.

Zhou G, Myers R, Li Y, Chen Y, Shen X, Fenyk-Melody J, Wu M, Ventre J, Doebber T, Fujii N, Musi N, Hirshman MF, Goodyear LJ & Moller DE (2001). Role of AMP-activated protein kinase in mechanism of metformin action. *J Clin Invest*, 108, pp.1167-1174.

Zhou L, Deepa SS, Etzler JC, Ryu J, Mao X, Fang Q, Liu DD, Torres JM, Jia W, Lechleiter JD, Liu F & Dong LQ (2009). Adiponectin activates AMP-activated protein kinase in muscle cells via APPL1/LKB1-dependent and phospholipase C/Ca2+/Ca2+/calmodulin-dependent protein kinase kinase-dependent pathways. *J Biol Chem*, 284, pp.22426-22435.

Zhu Z, Zhong J, Zhu S, Liu D, Van Der Giet M & Tepel M (2002). Angiotensin-(1-7) inhibits angiotensin II-induced signal transduction. *J Cardiovasc Pharmacol*, 40, pp.693-700.

Zuk PA, Zhu M, Ashjian P, De Ugarte DA, Huang JI, Mizuno H, Alfonso ZC, Fraser JK, Benhaim P & Hedrick MH (2002). Human adipose tissue is a source of multipotent stem cells. *Mol Biol Cell*, 13, pp.4279-4295.